Distribution Agreement

In presenting this thesis or dissertation as a partial fulfillment of the requirements for an advanced degree from Emory University, I hereby grant to Emory University and its agents the non-exclusive license to archive, make accessible, and display my thesis or dissertation in whole or in part in all forms of media, now or hereafter known, including display on the world wide web. I understand that I may select some access restrictions as part of the online submission of this thesis or dissertation. I retain all ownership rights to the copyright of the thesis or dissertation. I also retain the right to use in future works (such as articles or books) all or part of this thesis or dissertation.

Signature:

_____ _____

Sena Agezo Date

Quantifying animal social behavior during pair bond formation

By

Sena Agezo
Doctor of Philosophy

Graduate Division of Biological and Biomedical Science
Neuroscience

Gordon J. Berman, Ph.D.
Advisor

Robert C. Liu, Ph.D.
Advisor

Aubrey M. Kelly, Ph.D.
Committee Member

Samuel J. Sober, Ph.D.
Committee Member

Larry J. Young, Ph.D.
Committee Member

Accepted:

Kimberly Jacob Arriola, Ph.D., MPH
Dean of the James T. Laney School of Graduate Studies

Date

Quantifying animal social behavior during pair bond formation

By

Sena Agezo
M.S. & B.S., Drexel University, 2016

Advisors: Gordon J. Berman, Ph.D.,
Robert C. Liu, Ph.D.

An abstract of
A dissertation submitted to the Faculty of the
James T. Laney School of Graduate Studies of Emory University
in partial fulfillment of the requirements for the degree of
Doctor of Philosophy
in Graduate Division of Biological and Biomedical Science
Neuroscience
2023

Abstract

Quantifying animal social behavior during pair bond formation

By Sena Agezo

Pair bonding is a complex social process that involves behavioral changes across contexts, including sociosexual interactions and parental care. A pair bond is thus a complex state that manifests across an animal's behavioral repertoire. Despite such complexity, this state is typically characterized with reference to only a few behaviors, often only one at a time. For example, in prairie voles, a canonical mammalian model of pair bonding, a bond is usually inferred only by observing one behavior, partner huddling, or another resident-intruder attack. Here, we characterize how the process of pair bonding alters a complete repertoire of natural behaviors. Specifically, we investigate prairie voles with their oxytocin receptors knocked out since the receptors are thought to be necessary for pair bond formation.

We tracked the postures of voles during the early phase (3hrs) of a 48-hr cohabitation by leveraging the advances in deep-learning algorithms such as DeepLabCut. However, these algorithms exhibit poor tracking accuracy when the animals spend more time with each other, performing key social behaviors such as huddling and mutual grooming. Hence, we implemented a pipeline that combines multiple deep-learning-based tracking methods to obtain detailed and high-accuracy postural trajectories of multiple animals.

Using the postural trajectories, we implemented an unsupervised method to map the behavior of the animals and observed that prairie voles show a gradual temporal evolution of the behavioral repertoire from locomotory-like movements to more stationary-like behaviors. In addition, we found that the mutant voles, with the oxytocin receptors knocked out, show more stationary-like behavior than wild-type animals. However, contrary to the current knowledge in the field and despite the subtle behavioral difference we observed, we found that the oxytocin receptors are not necessary for pair bond formation in prairie voles.

Quantifying animal social behavior during pair bond formation

By

Sena Agezo
M.S. & B.S., Drexel University, 2016

Advisors: Gordon J. Berman, Ph.D.,
Robert C. Liu, Ph.D.

A dissertation submitted to the Faculty of the
James T. Laney School of Graduate Studies of Emory University
in partial fulfillment of the requirements for the degree of
Doctor of Philosophy
in Graduate Division of Biological and Biomedical Science
Neuroscience
2023

To my family and friends for all their love and support

TABLE OF CONTENTS

LIST OF FIGURES

LIST OF SYMBOLS AND ABBREVIATIONS

OT – Oxytocin

OTR – Oxytocin receptor

AVP – Arginine vasopressin

DLC – DeepLabCut

maDLC – multi-animal DeepLabCut

SLEAP – Social LEAP Estimate Animal Poses

ICV – intracerebroventricular

CRISPR – clustered regularly interspaced short palindromic repeats

Chapter 1. UNDERSTANDING THE ROLE OF THE OXYTOCIN SYSTEM IN PAIR BONDING THROUGH THE LENS OF THE PRAIRIE VOLE MODEL

1.1 Introduction

In this chapter, I will discuss the role of the oxytocin system in social behavior, specifically pair bonding. I will review the literature covering how the oxytocin system regulates the behavior of animals via its actions in different brain areas and talk about prairie voles, an animal model that has provided much of our knowledge about the oxytocin system and pair bonding. In addition, I will discuss the role of other neurochemicals, such as arginine vasopressin and dopamine, and their interactions with oxytocin to modulate social behaviors. Finally, I will conclude with the leading hypothesis about how oxytocin acts within the social brain network to regulate social behavior in animals.

1.2 Background

Social behaviors consist of a complex set of interactions between individuals. These interactions involve animals performing many different actions, with the repertoire of these behaviors evolving as the nature of the social interaction changes. Animals might engage in social interaction for a varied set of reasons, like for survival and reproduction. These social behaviors could be aggressive, which might take the form of fighting with other conspecific animals to gain a mate, for a new territory, to show dominance and maintain a social hierarchy, or to keep a territory (Varley and Symmes, 1966; Kravitz and Huber, 2003). In addition, these

social behaviors could be performed to protect them against other animals, like communicating the imminent approach of a predator or a competing rival clan group (Clutton-Brock et al., 1999; Ridley et al., 2013).

Alternatively, the animals might behave more affiliative toward each other and possibly, in the process, form social bonds (e.g., a parental behavior where either or both female and male animals care for their young). The social bond can be at a collective level, where a group of animals combines their efforts to care for and train their young (Kappeler, 1997; Kappeler and Van Schaik, 2002). Conversely, it can also be a pair bond that exists between the two adult sexes, where both parents care for the young together, have a selective preference for their partner, and share and protect their territory (Getz and Carter, 1980; Thalmann, 2001).

Studying how pair bonds are formed between two individuals is a research topic that underlies much of the work in this thesis. How do animals develop and maintain social bonds, particularly socially monogamous pair bonds? What neural circuits and states underlie the formation of these bonds? In the rest of this chapter, I will discuss pair bonds and the neurobiology behind them, reviewing studies investigating neurochemicals like oxytocin and its receptor and their involvement in facilitating the formation and maintenance of social bonds. There have been extensive and excellent reviews written on this subject, so I will refer the reader to these Refs (Sue Carter et al., 1995; Insel and Young, 2001; Burbach et al., 2006; Walum and Young, 2018; Froemke and Young, 2021).

1.3 Social Monogamy

Social monogamy is a sociosexual relationship between two individuals, with this association either being exclusively social and sexual or only social (Walum and Young, 2018). In an exclusively social and sexual bond, the adult individuals (a single breeding female and a

single breeding male) form an attachment where they only mate with each other, take care of their young, and defend their territory against intruders. However, in the solely social case, they perform all social behaviors like biparental care and territory defense except for exclusively mating with one partner.

Humans are likely to engage in an exclusive social and sexual monogamous pair bond, but solely social monogamy is more typical in the animal kingdom. This non-exclusively sociosexual monogamy is commonly observed within the avian species, approximately 90% of birds (Cockburn, 2006). With 9% of mammalian species considered socially monogamous compared to the 68% and 23% that are classified as solitary and living in social groups, respectively. Among this low percentage of mammals regarded as socially monogamous, primates make up 29% of them (Lukas and Clutton-Brock, 2013).

There are biological and evolutionary reasons why animals transitioned from solitary and group living into social monogamy, with one reason being the contribution of both sexes in providing for the young and protecting them from infanticide from other competing males (Chapais, 2021). Another reason is mate-guarding, where individual fights to protect their partner from an intruding conspecific mate or prevent them from seeking another mate (Chapais, 2021).

A trait that characterizes social monogamy is a pair bond, where the male and female cohabitate with each other and have a long-term selective attachment (Sue Carter et al., 1995). In humans, individuals forming pair bonds have the added advantage of promoting familial cooperation and encouraging diverse mate selection to prevent inbreeding (Gavrilets, 2012). Studies in humans also show a link between positive health and being in a social relationship (House et al., 1988), where individuals involved in social relationships had fewer depressive

symptoms and improved inflammatory responses (House et al., 1988; Kiecolt-Glaser and Newton, 2001; Kiecolt-Glaser et al., 2005). From observing the human and nonhuman benefits of being in a pair bond and with the goal of gaining knowledge about their neural underpinnings, the study of animal models in the laboratory that perform such behavior has become invaluable to the field of social neurobiology.

1.4 Prairie Voles: A Premier Animal Model for Pair Bonding

In studying a specific behavior and its neural underpinnings, especially in a laboratory environment, it is ideal to have a suitable animal model that exhibits appropriate ethological properties to gain a better biological understanding of the behavior. For example, we have gained considerable knowledge about motor learning and consolidation of learning through animal models like songbirds, whose juvenile animals can learn the songs of adult birds (Warren et al., 2011). Another example is the study of the auditory system, where bats serve as an excellent model because of their highly optimized echolocation behavior (Masters and Jacobs, 1989). Flies and worms have been extensively studied in how they interact with their environment to feed, mate, and fight to elucidate feeding, sexual, and aggressive behaviors (Avery and Horvitz, 1990; Mann et al., 2013; Cheriyamkunnel et al., 2021). Even in the overused and overgeneralized mice animal model, researchers have investigated behaviors such as parental behavior and vocalization and their associated neural mechanisms (Chong et al., 2020; Dunlap et al., 2020).

Prairie voles (*Microtus ochrogaster*), over the last three to four decades, have emerged as the premier model for studying animal pair bonding. The prairie voles are socially monogamous microtine rodents primarily found in central North America (Keller and Krebs, 1970; Ophir et al., 2007). In the wild, it is highly probable to capture a pair of male and female prairie voles in a

live trap compared to meadow voles (*Microtus pennsylvanicus*), which are considered socially promiscuous. The captured voles are likely to be the same pair if the trappings are repeated multiple times (Getz et al., 1981). In addition, when a male and a female prairie vole are paired together in the laboratory setting, they form long-lasting, enduring bonds (Getz et al., 1981). These stable social bonds are characterized by biparental care, where both sexes contribute equally to nurturing the young and defending their territory against intruders. On the contrary, such biparental behaviors are not observed in the meadow and montane voles (*Microtus montanus*).

When prairie voles are tested in a partner preference test, a simple behavioral paradigm to assess pair bond formation (Figure 1.1) (Williams et al., 1992), the paired individuals spend most of the time in side-by-side physical contact with their partners compared to strangers, animals that are novel to the pair (Gavish et al., 1983; Carter et al., 1988). In addition to the selective preference for their partners, paired males and females that have had sexual contact show highly aggressive behaviors toward unfamiliar conspecifics as a way to guard their mates compared to sexually naïve individuals (Getz and Carter, 1980; Getz et al., 1993). Owing to the prairie voles showing the following factors, (i) an apparent behavior to identify factors that initiate or inhibit the formation of attachment bonds, (ii) an attachment behavior that is selective and enduring, and finally, (iii) a measurable and manipulatable behavior, as defined by Insel and Young, they provide the appropriate model to study the neurobiology of pair bonding (Insel and Young, 2001).

From the studies into the neurobiology of pair bonding in prairie voles (and other non-monogamous species like mice and meadow voles), we have gained insight into the role of neuropeptides such as oxytocin, vasopressin, dopamine, and other related neurochemicals like

serotonin (5-HT) and the opioid signaling. Additionally, we are developing a clear picture of brain circuitry and areas that are regarded as the social brain centers. This network of brain regions, including the nucleus accumbens, the amygdala, the hippocampus, and the prefrontal cortex, have neuronal projections and receptors that, when manipulated, can alter the ability of the animal to form a social bond.

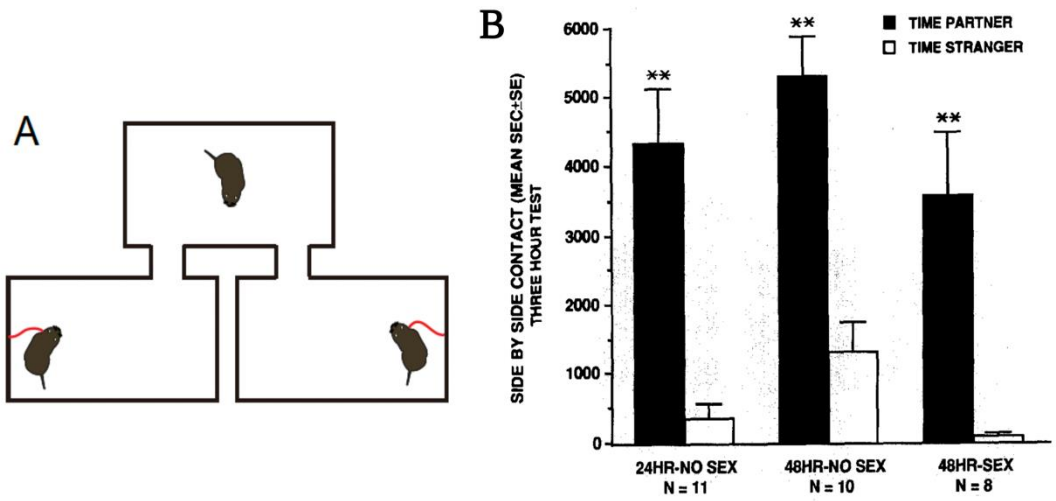

Figure 1.1. A partner preference test to assess pair bond formation. Female prairie voles were paired with male conspecifics under varying conditions. A. Schematic of partner preference test performed in a 3-chamber. B Time spent in side-by-side contact with the partner and the stranger during a 3-hr preference test (Adapted from Williams et al., 1992)

1.5 Oxytocin

Initially implicated in uterine contractions during labor and promoting milk ejection from the mammary gland during lactation (Dale, 1906; Freund-mercier et al., 1988), Oxytocin (OT) is a nine amino-acid peptide (Cys-Tyr-Ile-Gln-Asn-Cys-Pro-Leu-Gly-NH2) that regulates social behaviors like pair bonding and maternal care (Pedersen et al., 1982; Williams et al., 1994; Sue Carter et al., 1995; Young et al., 2001; Numan and Young, 2016).

OT is considered an evolutionarily conserved neuropeptide with oxytocin-like neurochemicals existing in varying species, from insects to fish to mammals (Stafflinger et al.,

2008). OT, and its closely related neurochemical, arginine vasopressin (to be discussed later), share genetic and biological similarities and are thought to have originated from an ancestral gene vasotocin, which is found in reptiles and other vertebrates (Acher et al., 1996). In species like birds and fish, OT has homologous, such as mesotocin and isotocin, which are associated with social behaviors, survival, and reproduction (Acher et al., 1996).

In the prairie vole, OT is synthesized in the paraventricular nucleus (PVN) and supraoptic nucleus (SON) of the hypothalamus (Bargmann and Scharrer, 1951). The PVN has magnocellular and parvocellular cells that make oxytocin, while the SON has only magnocellular cells which synthesize them. The OT synthesized by the magnocellular and parvocellular is released by three modes of transmission to the body and brain. The first of these modes is the endocrine release, where the PVN and SON cells, with their axonal fiber projection to the posterior pituitary gland, secrete OT into the bloodstream (van den Pol, 2012). The second mode of transmitting OT is via paracrine release, where OT is secreted from the dendrites and cell bodies of the neurons into the cerebrospinal fluid (de Kock et al., 2003). In both the endocrine and paracrine secretions, OT is meant to act as a hormone. Finally, in the third transmission mode, OT is released at the axon terminal via vesicles to the cell body and dendrites of neurons that synapse with the PVN and SON cells.

In the endocrine and paracrine secretions, the OT released into the bloodstream is implicated in having both peripheral and central functions to facilitate uterine contraction, lactation, and parental care (Dale, 1906; Summerlee and Lincoln, 1981; Gimpl and Fahrenholz, 2001; Francis et al., 2002). During the onset of labor and lactation, there is a significant increase in the OT receptors (to be discussed later) in the uterus and the mammary gland associated with an up-regulation of OT in the bloodstream to help promote uterine contraction and milk

production. And in parental care, involving mothers becoming attached to their infants, there is an upregulation of OT in the bloodstream, coupled with the paracrine release in the cerebrospinal fluid during parturition. At the same time, the synaptic transmission of OT via the axon terminals of the PVN and SON neurons is thought to promote maternal attachment in some species, like mice and rats, to their young (Dölen et al., 2013).

In addition to facilitating uterine contraction and parental care, the release of OT centrally in the brain plays an essential role in mediating pair bond formation in animals. When OT is infused via intracerebroventricular (ICV) injection into the prairie voles, the animals that receive OT instead of artificial cerebrospinal spinal fluid spend more time in side-by-side contact with their partner compared to a stranger, an indication that OT promotes partner preference (Williams et al., 1994). However, a peripheral (subcutaneous) injection of OT does not elicit this partner preference response. The central release of OT produces a preference for the partner in both male and female prairie voles (Cho et al., 1999a). It has been observed that during social interactions, the extracellular concentration of OT increases in the female prairie voles (Ross et al., 2009). And in human studies, although they need to be interpreted with caution, the infusion of OT via nasal spray is thought to promote prosocial behaviors such as increased contact with the eye region of human faces in males with and without autism during social interactions (Figure 1.2) (Guastella et al., 2008; Andari et al., 2010; Auyeung et al., 2015). After the intranasal infusion of OT, humans are likely to engage in trust-like behaviors and reduce fear-associated and betrayal-aversion behaviors during social interaction (Kirsch et al., 2005; Kosfeld et al., 2005). Even though there is skepticism as to the mode of delivery of OT, there is some evidence to show that intranasal infusion elicits increased elevation of OT in the blood and CSF

(Neumann et al., 2013; Modi et al., 2014; Freeman et al., 2016). The activity of OT is mediated by binding to their canonical receptors, oxytocin receptors (OTR).

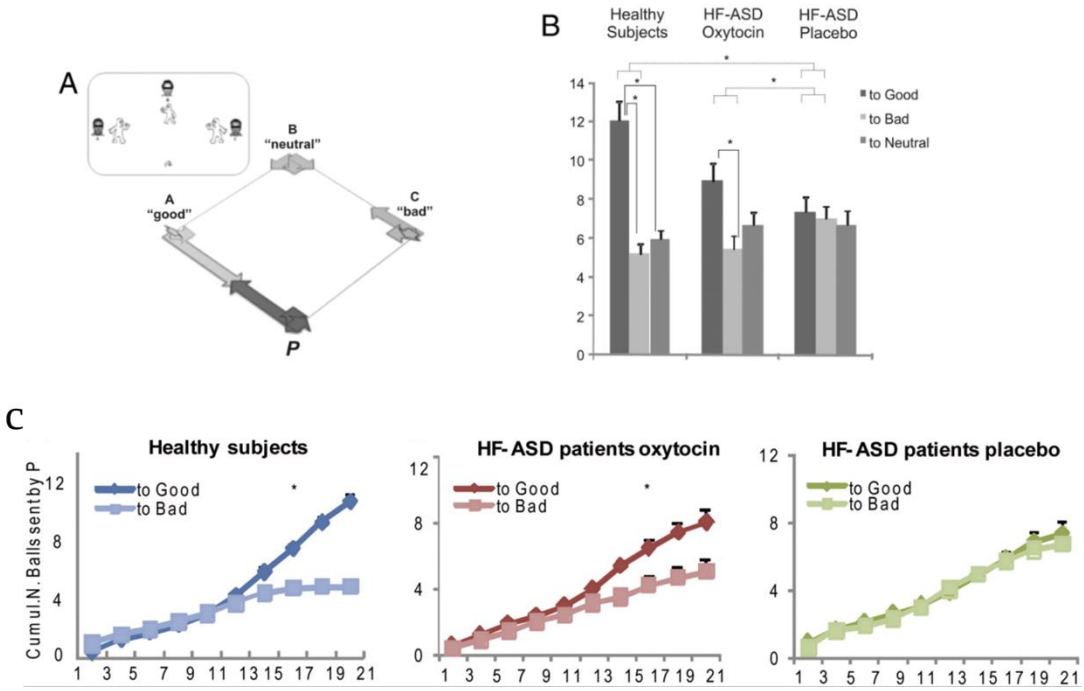

Figure 1.2. Oxytocin promotes prosocial behaviors in humans. A. A schematic of a Cyberball game and ball-toss distribution, where a participant engages in a multi-round ball-toss game over a computer network with three fictitious partners, classified as good, neutral, and bad. The "good" profile (A) sent, on average, 70%, of its played balls to the participant (P). The "neutral" profile (B) sent 30%, and player C (the "bad" profile) sent 10% of its played balls to the participant. B. Ball-toss distributions for healthy subjects and for patients with HF-ASD treated with oxytocin or placebo. C. Time course of ball tosses sent by participant P to players A (good) and C (bad) in a regularly spaced bin, an interval between player A's tosses n and n+2. (Adapted from Andari et al., 2010)

1.6 Oxytocin Receptors

The OTRs are G protein-coupled receptors encoded by a single gene that is conserved across species (Inoue et al., 1994). They are widely expressed throughout the body and brain and can be found in the uterus, kidney, heart, mammary gland, and brain (Gimpl and Fahrenholz, 2001). In the periphery, the binding of OT to the OTRs is implicated in mediating reproductive

functions in both females and males, like parturition and lactation and erectile function and copulation, respectively. In the brain, the OTRs are densely expressed in areas associated with the social brain network, such as the nucleus accumbens, the amygdala, the prefrontal cortex, and the olfactory bulb. The expression in the brain varies widely from one species to another. For example, even within closely related species like prairie voles and meadow voles, there is a higher concentration of OTRs in the nucleus accumbens and amygdala in the prairie voles than in the promiscuous meadow and montane voles (Shapiro and Insel, 1992; Olazábal and Young, 2006). Across species, there is an elevated expression of the OTR in the lateral septum of mice and meadow voles compared to the prairie vole and rats. At the same time, the prairie voles have higher OTRs in both the shell and core of the accumbens and the caudate putamen than in mice and rats (Olazábal and Young, 2006). Even within the same species, there is a natural variation of the OTR expression in the brain. Due to a single nucleotide polymorphism in the gene, some prairie voles have a high expression of OTR in the nucleus accumbens than others with low expression in the same brain region (King et al., 2016). Given the varying degree of OTR expression across different animal species, especially in the prairie voles, we have gained a wide sphere of knowledge about its possible role in social behavior.

Early work with OTRs in prairie voles showed how central they are to pair bond formation and other social behaviors. ICV infusion of oxytocin receptor antagonist (OTA) inhibits paired animals' preference for their partners (Williams et al., 1994). Even after mating, when an OTA is centrally infused into the brain of prairie voles, it reduces the partner preference formation (Insel and Hulihan, 1995). In subsequent studies, a site-specific injection of OTA into the nucleus accumbens or prelimbic cortex blocks mating-induced pair-bond formation in female prairie voles (Young and Wang, 2004). Using viral techniques such as RNA interference to

knock down the OTR in the accumbens, thereby reducing its density, inhibits the pair bonding (Keebaugh et al., 2015).

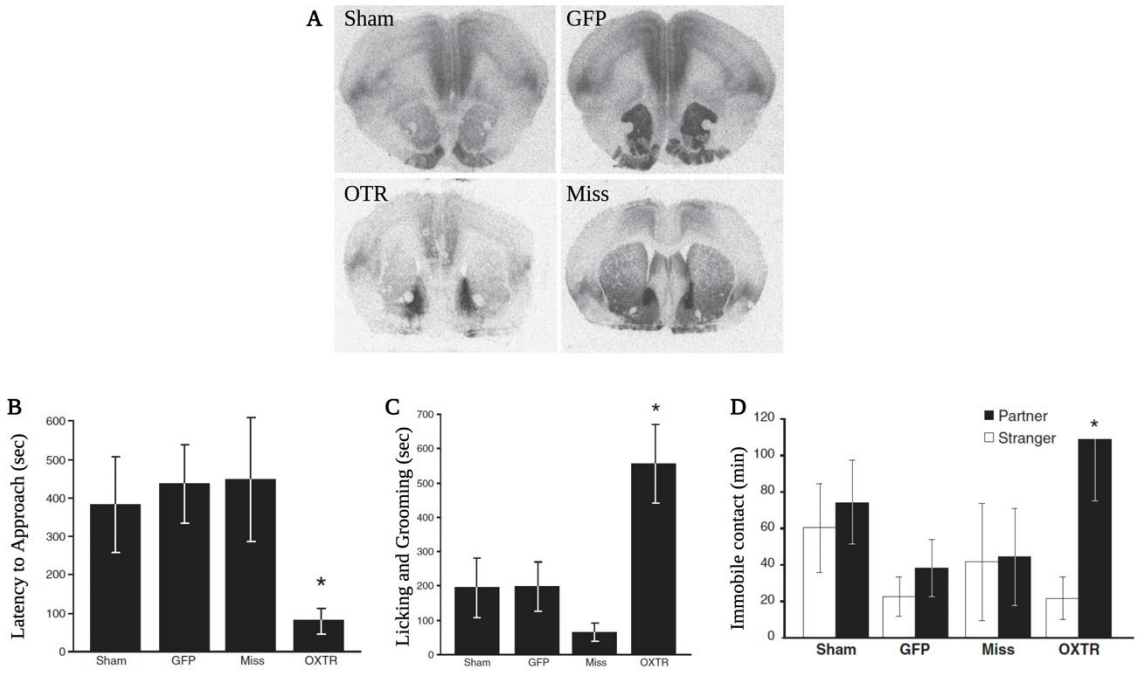

Figure 1.3. Overexpression of OTR facilitates alloparental behavior and partner preference in female prairie voles. A. Autoradiography shows the OXTR binding density in Sham, GFP, OTR, and Miss groups. The control group, "Sham," received no injection of AVV-OTR. The "GFP" control group received bilateral accumbal infusions of a virus expressing the GFP gene. The OXTR-expressing virus was bilaterally injected into the nucleus accumbens of the experimental group "OXTR." The other control group, "Miss," received bilateral injections outside the nucleus accumbens. B. The latency to approach pups in all four groups. C. Time spent licking and grooming pups. D. Time spent in immobile side-by-side contact with a partner or stranger after a cumulative 18 h cohabitation period. (Adapted from Keebaugh et al., 2011)

Conversely, taking advantage of this viral technique to overexpress the OTRs within the accumbens via viral-mediated gene transfer also facilitates the formation of partner preference in the prairie voles (Figure 1.3) (Keebaugh and Young, 2011). Related to the individual genetic variation of the OTRs in the accumbens, voles that overly express OTR show a significant preference for the partners compared to voles will low expression of them (King et al., 2016). In slice preparations, voles that had social experience through pair bonding significantly increased

the amplitude of the excitatory postsynaptic current and potential in the nucleus compared to virgin animals, which had no social encounter

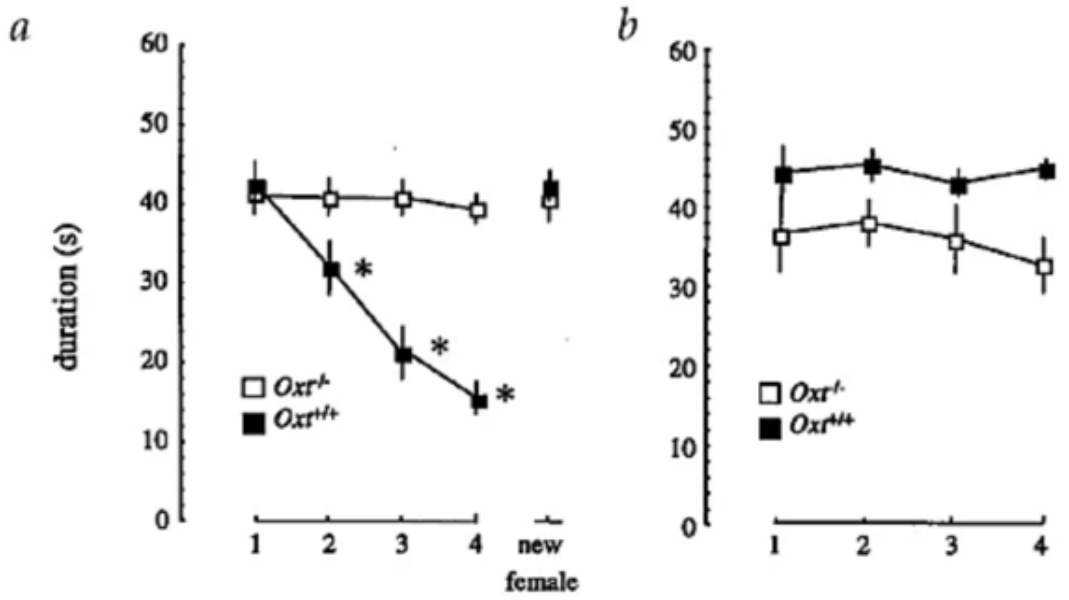

Figure 1.4. OT knock-out (OTKO) mice fail to display social recognition despite apparently normal olfactory and spatial learning abilities. A. Male mice were allowed to investigate the same ovariectomized (OVX) female during each of four successive 1-min trials. B. Mice investigated different OVX stimulus females in each repeated trial. (Adapted from Ferguson et al., 2000)

1.7 Influence of the Oxytocin System in the Social Brain Network

The OT system (OT and OTRs) are not only associated with the accumbens regarding social behavior. We have also learned much about their roles in social recognition and memory from other species, like mice and rats. In mutant mice, where the oxytocin gene has been knocked out, the mice fail to remember their social interactions with a conspecific animal that they were exposed to as compared to the wild-type animals (Figure 1.4) (Ferguson et al., 2000; MacBeth et al., 2009). The OT knockout mice spent approximately equal time investigating mice they interacted with in four sessions. On the contrary, the wild types spent lesser time on each subsequent session, which is the typical behavior of mice in exploring familiar individuals. The

lack of social recognition and memory was not due to the mice's inability to smell, recognize objects or have spatial memory, but it was a result of the OT being necessary for such a task. In the same studies, when OT was administered via acute intraventricular infusion to mutant mice, social memory was rescued, i.e., the mice spent lesser time in subsequent trials after exposure to the stimulus mice. However, an injection of OTA inhibited the social memory of the wild types but not the mutant mice. In a subsequent study, when OT was injected before an initial encounter with a stimulus animal, the mutant mice were likely to recognize the animal versus if the injection was given after the first social exposure (Figure 1.5) (Ferguson et al., 2001)

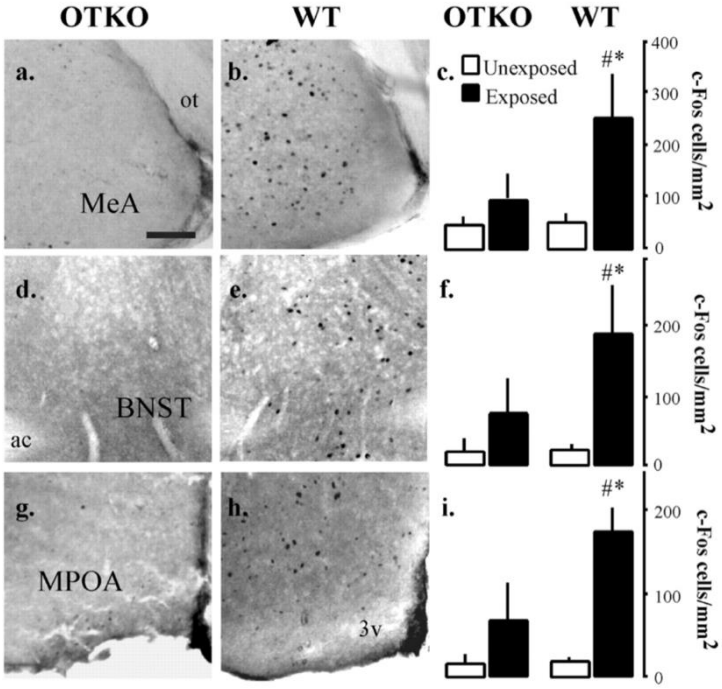

Figure 1.5. Significant induction of Fos-IR in wild type with intact OTRs. Male mice were considered Exposed if they had a social encounter with an ovariectomized female for 90 sec. Otherwise, they were deemed unexposed if they were not provided with a social experience. Photomicrographs showing c-Fos-immunoreactive cells after a social encounter in OTKO (a, d, g) and WT (b, e, h) males in the medial amygdala (MeA; a, b), the bed nucleus of the stria terminalis (BNST; d, e), and the medial preoptic area (MPOA; g, h). Measurement of the number of c-Fos cells per square millimeter in those brains, an indication of neural activation (c, f, i). (Adapted from Ferguson et al., 2001)

Further studies have narrowed down to specific brain regions to how the OT system modulates social recognition and memory. For example, as shown in experiments by Popik and van Ree, 1991, the infusion of OT in the medial preoptic area promoted the social recognition of adults of stimulus juvenile rats, where the resident rats spent less time on repeated exposure to the same juvenile than when they received a saline placebo (Popik and van Ree, 1991). Similarly, studies that have looked at early gene c-Fos, an immediate protein marker indicating a neural response, in the medial amygdala, the bed nucleus of the stria terminalis, and the medial preoptic area showed significant induction of Fos-IR in wild types than mutant OT knockout mice when they are repeatedly exposed to a stimulus animal (Ferguson et al., 2001). In addition, site-specific infusion of OT in the medial amygdala rescues the social recognition in mutant mice, and in contrast, injection of OTA into the same area of wild types inhibits the recognition.

Adding to growing knowledge about OT in the social brain network, using channelrhodopsin2, a light-activatable opsin that leads to excitation, to optogenetically stimulate the PVN in mice caused a significant increase in the social memory of the stimulus animals compared to a control that did not receive the same optogenetic stimulation (Figure 1.6A) (Oettl et al., 2016). And for other brain areas of interest like the anterior olfactory nucleus (AON), using a slice preparation to determine their role, when a selective OT agonist, TGOT, is applied or its OT fibers are ontogenetically activated, there is an increase in the firing activity of the AON cells, as captured by the high-frequency of both the excitatory postsynaptic current in AON and the inhibitory postsynaptic current in the main olfactory bulb (MOB), which receives projections from the AON (Figure 1.6B-C) (Oettl et al., 2016). This activation of OTR in AON is thought to modulate the firing activity of MOB cells by suppressing background firing activity and increasing the peak firing responses to odors.

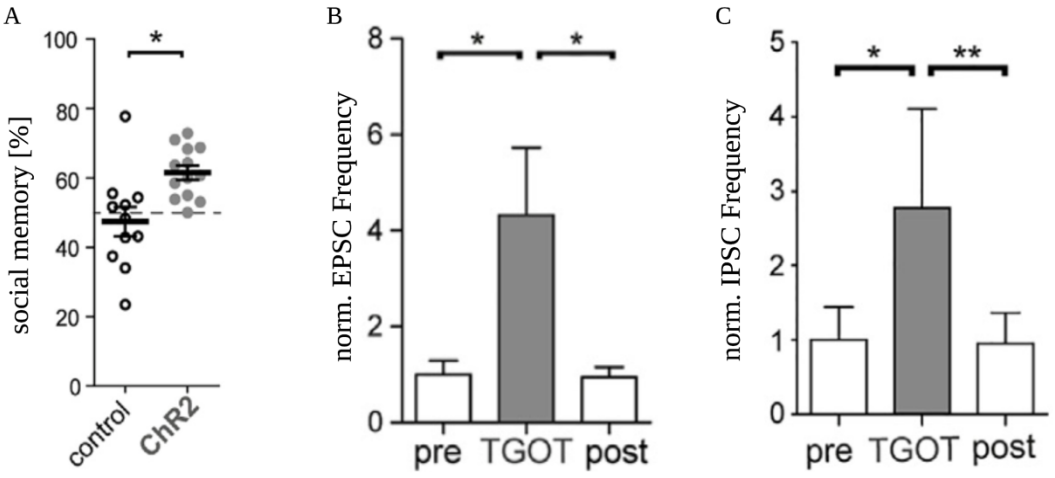

Figure 1.6. Oxytocin enhances social recognition by modulating the olfactory system. Adult female rats were exposed for 5 min to a same-sex juvenile rat (sample phase). After returning to the home cage for 120 min, the adult rat was re-exposed to the previous and, at the same time, to a novel same-sex juvenile for 3 min (recognition phase). A. Social recognition memory is expressed as the percentage of time the test animal spent exploring the novel social partner over the total time exploring both same-sex interaction partners. B. TGOT-induced normalized excitatory postsynaptic currents (sEPSC) rate in fast-spiking neurons in the AON. C. TGOT-induced normalized inhibitory postsynaptic currents (sIPSC) in mitral cells in the MOB. (Adapted from Oettl et al., 2016)

The OT system influences cognitive and memory centers like the prefrontal cortex (PFC) and hippocampus. In the PFC, an area associated with the brain's executive functions and goal-directed behavior, when the OTR expressing pyramidal-like neurons in the PFC are activated, they inhibit social recognition in mice, making them spend considerably equal time with novel and familiar animals (Tan et al., 2019). Likewise, looking at the hippocampus, the OTRs are expressed in the dentate gyrus, CA1, CA2, and CA3 cells. When the OTRs expressing neurons in the hippocampus of mice are blocked, the animals cannot form a social memory of their encounters (Raam et al., 2017). However, when TGOT is applied to slice preparation of the hippocampus, it increases the probability of evoked postsynaptic firing while simultaneously reducing the baseline activity of CA1 pyramidal cells (Owen et al., 2013).

1.8 Arginine Vasopressin

The OT system does not work by itself to modulate social behavior during pair bonding but has an interplay with other systems such as the arginine vasopressin (AVP), dopamine (DA), serotonin (5-HT), and opioids. AVP is a nine-amino acid (Cys-Tyr-Phe-Gln-Asn-Cys-Pro-Arg-Gly-NH2) that shares a similar protein structure to OT except at the third and eighth positions. AVP is thought to have evolved some few million years before oxytocin from their ancestral precursor vasotocin. It is also synthesized in the PVN and SON of the hypothalamus and released into the brain and body along similar pathways to OT (Barberis and Tribollet, 1996; Caldwell and Young, 2006). Unlike OT, AVP has three G protein-coupled receptors, V1aR, V1bR, and V2R. However, studies have shown that there is cross-talk between AVP and OTs: AVP can bind to OTRs and its three receptors, while OT has an affinity for its receptor, OTR, V1aR, and V1bR (Kimura et al., 1994; Chini et al., 1995; Hawtin et al., 2000; Song et al., 2014). Therefore, it is no doubt that AVP and its receptors have been implicated in facilitating pair bonding in voles.

An ICV infusion of AVP in male prairie voles induces partner preference, with the animals spending more time huddling with their partners than with strangers (Winslow et al., 1993; Cho et al., 1999b). Conversely, when antagonists are administered to the V1aRs in the ventral pallidum and the lateral septum, the male prairie voles do not prefer their partners over a stranger (Liu et al., 2001; Lim and Young, 2004). Furthermore, using viral-vector-mediated techniques, like RNA interference, to knock down the V1aRs produces similar results of voles not showing any preference (Barrett et al., 2013).

However, unlike the OT system, which is thought to promote affiliative behaviors, the AVP system is associated with aggressive behaviors like fighting and defense (Ferris et al., 1997;

Veenema et al., 2007; Veenema and Neumann, 2008). And these aggressive behaviors are viewed as a mate-guarding approach adopted by prairie voles to protect their partners, offspring, and territory against intruders and as a way to maintain their social bonds (Walum and Young, 2018).

1.9 Dopamine

In addition to the OT and AVP systems, DA helps facilitate the pair bond formation between prairie voles. The nucleus accumbens, which expresses receptors for dopamine, receives dopaminergic neurons from the ventral tegmental area. Studies have shown that when DA agonists are also peripherally administered, male and female prairie voles without mating with their opposite-sex conspecific animal show a preference for the partners. Conversely, an infusion of nonspecific DA antagonists peripherally into the body blocks mating-induced partner preference in both male and female prairie voles (Wang et al., 1999; Aragona et al., 2003). In addition, a site-specific injection of the DA antagonist into the accumbens blocks mating-induced partner preference.

It is known that the nucleus accumbens has two types of DA receptors, D1 and D2 receptors. Infusion of selective D2-like receptor (but not D1-like receptor) antagonist inhibits mating-induced partner preference in both male and female prairie voles (Wang et al., 1999; Liu and Wang, 2003). On the contract, injecting a D2-like receptor (but not a D1-like receptor) agonists without mating facilitates partner preference. It is an indication that D2-like receptors are necessary for the formation of a pair bond.

The D1-like receptors, on the other hand, are involved in the maintenance of the pair bonds. After the voles have been paired for a while (at least more than 48 hours), D1-like (but

not D2-like) receptors are expressed more in the nucleus accumbens. Such that blockade of the D1-like (but not D2-like) receptors within the nucleus accumbens abolish the aggressive behavior towards strangers (Aragona et al., 2006).

1.10 Opioids

The activity of DA is conjoined with that of opioids. The neurons that express D2-like receptors contain enkephalin, an endogenous ligand for μ-opioid receptors that mediate motivation and positive hedonics (Peciña and Berridge, 2005), whereas neurons containing dynorphin, the endogenous ligand for κ-opioid receptors that mediates aversion and negative affect, express D1-like receptors (Stevens Negus, 2011). Peripheral administration of μ-opioid receptor antagonists prevents bond formation (Burkett et al., 2011). Similarly, site-specific injection of μ-opioid receptor antagonists into the caudate putamen and NAc shell (but not NAc core) blocks partner preference (Burkett et al., 2011; Resendez et al., 2013).

Conversely, peripherally and site-specific administration of κ-opioid receptor antagonists significantly decreases selective aggression in pair-bonded male prairie voles toward an intruder (Resendez et al., 2012). However, this blockade of the κ-opioid receptor does not affect their affiliative behaviors.

The current hypothesis in the field is that both D1-like and κ-opioid receptors interact to mediate selective aggression. Therefore, if either one or both receptors are activated, voles are likely to engage in an attacking behavior (Resendez et al., 2016).

1.11 Endocannabinoids

Recent research from our lab has shed light on the interaction between endocannabinoids (eCBs) and the OT system in pair-bonded voles. The eCBs are thought to act as retrograde regulators of synaptic transmission between cells (Castillo et al., 2012). Currently, there are two known types of eCB receptors, CB1 and CB2 receptors, and among these eCB receptors, the CB1 has been implicated in pair bonding. When CB1 receptors are blocked with an antagonist in slice preparations of pair-bonded females (but not virgin females), a TGOT-induced excitatory postsynaptic potentiation is inhibited, possibly indicating the eCB system is necessary for OT activation (Borie et al., 2021). Conversely, when a CB1 agonist is applied, there is an increase in the excitatory postsynaptic potentiation in the cells, similar to if TGOT was applied to those cells.

1.12 The social salience hypothesis

Given the knowledge that we have garnered from the studies on the influence of the OT system in regulating social behaviors in prairie voles, mice, rats, and primates, a leading question that arises is how does the OT system work within the social brain network to facilitate the formation of a pair bond between animals? One leading hypothesis in the field is the social salience hypothesis.

The social salience hypothesis postulates that OT is released from the PVN into the social brain centers during social interaction to make the social information salient. This salience is achieved through recognizing an individual's pleasurable and rewarding encounter with its conspecific and developing a memory about the individual's identity. The process is

accompanied by a plasticity that occurs in brain regions such that a subsequent exposure with the individual, even after a brief separation, evokes the rewarding effect (Figure 1.7).

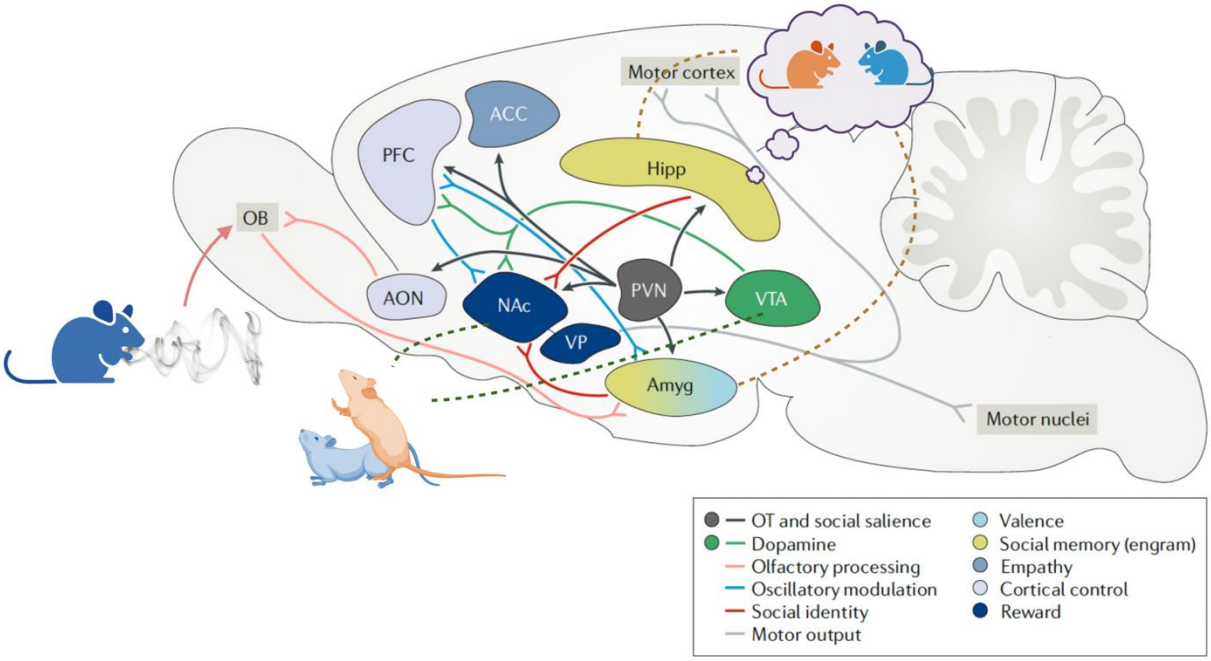

Figure 1.7. The oxytocin system and other neurochemicals in the social brain network. During social interaction, odorant cues released from a soon-to-be partner are processed in the main olfactory bulb (MOB). The PVN releases OT to bind the receptors in the anterior olfactory nucleus (AON) to activate the excitatory neurons, which activate MOB's inhibitory neurons. The activation of MOB by the OT fibers of the AON causes it to suppress the spontaneous firing activity, which might be responding to random odorants, and amplify the social cue that is received from the partner. The salient sensory information is transferred along one of several possible pathways to the amygdala, which receives projections from MOB and accessory olfactory bulb. OT acts in the medial amygdala (MeA) and basolateral amygdala (BLA) to facilitate olfactory learning and memory. In addition, a social engram of neurons within the hippocampus (Hipp) is activated to retain information about the partner. Concurrently, rewarding experiences such as mating during social interaction activate the VTA to release dopamine into the nucleus accumbens (NAc) and prefrontal cortex (PFC). The connection between PFC and NAc under the regulation of OT guides the animal's behaviors in the social context. (Adapted from Walum and Young, 2018)

1.12.1 Social Sensory Stimulus Transmission

To put the social salience in a better context of the social brain, given the knowledge gained so far, when an animal, for example, a prairie vole, is paired with a conspecific, the vole receives visual, auditory, and odorant cues from the other individual. Although the visual, auditory, and somatosensory cues have not been extensively explored regarding the social salience model for bond formation, much is known about the sensory information via olfaction.

The odorant cues from the individual soon-to-be partner are processed in the main olfactory bulb (MOB), which has few OT terminals and receptors (Vaccari et al., 1998). The MOB receives projections from an OTR-dense anterior olfactory nucleus (AON) (Freund-Mercier et al., 1987), which directly receives OT neurons from the PVN (Knobloch et al., 2012). According to the social salience model, the PVN releases OT to bind to the receptors in AON to activate the excitatory neurons, which then activates MOB's inhibitory neurons (Oettl et al., 2016). The activation of MOB by the OT fibers of the AON causes it to suppress the spontaneous firing activity, which might be responding to random odorants, and amplify the social cue that is received from the partner. This manner of OTR recruitment shows the OT system's role in increasing the signal-to-noise ratio, a component of the salience hypothesis.

The salient sensory information is then transferred along one of several possible pathways to the amygdala, which receives projections from MOB and the accessory olfactory bulb. In the amygdala, specifically in the medial amygdala, MeA, the OT system facilitates encoding social information about the partner's identity. Studies have shown that when the OTRs in MeA are inhibited with antagonists, mice are unable to recognize a familiar animal, and inversely when OT is infused into the MeA of OT knockout mice, the social recognition is rescued (Ferguson et al., 2000, 2001).

Another amygdala area implicated in the circuitry for the social salience model is the basolateral amygdala (BLA), which receives projections from the OT expressing glutamatergic neurons of the prefrontal cortex (PFC) (Tan et al., 2019). It is thought that OT enables social recognition by coordinating the temporal and spatial coupling of social stimuli between the PFC, BLA, and hippocampus. Hence, any dysregulation that disrupts the synchronization within this circuitry leads to an impairment of the social memory of a partner. As evidenced by a study by Tan and colleagues (Tan et al., 2019), when they optogenetically activated OTR expressing pyramidal-like PFC neurons, either at the cell body or the axon terminals to BLA, they impaired the social recognition of familiar mice.

1.12.2 Social Recognition and Memory

As part of the bond formation, the animals must recognize their partners so that they do not waste time trying to refamiliarize themselves. In addition to the recognition, the animals must create a memory (social) of their encounters with their partner since, during their interactions, they could have rewarding experiences such as mating (Mermelstein and Becker, 1995; Becker et al., 2001; Ross et al., 2009). To form a social memory of the partner, the brain engages the hippocampus, an area historically associated with memory formation (Duvernoy, 1988). The hippocampus receives projection from the PVN and expresses OTRs in both the dorsal and ventral parts. The hippocampus also sends projections to the nucleus accumbens via ventral CA1 neurons. Inhibition of these projections prevents the animals from remembering the encounters with their conspecific partner (Okuyama et al., 2016). Therefore, during a social interaction with a partner, the information about the partner is encoded in the neurons in the hippocampus. However, this encoding is not on all the neurons; instead, a subset of them, which is referred to as an engram. Such that the reactivation of this engram of cells leads to recall of the memory

about the partner. In addition to having a social memory engram, the activation of OTR-expressing neurons leads to an enhanced signal-to-noise ratio by increasing the probability of firing activity and reducing spontaneous activity (Owen et al., 2013).

1.12.3 Social Gating

With the animals having encoded a social recognition and memory of their partners, they would have to create a positive, rewarding association with the behaviors such as mating, huddling, and allogrooming they shared with them. This social information is transferred to the nucleus accumbens, an area thought to promote the likelihood and vigor of behaviors to achieve motivationally goals either with rewarding or avoidance of aversive consequences (Floresco, 2015). The nucleus accumbens receives cortical and limbic projections from the prefrontal cortex, amygdala, hippocampus, and dopaminergic inputs from the ventral tegmental area (VTA) (Floresco et al., 1997, 1999, 2008). One can view the accumbens as a servant to many masters, and one of its requirements is to gate social behavior. As seen in other brain areas expressing OTRs, the nucleus accumbens receives many projections from the PVN. The OT released by the PVN binds to the high-concentration OTRs in accumbens and, in so doing, modulates the social behavior of animals. The interplay of the OT system with other neurochemical systems like AVP and DA facilitates the performance of prosocial and affiliative behaviors in a manner that increases the signal-to-noise ratio of social cues received from a conspecific partner.

In summary, the social salience hypothesis presents a model through which we observe the OT increasing the signal of social cues between animals and suppressing the noise of later signals from other animals or objects so that a pair bond is established and maintained.

1.13 Concluding Remarks

It may look like we have a clear picture of the OT system's role in forming pair bonds, especially in prairie voles. However, a recent publication by Berendzen and colleagues paints a different view. They showed that by using advanced viral techniques, like CRISPR-Cas9, to knock out the OTR, prairie voles exhibit a strong preference for a partner (Berendzen et al., 2022). The mutant voles, with OTR, knocked out globally both centrally and peripherally, are capable of forming pair bonds, i.e., they spend a significant time in side-by-side contact with their partner compared to strangers when assayed with the partner preference paradigm. As you will read in chapter 4 of this manuscript, we also replicated these findings in our experiments.

Another aspect of pair bond formation that has yet to be explored is the behavioral dynamics of forming bonds. Most studies discussed in this chapter only measured the voles' behavior after forming a bond. They did not quantify the social behaviors of the animals as they interacted with one another. In chapter 2, we will consider how to measure animal social behavior. Then in chapter 3, we will discuss the advancement we have made to improve the detailed tracking of social behavior to enable the investigation of the behavioral dynamics of forming pair bonds. Chapter 4 investigates how knocking out OTRs alters the voles' social behavior during pair bond formation. Finally, we will end with a chapter on future directions and possible experiments to further our understanding of animals' social behavior.

Chapter 2. THE ENIGMA OF QUANTIFYING SOCIAL BEHAVIOR

2.1 Introduction

In this chapter, I will present our perspective on measuring animal social behaviors. First, I will explain what has been done to measure behavior in a general context, from individual to collective behaviors. Second, I will talk about the gap in measuring social behavior and the challenges faced in trying to do so. Third, I will then present our framework for addressing this gap and what has been done to measure behaviors in social contexts. Finally, I will conclude with why measuring social behavior accurately and precisely is important.

2.2 Background

In the mid-twentieth century, when Nikolaas Tinbergen and Konrad Lorenz presented their viewpoint of measuring animal behavior (Tinbergen, 1952, 1963; Lorenz, 1966; Hess et al., 1982), it was contrary to the popular approach adopted by Skinner and other behaviorists (Jones and Skinner, 1939), which focused on measuring a response to stimulus in learned behavior. For example, instead of quantifying the number of times a rat pressed a lever for food in a controlled experimental setup, Tinbergen and Lorenz were more interested in measuring the innate behavior of the animal in a naturalistic setting. For example, the gaping beak reaction of young thrushes to the presence of food from their mother or two male sticklebacks fighting during nuptials (Tinbergen, 1952). To this end, they had one central question in mind, and that was why animals behave as they do.

To answer this trivial but complex question, one needs to understand the internal and external causes of the behavior and, to an extent, the ontogeny of the behavior. Beyond that, the appropriate language is required to describe the set of actions that the animal performed to

execute the behavior. The language can take the form of descriptive words indicating every sequence of behavioral steps; for example, in the gaping reaction of young thrushes, the young birds open their beaks wide when they observe their parent tower over them with food. However, this language could be more precise if some metrics were associated with it, i.e., the distance and height of the parent bird need to be from their young to elicit the gaping reaction from the chicks.

The goal of attaining such quantitative precision and details in describing innate behavior gave rise to the computational ethology field. The field of computational ethology relies on applying mathematics and physics to quantify the innate behavior of animals in their naturalistic environments. In this field, two areas that have greatly benefited from the progress made are the studies of animals' individualistic and collective behaviors. In regard to collective behaviors, we are referring to behaviors of large groups of animals, e.g., a swarm of bees, and a flock of birds.

In individualistic behaviors, i.e., the sequences and repertoire of behaviors performed by a single animal, there has been substantial progress in understanding the movement dynamics of the animal (Richard and Dawkins, 1973; Stephens et al., 2008; Branson et al., 2009; Berman et al., 2014; Wiltschko et al., 2015). Several nicely written reviews cover the progress of quantifying single animal behaviors (Anderson and Perona, 2014; Brown and De Bivort, 2018; Datta et al., 2019; Pereira et al., 2020). For example, work by Stephens and colleagues showed that the motion of *C. elegans* can be reduced to a set of low-dimensional representations sufficient to describe the animal's behavior (Stephens et al., 2008). By recording the movement of the *C. elegans* under a microscope and assuming several arc lengths annotated along the body of the animal were descriptive of their posture, they applied a computational approach (principal component analysis) to decompose the posture into four modes that represented the forward and backward motion of the nematode, its turning behavior, and Omega configuration, and the shape

of the head and tail region of the worm (Figure 2.1). Given the low-dimensional representation, they found equations that described some animal motions and were able to quantitatively predict the response of the animals when they altered the temperature of their environment.

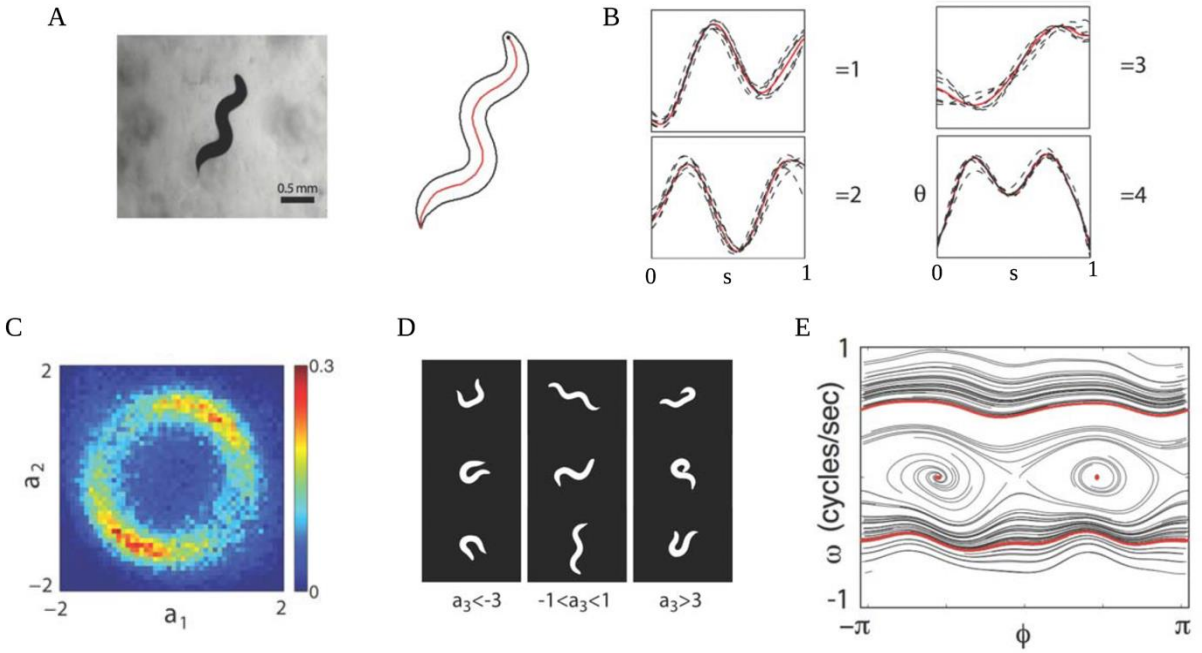

Figure 2.1. Low-dimensional representation of the behavioral dynamics of C. elegans. A. Image of a *C. elegans* captured under microscopy and the tracking of a curve along the center of the body. B. Dimensional decomposition of the posture into four eigenmodes (with their eigenvectors - referred to as eigenworms) that capture 95% of the shape variance of the animal. The population-mean eigenvectors (red) are highly reproducible across individual worms (black). C. The probability distribution of the first two mode amplitudes, r(a1, a2), shows a ring of nearly constant amplitude. D. At different positive and negative amplitudes for the third mode, the animal assumes different body postures with bends in the dorsal and ventral directions. E. Trajectories in the deterministic dynamics. A selection of early-time trajectories is shown in black. At late times these same trajectories collapse to one of four attractors (red): forward and backward crawling and two pause states. (Adapted from Stephens et al., 2008)

Like quantifying individual behavior, theoretical and computational models have spurred an understanding of collective animal behaviors. Theoretical models like the agent-based model have been developed to define a set of rules to govern the behavioral dynamics of animals in large groups (Aoki, 1980; Morgan and Okubo, 1981; Reynolds, 1987; Couzin and Krause, 2003).

These rules consider the agent's direction (an individual animal within the group), the alignment of the agent relative to other individuals, and the force factor in determining the attraction and repulsion between the agents. For example, Couzin and colleagues showed that by slightly modifying the underlying rules that govern the dynamics of interactions among the animals, they could explain different collective behavioral states of animals (Couzin and Krause, 2003). By altering the distances an agent maintains to remain in certain zones, such as the zones of attraction, orientation, and repulsion relative to other individuals (Figure 2.2A), they could influence the group polarization and group angular momentum (Figure 2.2B). A change in the group polarization and momentum meant the collective behaviors transitioned from a swarm-like state to a highly parallelized state (Figure 2.2C). Hence, when animals exhibited attraction and repulsion behaviors but low parallel alignment with their neighbors and low momentum, they exhibited swarm-like behaviors, as seen in mosquitoes. And as the behavioral interactions build up to have a high degree of alignment and maintain a strong force of attraction and repulsion between the animals, they show a dynamic parallel group like the aggregation of bird flocks and a school of fish.

Despite the wealth of understanding gained from both ends of the spectrum of quantifying individualistic and collective behaviors, there is a considerable gap in knowledge regarding measuring social behavior in two to three animals. We do not have the same precise and detailed theoretical and computational models to explain the social interactions between two or three animals.

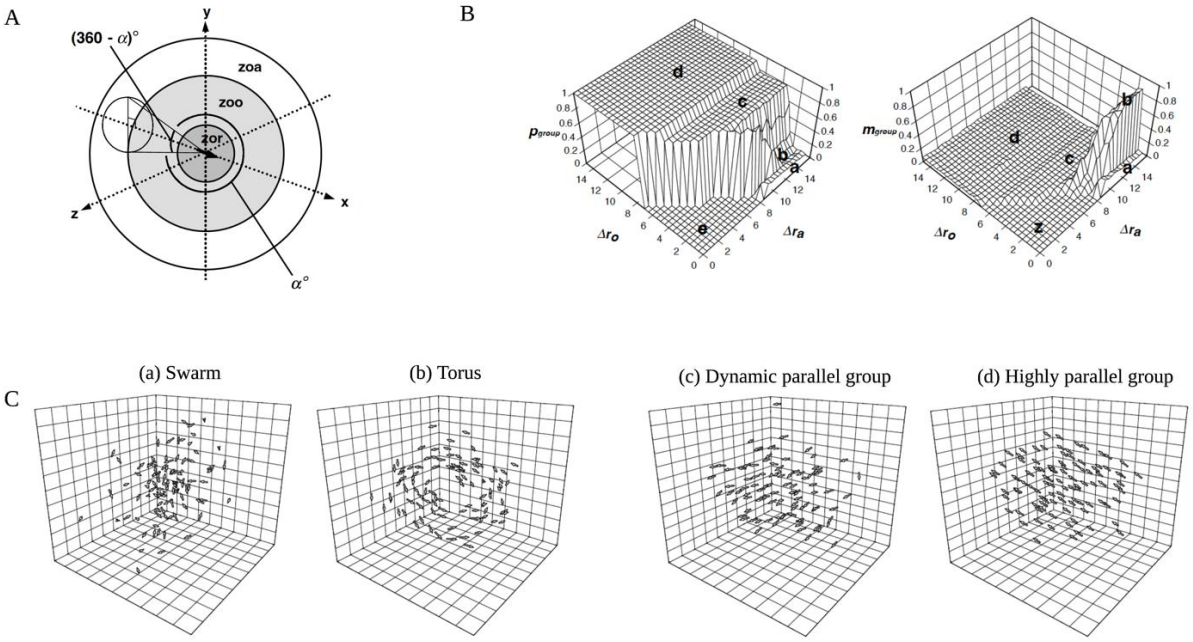

Figure 2.2. Dynamics of collective behaviors in animals. A. A representation of an individual in the model centered at the origin: zor = zone of repulsion, zoo = zone of orientation, zoa = zone of attraction. The possible ‘‘blind volume’’ behind an individual is also shown. A = field of perception. B. A plot of the group polarization p_{group} (left) and angular momentum m_{group} (right) as a function of changes in the size of the zone of orientation Δro and zone of attraction Δra: The areas denoted as (a–d) correspond to the area of parameter space in which the collective behaviors (C), respectively, are found. Area (e) corresponds to the region in parameter space, where groups have a greater than 50% chance of fragmenting. (C) The collective behaviors exhibited by the model: (a) swarm, (b) torus, (c) dynamic parallel group, (d) highly parallel group. (Adapted from Couzin and Krause, 2003)

2.3 The question of social behavior

The limitation of not having the same level of a detailed mathematical framework for social interaction between two or three animals might be due to being unable to clearly distinguish the animals' behaviors. For example, when an animal approaches another and is in face-to-face contact for a short moment with them, is the behavior classified as an approach to oral investigation or just an approach (see a video sample of the described behavior in prairie voles - https://github.com/senakoko/Thesis_Videos/tree/main/Chapter_2_Videos)? What if a few

seconds after the animal that approached attacks the other, is the entire bout considered an approach-to-attack, or it needs to be broken down into sub-modules describing every sequence? Alternatively, the difficulty of developing detailed metrics to quantify social behavior might primarily lie in its definition. Do we take the idea that when two or three animals are performing a set of behaviors within the presence of each other as a social behavior? Or do the animals need to interact with one another before we say they are engaged in social behavior? Or does the context of being a social setting dictate that any sequence of animal behaviors should be considered social behavior? Where and when does one behavior start and stop, and when does another follow during social interactions? One quickly begins to appreciate how difficult it is to define 'social behavior' for a few animals. In the rest of this chapter, we present our framework for measuring social behavior.

2.4 Social Behavior

To provide this computational and mathematical model to measure social behavior, we have first to answer the question of what social behavior is. Taking on a simplistic view, we define social behavior as any movement that animals perform that is either affected by or affects another individual(s). These behaviors can have a noticeable direct cause-response effect, such as fighting or mating between animals, or a subtle form, such as the posture and orientation of the animals before engaging in a fight. Even with this simplistic definition, several questions arise, and an example is at what time scale are we considering social behavior to happen? The time spent performing the social behavior can range from a quick thrust forward to attack another individual, which might indicate a short time scale of seconds, to longer time scales, for example, a parental care behavior of feeding the young.

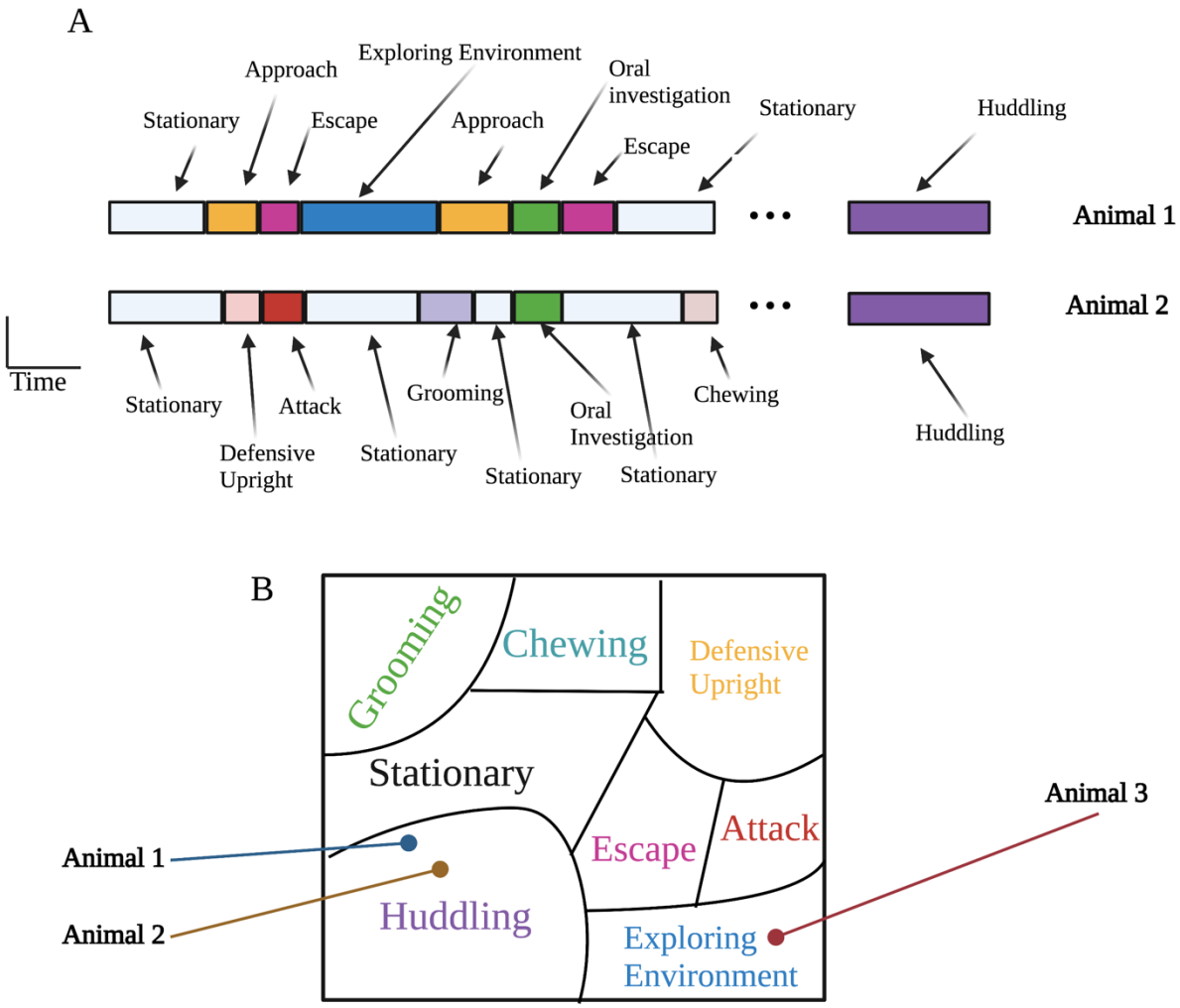

Figure 2.3. A schematic of the representation of animals' behavioral repertoire. A. A hypothetical ethogram that shows a moment-by-moment classification of each animal's behavior. B. A theoretical behavioral space with the behaviors of the animals clustered together based on their stereotypy.

2.5 Framework for measuring social behavior

To quantify the social behavior of animals, we propose a framework that focuses on measuring the animals' moment-by-moment social behaviors (i.e., an ethogram) as they interact with each other (Figure 2.3A). In our framework, we will adopt the short time scale of social behavior from milliseconds to minutes to allow us to observe the gradual temporal evolution of the animal's behavior, marked with different frequencies. To this end, we can capture when a

behavior initially occurs, how often it occurs, and when it gradually tapers off or stop to happen. In addition, given that we would have an ethogram of both animals, we can consider synchronization among the individuals, possibly due to imitations or just spontaneous activities that happen to be performed simultaneously.

In addition to the ethogram framework, we propose creating a representation that captures the animals' stereotyped and non-stereotyped behavioral patterns (Figure 2.3B). Therefore, we build a two- or three-dimensional behavioral space where frequently occurring (stereotyped) behaviors are clustered in their own regions, and non-commonly observed (non-stereotyped) behaviors are grouped by themselves. This idea of creating a behavioral space that maps the social behavior of the animals would allow us to identify behaviors that are either unique to each individual or shared among the group. As we shall see later in this chapter, we can quantify behavioral transitions based on this map.

2.6 Developing a pipeline for the framework

To measure the social behavior of the animals, we have first to record the social interactions, track their postures, then classify and analyze their behaviors. The first step of recording social behaviors is critical in determining the output of the behavioral measure. It is because the recording medium can take several modes, from videography to microphone to movement detectors like accelerometers and IR beam-break sensors. Each medium for recording the behavior would have its unique advantage; for example, microphones are ideal for capturing sound-generated behaviors like vocalizations. For example, an adult songbird teaching a juvenile bird how to sing, a mating call between frogs and meerkats making sounds to alert its gang of a possible intruder are social behaviors. IR beam-break sensors are suitable for determining when

an animal crosses a threshold to interact with another animal. The number of times the beam is broken can be considered a measure of the interest level that the animal shows toward the other.

2.6.1 Videography

However, in our framework for measuring social behavior, we will limit our recording mode principally to videography, although measured acoustic information can be later embedded into the framework to expand the context of the behavior. The video recording provides information about the movement dynamics (i.e., kinematics) of the animals and their environment, which not be captured by the microphone and other recording devices. In addition, it offers a high spatiotemporal resolution of the animals' behaviors.

Videography has benefited considerably from the advancements in developing high-speed and high-resolution recording cameras. There are designs of 2-dimensional cameras that have a resolution and frame rates capable of capturing the detailed, subtle, and fast-moving body parts of an animal that define their behavior. For example, some cameras can capture the fast wing flapping of birds or insects and a Sierra Nevada salamander shooting out its tongue in less than 20 milliseconds to catch an insect (Deban and Richardson, 2011). In addition, some cameras can provide depth information to create a 3-dimensional (3D) resolution (Hong et al., 2015; Wiltschko et al., 2015) of the animals. Even with 2D cameras, 3D reconstructions of the animals can be generated based on how the cameras are positioned (Nath et al., 2019; Dunn et al., 2021; Marshall et al., 2021). We would refer the reader to extensive reviews on video recording in these references (Dell et al., 2014; Robie et al., 2017).

2.6.2 Tracking

After recording the social behaviors, the next step in the pipeline for the framework is to track the animals' positions and postures. The early technology in this field of animal tracking was centered around annotating their center of mass. These methods were computer vision and machine learning-based approaches used to track the position and posture of animals (Spink et al., 2001; Branson et al., 2009; Pérez-Escudero et al., 2014; Hong et al., 2015). However, over the last decade, owing to the advancement in deep learning knowledge, there has been an explosion of methods that have led to identifying multiple body points besides the centroid of the animal (Mathis et al., 2018; Graving et al., 2019; Pereira et al., 2019; Lauer et al., 2021). Researchers can simultaneously track multiple animals' noses, limbs, tails, and other body points. Not only are the postures tracked in the 2D, but there are also 3D annotations of the animals that can be labeled.

Despite highlighting the advances in methods to track the postures of multiple animals, there are still limitations that we would like to point out. The multi-animal tracking tools cannot maintain the animal's identities robustly and reliably throughout the entire recording. This issue is more prominent when the animals are near each other. The issue of swapping identities could be less of a problem if knowing the animal's identities was optional. However, in most cases knowing the identity is essential because it could provide insight into the temporal evolution of social behavior for a specific animal. For example, in an experiment involving male and female prairie voles during cohabitation to form social bonds, it is important to know their identities because there might be a sexual dimorphism regarding how they interact. For example, males might show more aggressive behaviors than females, which might be more defensive. In the next

chapter, I will delve more into the limitations of the multi-animal deep learning approaches and the solutions we have developed to resolve them.

2.7 Extracting ethograms

For this framework we have set up, we would assume that we have perfect 2D or 3D tracking with no swapping errors or mislabeled body points of the postures of the animals. With the perfectly tracked points, we can build a behavioral classifier to extract the behaviors performed by each animal. As with all classifiers, they need to be trained with a set of features and predefined behaviors. These features can be obtained from the animals' position, orientation, distance, and speed from the tracked body points. The identification of behaviors to train the classifier remains to be the challenging part. As discussed earlier, the precise labeling of the behavior seen can vary widely from observer to observer. Although to the animal, its intention of the behavior it desires to perform is known, scientists would never know it, but instead must impose a description based on their knowledge and expectation. To resolve this dilemma, we suggest the behavioral annotation be done by three individuals (although a larger number would be ideal but not feasible because of limited personnel to score behaviors in most laboratories). As suggested by the scorers, the consensus definition of behavior and its average start and stop times can be used in the classification. Given the features and defined behaviors, a machine learning classifier such as a support vector machine (SVM), adaptive boosting (AdaBoost), and random decision forest (TreeBagger) or a deep learning recurrent neural network can be trained to identify a moment-by-moment classification of the behaviors.

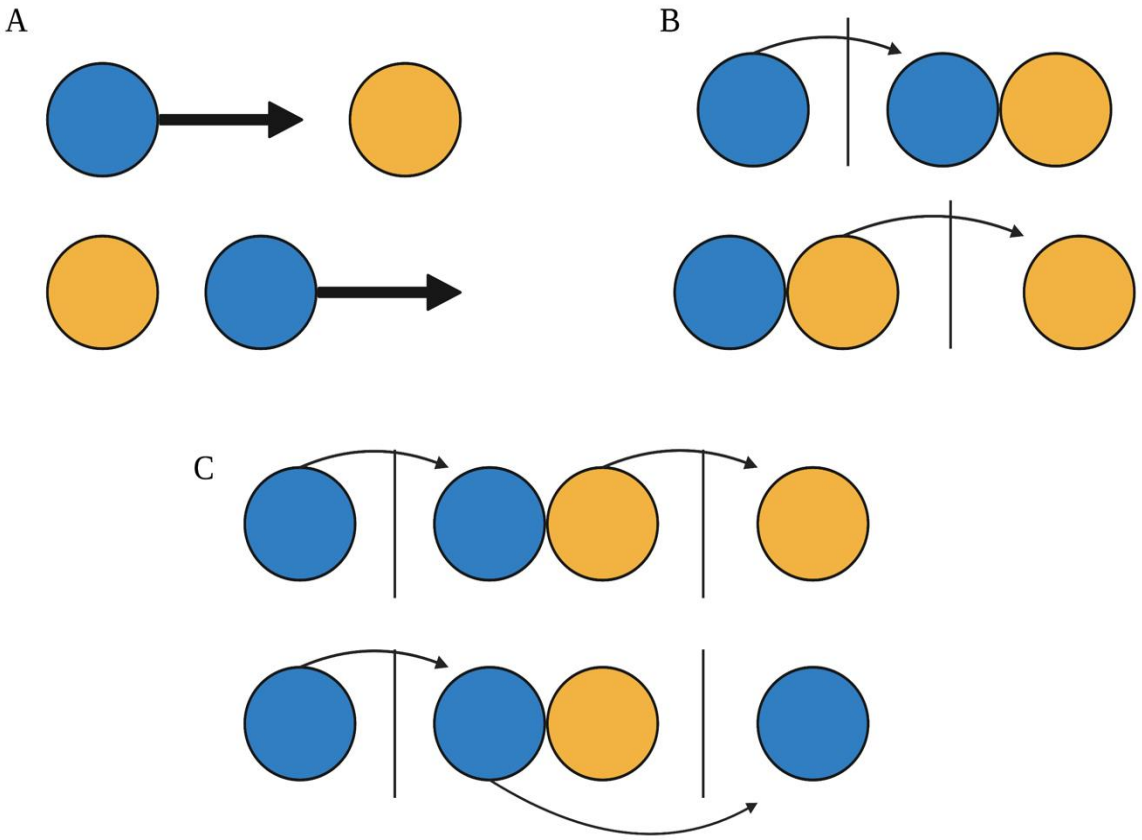

Figure 2.4. A schematic representation of grouping behaviors into orders for animals (a) and (b). A. Examples of a first-order grouping showing an individual (a) approaching another stationary animal (b) and an animal (a) moving away, either escaping or ordinary departure, from the other individual (b). B. A second-order grouping shows an animal (a) approaching another and then huddling with them (a) or the two animals huddling and one (b) departing. C. Examples of a third order where an individual (a) approaches another to probably orally or anogenitally investigate the other animal (b), where either animal (a) or (b) escapes. (Adapted from de Chaumont et al., 2012)

This ethogram of behavior provides a basis for understanding the spatiotemporal evolution of social behaviors among individuals. An approach that can be adopted is to group the behaviors into three event categories (de Chaumont et al., 2012). These groupings can reveal how behaviors emerge for a set of actions as the animals interact with one another. For example, A single continuous movement of an animal towards, away from, and following other individuals can be categorized as a first-order event (Figure 2.4A). This event is based on the

relative speed of movement and change in distance between the animals. When two first-order events are combined, for example, two individuals have side-by-side contact, and then one moves away to interact with an object or another animal, that can be considered a second-order event (Figure 2.4B). A third-order event can be extracted in the last categorization when two second-order events are temporally concatenated (Figure 2.4C). In this event, one animal goes to contact with another, both have a brief period of social interaction, either side-by-side contact, oral-oral interaction, or oral-genital, and one animal then escapes. From the temporal evolution, you can create a hierarchical structure of behavior transition. The hierarchical behavioral transition (to be discussed later in this chapter) would show the likelihood of certain behaviors occurring before or after others (de Chaumont et al., 2012).

2.8 Mapping behavior into a space

Although creating an ethogram of the moment-by-moment behavior through the prescribed approach presented above might capture the social behaviors of the animals, it is likely to be biased by the subjective classifications of the human annotators. Also, due to anthropomorphic expectations, subtle interactions might be overlooked. Hence, we propose mapping the postural dynamics of the animals into a space that maps their stereotyped behaviors. This theoretical framework gained initial precedence in single-animal behavioral quantification by mapping their movements into a representation that reveals their behavioral repertoire (Berman et al., 2014). In this approach, an unsupervised method (MotionMapper) creates a 2D probabilistic space of the stereotyped behaviors based on the animals' video data or tracked points (Figure 2.5).

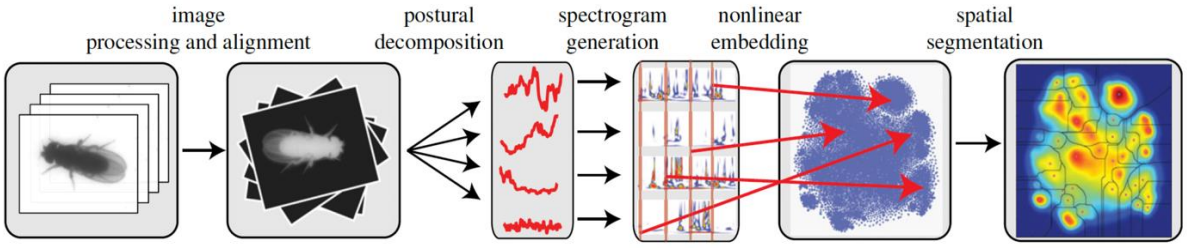

Figure 2.5. A pipeline for mapping behavior into a lower-dimensional representation. Images from a video of a behaving animal are rotationally and translationally aligned to be invariant. The image data is decomposed into a low-dimensional embedding. A wavelet transform is then applied to the decomposed postural data to generate a spectrogram. These spectrograms are used to construct spectral feature vectors that we embed into two dimensions using t-distributed stochastic neighbor embedding (t-SNE). Lastly, a watershed transform is applied to identify resolvable peaks associated with stereotyped behaviors in the distribution (Adapted from Berman et. al., 2014)

The MotionMapper algorithm takes the postural time series of the animal's movement as inputs to build the behavioral space. However, in the context of social behavior, certain choices that differ from those used in the original implementation for a single animal need to be made. Are the postural time series of each animal treated separately, or is a single postural time series that describes shared information between the animal used as the basis for mapping the social behavior? Either choice would have its advantage, where a separate postural time series provides a clear picture of each animal's posture that allows unique identification of an individual's behavior at any given time within the behavioral space. Alternatively, in using the shared postural time series, the redundancy in knowing each animal's posture is avoided because social behaviors should produce distinctive effects on the postures of the individuals to allow their identification. A third choice for the time series would be to have both individual and shared information about the poses of the animals. It will be an over-parameterization, but it ensures redundancy in the postural dynamics.

In either case, this postural time series that describes the body configuration of the animal remains a high-dimensional measurement, and so, similar to other approaches that can infer the behavior of animals by performing a postural decomposition (Stephens et al., 2008), MotionMapper performs a dimensionality reduction technique, like Principal Component Analysis (PCA), to reduce the postural data in a low-dimensional time series.

To extract the stereotyped behaviors but ensure that their dynamics naturally emerge for the reduced postural time series, MotioMapper performs a wavelet transformation on the data. This wavelet transformation creates a multi-scale time and frequency resolution allowing for the representation of the postural dynamics at different time scales. This idea of transforming the data from the time to frequency domain is critical to the concept of quantifying the stereotypy of behavior. It is because several different approaches could have been taken to extract the stereotyped behaviors (See (Berman, 2018) for extensive discussion on this topic).

An alternative approach to wavelet transformation is to fit a statistical model, like an Autoregressive Hidden Markov Model (AR-HMM) (as executed in the Motion Sequencing (MoSeq) approach), to the postural data (Wiltschko et al., 2015). This method extracts sub-second (200-400 milliseconds) motifs from the time series data. Although MoSeq pulls dynamical and behavioral representations from the time series, as Berman points out, the approach is highly dependent on the time scale selected to define the behavioral states (Berman, 2018). It is a limitation because the animal's behaviors might happen at different time scales. Therefore, one must choose and test several time scales to model their desired behaviors.

A substitute method is to find predefined modules of behaviors of varying time lengths within the data. These modules serve as behavioral templates so that time series patterns that match them are used to extract the behaviors (Schwarz et al., 2015; Gomez-Marin et al., 2016).

Although there is an advantage of obtaining the desired behaviors, this approach is limited by having to know all desired behaviors that an animal is likely to perform. It removes the ability to identify subtle and unknown behaviors in the animal's repertoire.

Transforming the postural time series data into the frequency by performing a wavelet transformation removes the burden on the user to define the time series templates or their durations to match the data accurately.

The process of transforming data into the frequency domain creates high-dimensional data. To ensure that the local structure is preserved when performing a dimensional reduction on the data, MotionMapper uses a non-linear embedding algorithm, t-stochastic nearest neighbor embedding (tSNE) (Van Der Maaten and Hinton, 2008). Using tSNE means points close to each other in the high dimensional space would be preserved to be together in the lower dimensional. Unlike PCA, where the goal is to capture the variance and preserve the global distance structure within the data, the tSNE algorithm is a manifold learning technique that seeks the preservation of local distance over global ones.

With the data in a reduced dimensional form, MotionMapper chooses a watershed algorithm to cluster the behavioral states. The watershed algorithm captures repeated motifs as stereotyped behaviors by assigning data points to the same cluster that reach the same local maximum by ascending a local gradient. Conversely, to assign the cluster, a Gaussian Mixture Model (GMM) can be fitted to the data (Todd et al., 2017). The GMM assumes the data is drawn from a probability distribution formed by summing mixture components and assigns points to cluster if its mixture component has the maximum posterior probability.

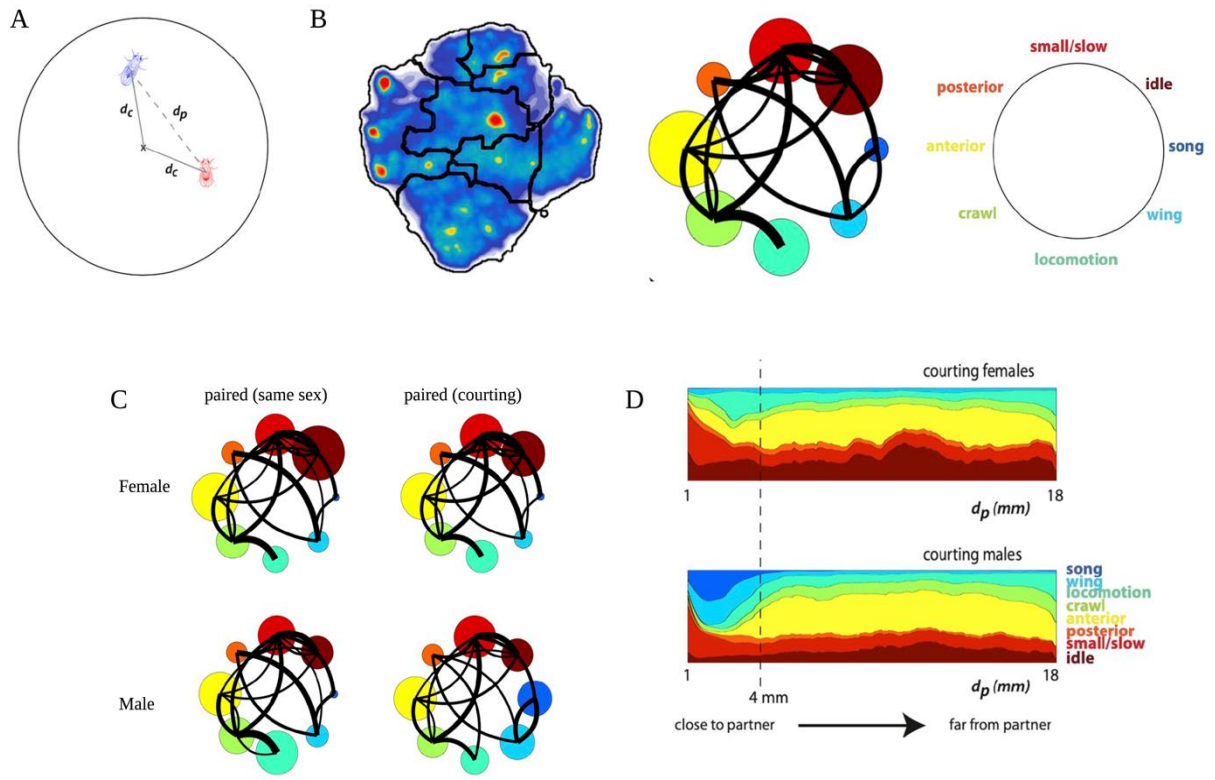

Figure 2.6. A behavioral mapping of social behavior of paired fruit flies. A. A schematic of the arena with the paired fruit flies. Flies of the same sex or opposite sex were paired together and videotaped for 30 minutes to record their behaviors. B. A map (left) showing the 2D projection of the behavior of the flies. Black lines indicate coarse-grained regions based on hand labeling. A bubble plot (middle) summarizing the relative densities and transitions between coarse behavior regions. The right plot shows the names of the classified coarse-grained regions from the map. C. A comparison of the relative densities of the female and male flies when paired with either the same or opposite sex. D. Stacked behavioral density plots show the frequency of each coarse behavior given distance to the interaction partner d_p. A sliding window of 1 mm was used to calculate density at.1 mm increments with centers ranging from.1 to 18 mm. (Adapted from Klibaite and Shaevitz, 2020)

Although MotionMapper was initially developed to map the behavior of single animals, there are recent publications to show that it can be extended to a social context to uncover sequences of social behaviors shared among animals. For example, the MotionMapper has been used to study how fruit flies alter their behaviors in different social pairings (Klibaite and Shaevitz, 2020). Here, the authors showed that from the extraction of a repertoire of stereotyped behaviors, paired fruit flies performed more posterior grooming and wing movements during

social interactions than when they were in a non-social context of being alone. Females in a same-sex pairing or opposite-sex pairing with males were less likely to move around compared to a same-sex pairing of males (Figure 2.6C). This increased locomotory activity might be due to the high likelihood of the males fighting each other. They also observed that by comparing how similar the behavioral maps of the flies are, courting males showed a more different behavioral repertoire than other fly pairings, which was likely driven by courtship-specific song and wing behaviors (Figure 2.6D). In addition, they observed that paired flies were likely to synchronize their behaviors.

2.9 Measuring hierarchy and predictability in social behaviors

Animals might go through a sequence of actions to perform a behavior, with some actions occurring before or having precedence over others. The structure that exists within these sequences is a possible indication of a temporal organization of the behaviors. For example, there is a high probability that tongue grooming precedes front leg grooming in flies, but the inverse is not true, with almost zero probability (Richard and Dawkins, 1976). In addition, the fly grooming movement falls into two clusters, anterior and posterior grooming activities. Hence, a fly is likely to perform interchangeably tongue and head grooming for anterior movement and abdomen and wing grooming for posterior actions. If the flies were covered in dust, they performed a predictable, sequential cleaning of the anterior parts, the head and antennae, the abdomen, and their wings and thorax (Seeds et al., 2014). What this temporal organization offers is an idea of hierarchy and the predictability of behavior.

The hierarchical organization of behavior, although primarily explored in single animal behavior, can be extended to study the social behaviors of animals. During social interaction,

paired male flies cycle through a loop of fast approach, slow approach, and wing threat (Chen et al., 2002). When it performs a wing threat, a fast or slow approach likely follows this behavior. However, in the fast approach phase, they are likely to also engage in boxing and tussling, which is not seen when they are in slow approach and wing threat behaviors.

Markovian and non-Markovian models can be adapted to measure hierarchical structure in social behaviors. One can fit a Markov and its variant of hidden Markov models to the transitions of behavioral repertoire obtained from the behavioral states of spatiotemporal and time-frequency analysis (Chen et al., 2002; Wiltschko et al., 2015). However, using a Markov model, one inherently assumes that social behavior happens in a single discrete timescale and that the current behavior is defined only by the one preceding it. Alternatively, one can take a longer time scale where a current behavioral state depends on a history of previous states.

With this assumption, a non-Markovian approach, like the information bottleneck, can be applied to the transition matrix of the behavioral states (Tishby et al., 2000). The information bottleneck method, an approach initially developed to assign the relevance of information quantitatively, can be extended to extract hierarchy out of a sequence of behaviors (Berman et al., 2016). In this framework, the goal is to maximize the information about a future behavioral state while holding the information about the past states fixed. Berman et al. showed that by using the information bottleneck method, they observed fly behavioral repertoire to be organized in a hierarchical manner (Berman et al., 2016). The fine-grained behaviors of the flies, such as right and left-wing grooming and wing waggle, were predictive of short-time structure and coarser representation, like wing movement and locomotion, predict actions that with further away in time.

2.10 Why care about measuring social behavior?

In as much as the common saying goes, “humans are social creatures,” and there is an inherent desire to understand our social nature, a wide variety of species, from *C. elegans*, fruit flies, birds, fish, and rodents to non-human primates, engage in some form of social behavior (Tinbergen, 1952; Anderson, 1998; De Bono et al., 2002; Bialek et al., 2014; Durisko et al., 2014). These evolutionary preserved social behaviors might serve different purposes, from feeding, courtship, fighting, and migration to animal decision-making.

As Chiel and Beer put it, the brain has a body, and its motor output is reflected in the behavior (Chiel and Beer, 1997). Hence, measuring social behavior can provide insights into how the brain processes input signals from the environment, including social cues, and couples that with its internal state to dictate its actions. By carefully quantifying the movements of animals in space, time, and frequency domains, we can understand what states the brain is in and what information it considers relevant prior to executing an action. Since neuroscience has greatly advanced in being able to record multiple neural activities across different brain regions in multiple animals (Kawasaki et al., 2013; Dikker et al., 2017; Zhang and Yartsev, 2019; Anpilov et al., 2020), it is desirable that the precise quantification of social behavior can match the field. With it, we can gain insights into the neural activity that underlies social experiences. One can leverage the information quantified from social behaviors to detect social deficits such as autism. For example, using the distance between a tracked point on the head and center of animals and their behavior classifier, Hong et al. showed that an autistic-like mouse model, Black and Tan Brachyury (BTBR), spent significantly less time socially investigating a conspecific compared to wild-type animals.

In addition, measuring social behavior would help uncover how genetic variations might mediate social interactions. In studying the social investigation behavior of mice, Hong et al. showed that two strains of mice behaved differently towards conspecifics. The standard strain wild type, C57BL/6N, male mice closely investigate other males for longer durations. However, strains considered aggressive, NZB/B1NJ, exhibited more attack and less close investigation behaviors towards intruder males.

2.11 Concluding Remarks

In this chapter, we have discussed social behavior and the challenge most scientists face in measuring it. We then provided a framework on how to quantify social behavior. This framework entailed building a moment-by-moment classification of behavior and projecting the behavioral repertoire of the animals into a space based on their stereotypy. We talked about the choices a scientist has to make when selecting this framework and the biases inherited from them. For example, in building moment-by-moment classification through a supervised approach, the scientist is inherently biased toward the selections of the labeling generated by the human annotators. With creating a social behavioral map, although the representations are generated from the data, the choices in the algorithms used dictate the outcomes. In addition, the behavioral map representation primarily relies on stereotyped behaviors and less on non-stereotyped behaviors. Therefore, the less occurring non-stereotyped behaviors, which are likely to precede and dictate the stereotyped behavior, are overlooked, and hence, a complete representation of the social behavior of the animals is not obtained. Despite these limitations, we anticipate that as better theoretical frameworks are developed, and advancements are made in tools to study behavior, we will build a clearer picture of the dynamics of social behavior.

Chapter 3. DEVELOPING A PIPELINE FOR ROBUSTLY AND PRECISELY TRACKING MULTIPLE ANIMALS IN A SOCIAL CONTEXT

3.1 Introduction

In this chapter, I will present a pipeline that we developed to track the postures of multiple animals robustly. First, I will give a history of tracking animal behavior and the advancements made. Then, I will discuss the limitations of the tracking tools currently applied to label the positions and poses of animals in a social context. Subsequently, I will present our approach to building a pipeline that addresses the limitations of the current tools. Finally, I will propose suggestions for altering the pipeline to improve its robustness in more complicated scenarios in a social context.

3.2 Background

As discussed in the previous chapter, tracking the postures of animals is essential to the process of measuring animal social behavior. After videotaping the social interactions of the animals, the next step in the framework to quantify their social behaviors is to track them. The tracked information provides insights into the spatiotemporal position, orientation, and poses of the animals that serve as inputs to either creating a moment-by-moment classification of the social behavior or building a behavioral space representing the stereotyped behaviors of the animals.

Before the development of computer-automated tracking tools, tracking animal behavior mainly required humans to label the animal's positions and trajectories (Bayne and Scullard,

1978; Buelthoff et al., 1980; Moran et al., 1981). This human annotation approach meant a poor spatiotemporal resolution of the animal's poses, with overlooked time points. In addition, it was highly time-consuming, imprecise, subjective, and labor-intensive. However, as computers became cheaper and more available, and with the development of theoretical and mathematical approaches to track behavior, there was a gradual shift to more automated tracking methods, which meant better spatiotemporal resolution of the animal's posture (Bar-Shalom et al., 1990; Noldus et al., 2001; Spink et al., 2001).

Much of the early automation was driven by computer vision and machine-learning approaches, with the primary goal of tracking the center of mass of an animal and its head orientation over time (Branson et al., 2009; Dankert et al., 2009). Subsequently, owing to the advancement in deep learning knowledge in the last decade, there has been an explosion of methods that have led to identifying multiple body points besides the centroid of the animal (Mathis et al., 2018; Graving et al., 2019; Pereira et al., 2019; Lauer et al., 2021). Now, researchers can simultaneously track multiple animals' noses, wings, limbs, tails, and other body points, from insects, rodents, and non-human and human primates. Hence, providing adequate data points to quantify animal social behaviors.

As it will be further discussed later in this chapter, despite these advancements, there are still lingering issues where tracked-body points switch with one another on the same animal or are swapped with those of a different animal. The limitation is more prominent when the animals are close to each other. To such an extent that when we use the tracked points to build a behavioral space of the social behavior of prairie voles (based on the framework discussed in the previous chapter), we find that some of the clustered behavioral regions are made from spurious tracking (Figure 3.1).

Given the poor tracking issues that lead to spurious behavioral maps, we decided to develop a pipeline that combines an Autoencoder, a deep learning network, with the existing tracking methods to fix the swapping issues robustly. This pipeline was primarily tested with rodents, specifically prairie voles; nonetheless, we think it can be extended to other animal models, like flies and primates.

In the rest of this chapter, I will highlight the earlier tracking work with computer vision, machine learning, and deep learning. Subsequently, I will discuss in detail the pipeline we developed, explaining its features, successes, and limitations in the sections.

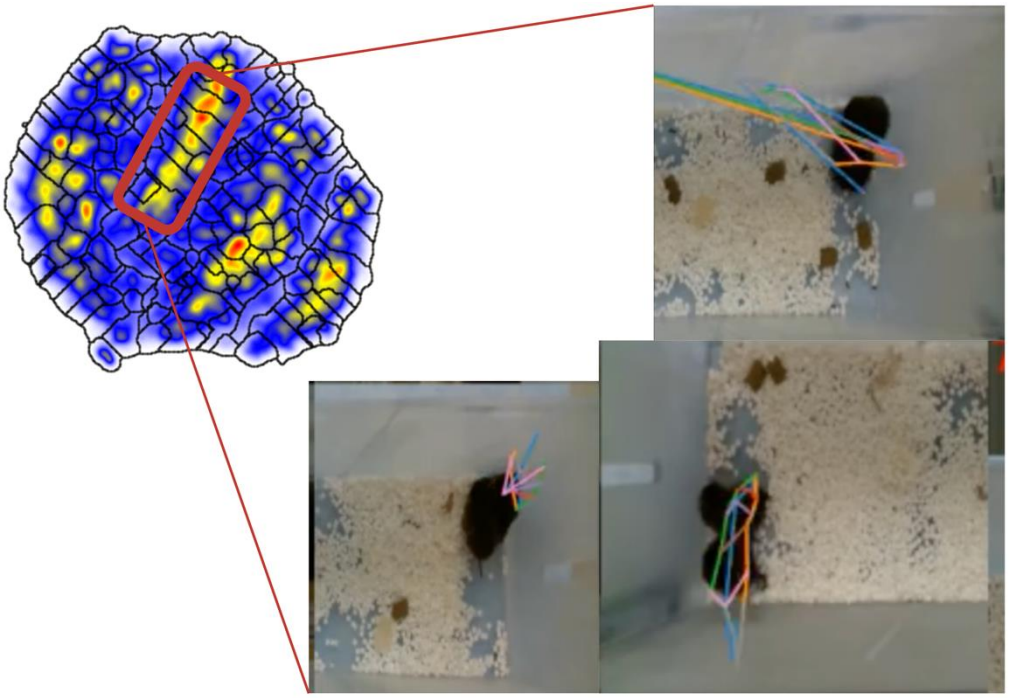

Figure 3.1. A behavioral space for prairie voles created with a multi-animal tracking tool. Male and Female prairie voles were paired for 24 hours. We recorded their behavior during the first 2 hours of cohabitation. Then, we applied a multi-animal DeepLabCut to track their postures. Given the poses, we built a behavioral map based on the approach outlined in the previous chapter. The map shows regions with peaks that are meant to indicate stereotyped behaviors. However, some of these peaks are generated by bad tracking errors (Red box). Refer to this link for samples of videos from these regions: https://github.com/senakoko/Thesis_Videos/tree/main/Chapter_3_Videos/Figure_3.1_Videos

3.3 Behavior tracking using computer vision and machine learning

The initial approach to automated animal behavior tracking involved using computer vision and machine learning tools to identify a single point (center of mass) of an individual animal (Noldus et al., 2001; Spink et al., 2001). With the tracked center of mass, researchers could monitor the animal's trajectory and quantify its distance traveled, speed, and time spent at a location. This meant scientists could achieve high throughput in investigating exploratory behaviors and their related neurological underpinnings like anxiety, stress, social novelty, and sociality (Spink et al., 2001; Post et al., 2011).

However, to achieve this goal of tracking an animal's centroid position, these methods relied on having a single animal in behavioral setups that were optimized to allow object-background segmentation and have fewer objects (e.g., food pellets, beddings) in the recording apparatus. Therefore, further advancements were needed to overcome these limitations to allow for quantifying single animal behavior in more naturalistic settings (Branson et al., 2009). The new methods that were developed were expanded to apply to more social paradigms involving two or more animals (Dankert et al., 2009; Pérez-Escudero et al., 2014). Hence, scientists could now leverage the ability to track multiple animals to study their collective behavior. For example, taking advantage of the ability to track multiple animals, Pérez-Escudero and colleagues observed that adult zebrafish, having explored their environment for a period (approximately 3 hours), spontaneously switched from shoaling to territorial behavior. In addition, when they studied the social behavior of multiple medaka fish, they saw a hierarchical structure of leadership-followership behavior within the group, which was preserved over multiple days and was very stable.

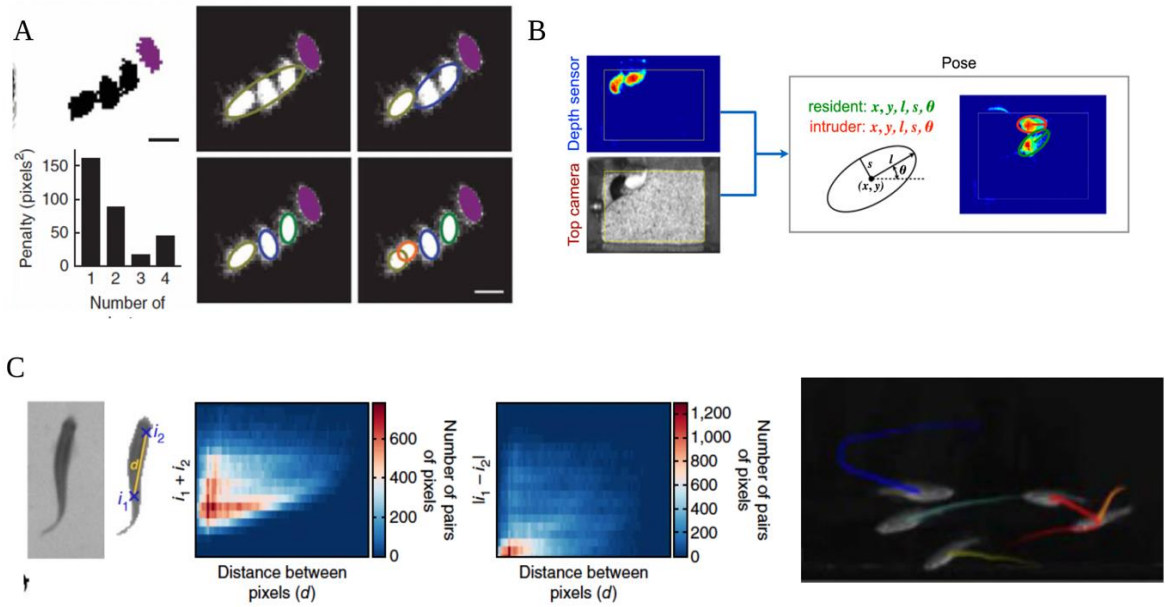

Figure 3.2. Computer vision and machine learning tools to track animal behavior. A. Tracking of multiple fruit flies. Foreground pixels are grouped to detect individual flies. The purple component corresponds to one fly; the large black part corresponds to three. The tracker splits this large component into 1–4 clusters. The penalty based on cluster size is shown for each choice. B. Pose estimation of two mice with distinct coat colors using information from both the top view camera and depth sensor. An ellipse that best fits an animal detected in the segmented 3D video frames is used to describe the animal's position, orientation, shape, and scale.C. Tracking of multiple adult zebrafish. The method consisted of identifying fingerprints or signatures of the animals that served as reference images. The fingerprints were made based on the intensity and contrast maps extracted from the video frames. By aggregating enough reference images, they could accurately track each individual. (Adapted from Branson et al., 2009, Hong et al., 2015, and Pérez-Escudero et al., 2014)

Subsequently, these computer vision methods were extended to label other body points, such as an animal's nose, mid-body, and tail, to expand from only tracking the animal's center of mass. For example, labeling the additional body points in rodents was beneficial for researchers to build machine learning classifiers that could be used to extract affiliative and investigation-like behaviors, which include oral-oral, oral-genital, and side-by-side contacts (de Chaumont et al., 2012). The initial iterations of the methods were developed for 2D videos, which meant they were limited to handling the vertical movements of the animals, like rearing, mounting during

sex, and resolving occlusions between the animals. However, as technology advanced to introduce 3D cameras with depth-sensing capabilities, the methods were adapted to utilize 3D information to capture the animal's behavior (Hong et al., 2015).

Despite the advancement, researchers had to adopt artificial means to make the methods work, especially in the social context. For example, they had to color the fur of the animals or use animals that had distinct coat colors because when the animals spent long durations near each other, like during huddling, and crossed each other's paths multiple times, the tracked points were swapped. Hence, more sophisticated tools using deep learning methods had to be leveraged to tackle the tracking issue.

3.4 Behavior tracking with deep learning approaches

The technological advancement in computing systems, marked by the development of graphical processing units (GPUs) and high multithreading and multiprocessing central processing units (CPUs), segued into the application of deep learning methods. As defined by Francois Chollet (François Chollet, 2017), "*Deep learning is a specific subfield of machine learning: a new take on learning representations from data that puts an emphasis on learning successive layers of increasingly meaningful representations.*" Deep learning is built on the idea of the neural network structure of the brain. To illustrate a simplistic relationship between machine learning and deep learning – take a function $y = f^*(x)$, where in machine learning, the goal would be to learn the rules that map input x to the output y. In deep learning, the relationship would be considered as a neural network structure with "layers," where $\boldsymbol{y = f^3(f^2\left(f^1(x)\right))}$ (Goodfellow lan, Bengio Yoshua, 2016).

The use of deep learning approaches In tracking animal behavior was preceded by advances in the field of annotating the behaviors of humans (Andriluka et al., 2014; Insafutdinov et al., 2016). For example, Insafutdinov and colleagues showed that deep learning-based techniques could be used to estimate the poses of humans in complicated real-world settings, such as people dancing and walking, while still maintaining the identities of the individuals.

Figure 3.3. An example illustrating an application of deep-learning tools for human pose estimation of multiple people in real-world images. (Adapted from Insafutdinov et al., 2016)

Following this advancement, some groups studying animal behavior, including the Mathis and Murthy labs, leveraged deep-learning tools to track animals. Mathis et al. published DeepLabCut (DLC) (Mathis et al., 2018), and Pereira et al. released LEAP Estimate Animal Poses (LEAP) (Pereira et al., 2019). DLC and LEAP, the two most popular tools in the field,

have similar backbones for using a convolutional neural network (CNN) in their architecture, but their implementations for how to track the animal pose slightly differ (to be discussed shortly).

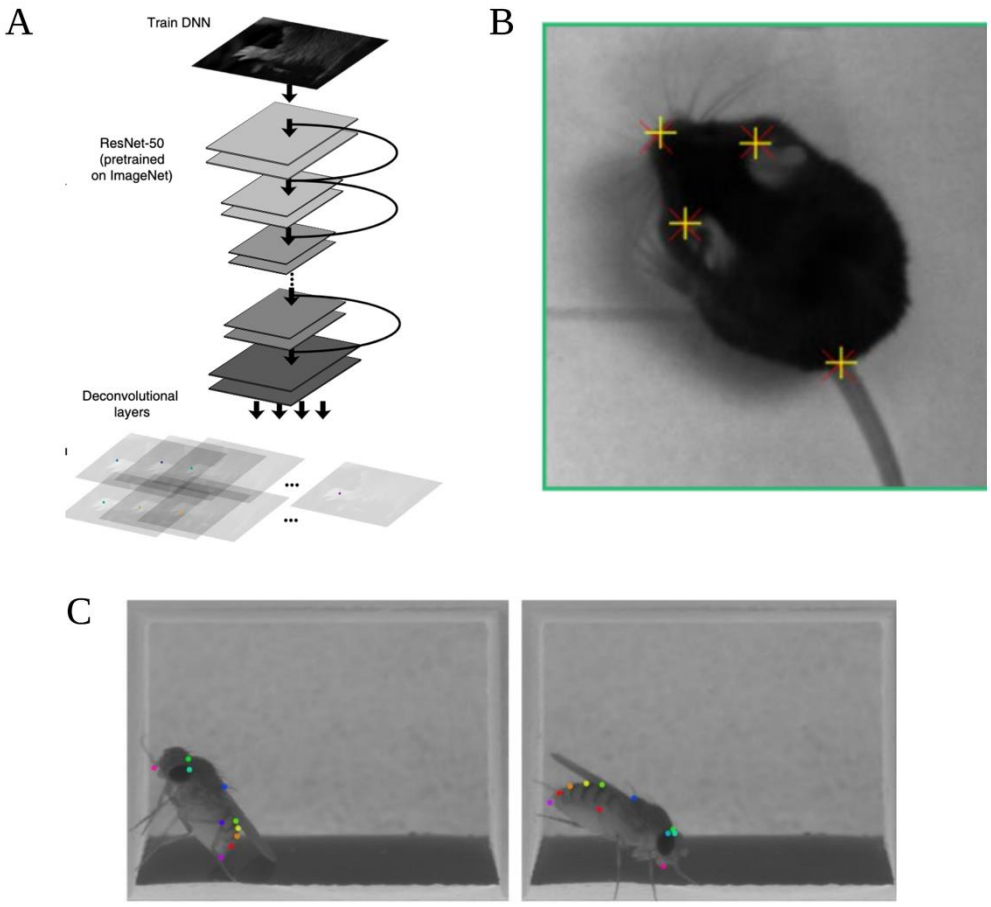

Figure 3.4. An example illustrating an application of DeepLabCut to track the pose of a mouse and a fly. A. A typical architecture of a deep neural network (DNN) is used in predicting the body-part locations based on the corresponding image. B. Example of body part prediction for a mouse showing the network's prediction (yellow cross) matching human annotator's labels (red cross). C. Example frames and body part predictions for a fly in different poses. (Adapted from Mathis et. al., 2018)

Given that our research primarily focuses on studying prairie voles, we will continue our discussion regarding the use of these tools in studying rodent behavior. However, it should be noted that these tools, among several others (Graving et al., 2019; Günel et al., 2019; Shukla and Arac, 2020; Liu et al., 2021), are species-agnostic and can be used to track behavior in other

animals, like fruit flies, fish, and primates, which was not the case in the computer vision methods that were tailored to specific animal groups.

By deploying these tools in tracking rodent behavior, one went from only being able to track a centroid and the head of an animal to tracking the tail, ears, and limbs (Figure 3.4). Therefore, instead of having only the centroid and head, which would likely tell the position and orientation of the animal, we could recreate a behavior such as grooming and rearing from the animal's pose.

The deep-learning framework was not only beneficial for creating postures, but it also expanded the capabilities of methods like idTracker (Pérez-Escudero et al., 2014), which used a computer vision approach to identify multiple animals (20-30). In the original method, the identification was achieved by finding a fingerprint of an animal which was based on an image intensity of a reference frame of the individual. This signature was used then to maintain the animal's identity in the video data. However, by implementing a CNN backbone, Romero-Ferrero et al. published idTracker.AI (Romero-Ferrero et al., 2019), which could track up to 100 animals while maintaining their identities. In this new implementation, they had a CNN that would learn the uniqueness of the individuals and a second CNN that could handle complex scenarios like when they crossed each other's path.

Notwithstanding, idTracker.AI was only designed to track centroids, and DLC and LEAP could only label the poses of a single animal but not multiple ones. Lauer et al. developed a multi-animal tracking tool called multiple animal DeepLabCut, maDLC, (Lauer et al., 2022), built on earlier work, DLC, and similarly, Pereira et al. also published Social LEAP (SLEAP)(Pereira et al., 2022), an advancement on LEAP to track multiple animals.

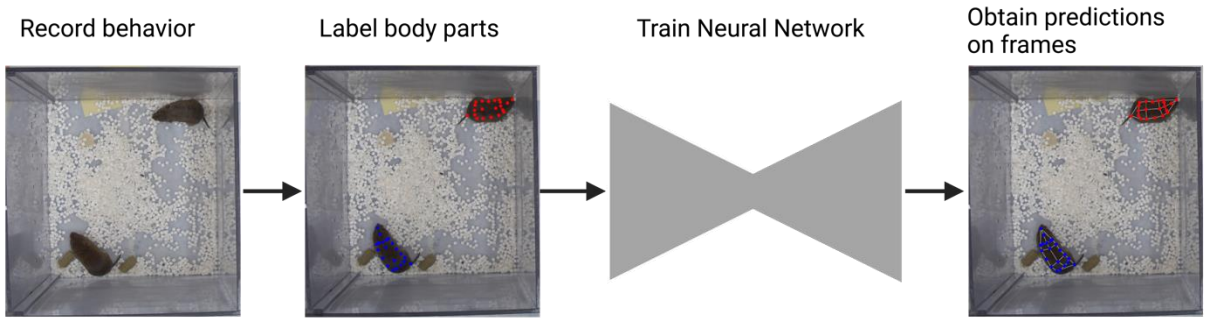

Figure 3.5. A standard workflow pipeline for using deep-learning-based markerless tracking methods. First, take a raw video of the animals and then label desired points on body parts. A deep neural network is trained on the labels from human annotators. The network infers animal's body points on video data.

As in previous versions, maDLC and SLEAP had different implementations of CNNs and methods to annotate body points on multiple animals and maintain their identities. maDLC implemented a bottom-up approach, and SLEAP used both a bottom-up and a top-down process.

In the bottom-up approach, they first estimate the labeled body points on all the animals and then group the points belonging to each individual based on their connectivity. The implementation is performed with only one network. In contrast, the top-down approach requires two networks. The first network locates the anchor point, and the second connects the other body points to the reference. Based on the number of animals one needs to track, it is usually more efficient to use the bottom-up approach to track the dataset with many animals and the top-down with data with fewer animals.

Despite the successes of maDLC and SLEAP in estimating the poses of multiple animals, when we apply them to prairie voles, we notice that they cannot maintain the animals' identities throughout the entire recording (see an example video here: Bad Tracking). When the animals are some distance from each other, both methods perform well in maintaining the animals' identities. However, the likelihood of swapped identities becomes significantly higher when the animals get closer to each other in mating or huddling. The methods fail to switch the key points

back to the initial tracking animals. This limitation would be a problem if one needed to build a behavioral representation of the animal, which relied on their identities.

3.5 Pipeline to fix pose estimation

Given the tracking limitations during social contexts when the animals are close to each other for long periods, I developed a pipeline that combines a different deep learning method, an Autoencoder, with the output of the tools, like maDLC and SLEAP to obtain detailed and high-accuracy postural trajectories of multiple animals. I will explain our approach and the choice made in the rest of the chapter.

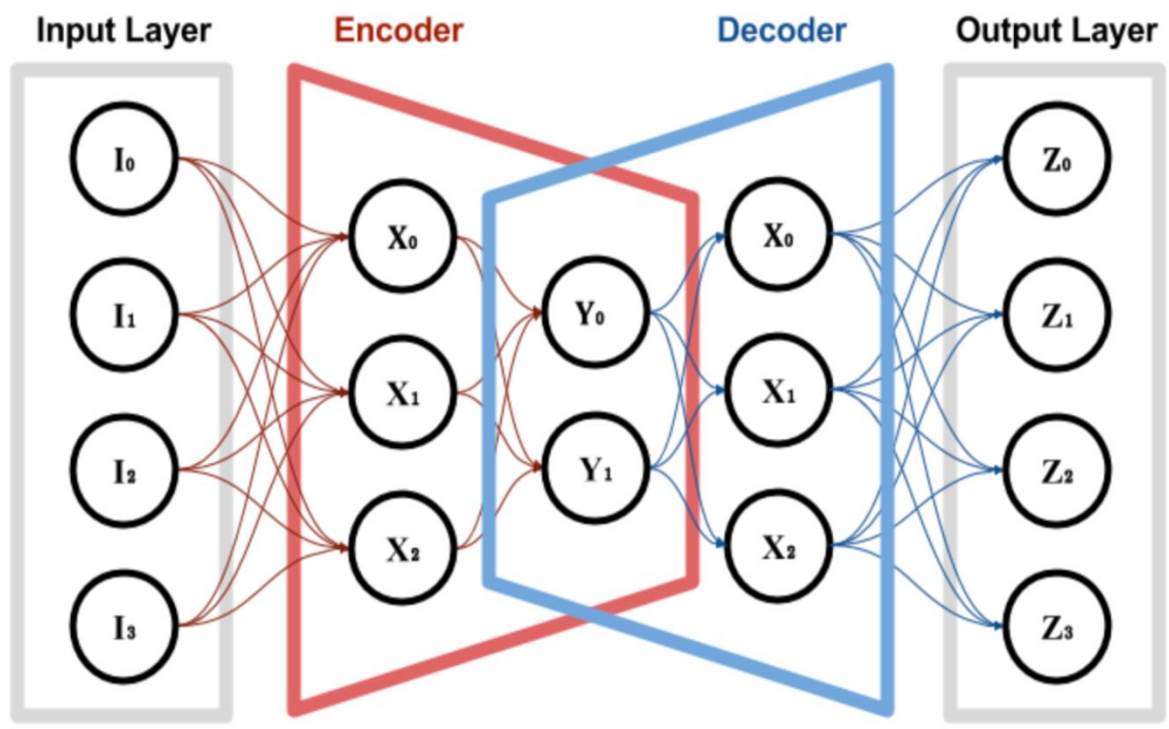

Figure 3.6. A typical architecture of an autoencoder. The autoencoder comprises two main parts – the encoder and the decoder. The encoder produces a latent representation from the input data, fed into the input layer. The decoder transforms the latent representation into an output, which is identical but not the same as the input. (Adapted from Géron, 2019)

3.5.1 Autoencoders

Autoencoders are deep-learning neural networks designed to learn the underlying non-linear function of a data input by encoding the information into a latent (dimensional reduced) representation (Géron, 2019). The term deep describes the number of neural layers created for the encoder and decoder; usually, more than two layers can be considered a deep network.

What is typical for autoencoders is that they have an encoder and decoder part of the network, where they (encoder and decoder) are identical but inverse (Figure 3.6). They are identical in the number of neurons in the network and the connections between the neuron nodes. Conversely, they are inverse in that the encoder is designed to take a data input of a high dimension and reduce it into a latent representation, which is usually a lower dimension. The decoder, in its part, is meant to take the latent representation generated by the encoder and recreate an outer representation approximately like the input data. It is critical that the outer representation is not the same as the input data because that would mean the autoencoder only copied the input data to the output. The goal of the autoencoder, like every other deep learning approach, is to learn from the data. Essentially, the autoencoder must learn the functions that govern the input data. The advantage of learning from the data, but not merely copying from the data, is that the autoencoder can act as a filter for noise that might be embedded in the data. For example, if we had a function $y = f^*(x) + n(x)$, where 'f*(x)' is the actual function and n(x) is the added noise. The autoencoder would filter out the noise, n(x), and retain the true function $y = f^*(x)$.

In addition to acting as a noise filter, the autoencoder can be considered a nonlinear dimensionality reduction technique used to reduce data dimensions. For example, in creating the latent representation from the data, which can be regarded as having a high dimension, the

autoencoder compresses the data (the encoding process) to a low dimension. If the activation function (to be discussed later) is linear, the autoencoder essentially becomes a principal component analysis (PCA) (Géron, 2019). We would later see the benefit of the autoencoder being a dimensional reduction technique in Chapter 4 for creating a behavioral repertoire of social behavior.

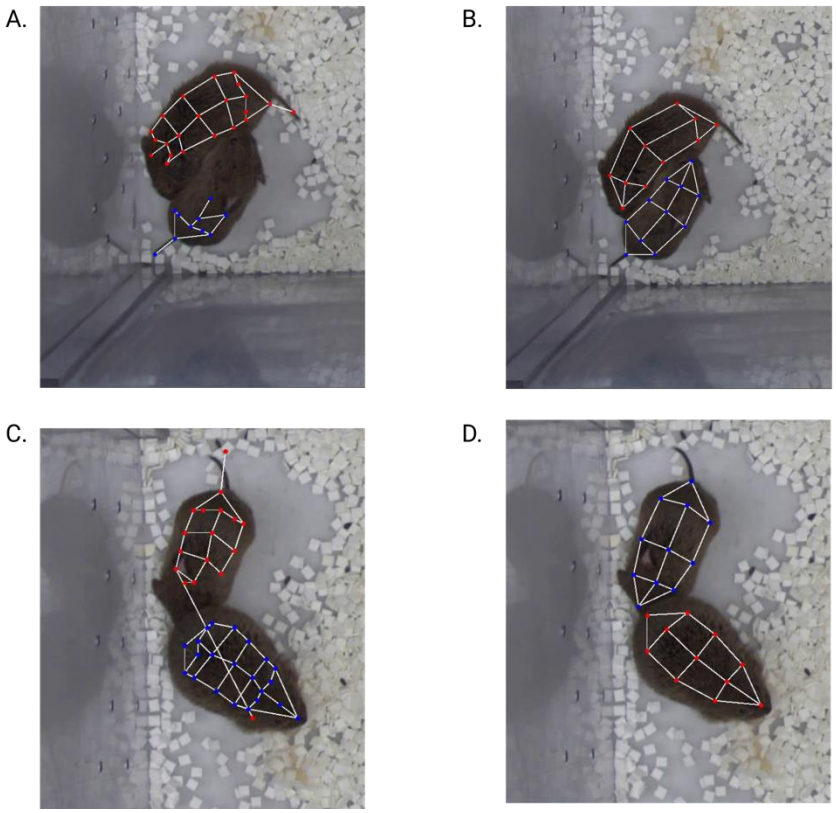

Figure 3.7. Comparison between pose estimation generated by tracking tools (e.g., SLEAP) and Autoencoder. A) SLEAP tracked points show unlabeled body points on the animal. B) Applying the autoencoder labels the missed body points from A. C) SLEAP tracking wrongly labels a body point for one vole on the other. D) Autoencoder fixes swapped body points

3.5.2 Autoencoder Architecture

In designing the architecture for the autoencoder, we had to make several choices, from the type of autoencoder to the formatting of the input data to the number of neurons in the network to the selection of the activation function and the optimizers. We needed to build a tool

to improve the tracked points generated by either maDLC or SLEAP and so go from figures 3.7A and 3.7C to figures 3.7C and 3.7D (see example videos: Bad Tracking and Good Tracking). In general, we had to decide on the following:

(i) Type of Autoencoder

(ii) The structure of the data input

(iii) The number of layers

(iv) The number of neurons in each layer

(v) The activation functions

(vi) Add batch normalization or dropout or both

(vii) The loss function(s)

(viii) The optimizers

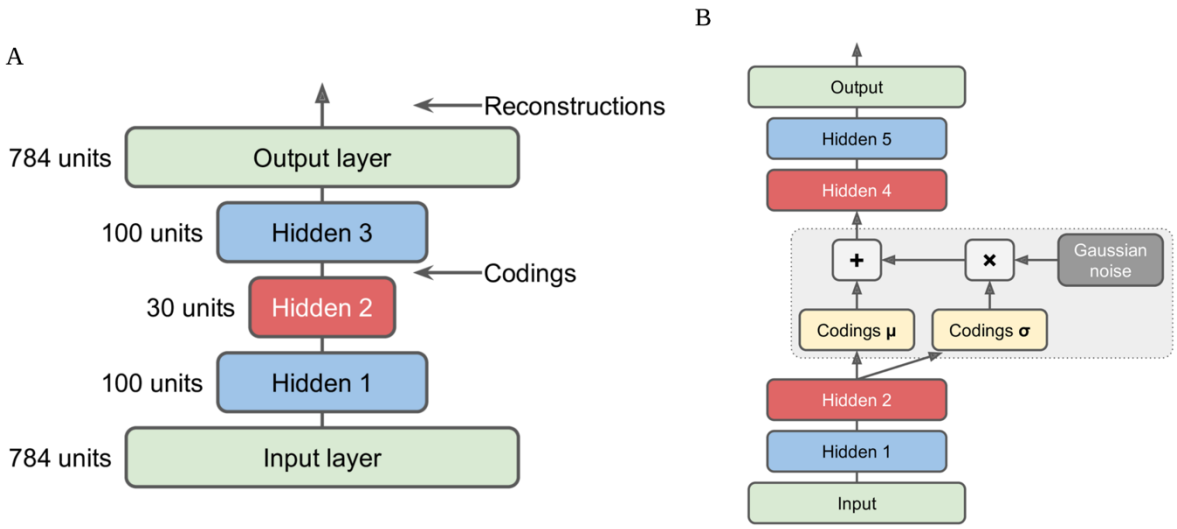

Figure 3.8. A block diagram figure of autoencoders. A. A schematic of a stacked autoencoder. B. An illustration of a variational autoencoder. (Adapted from Géron, 2019)

I will take each listed point above and explain the decisions we made behind them and why we made them. I have written a python package with the complete code to implement the autoencoder on tracked data (https://github.com/senakoko/AutoPoseMapper).

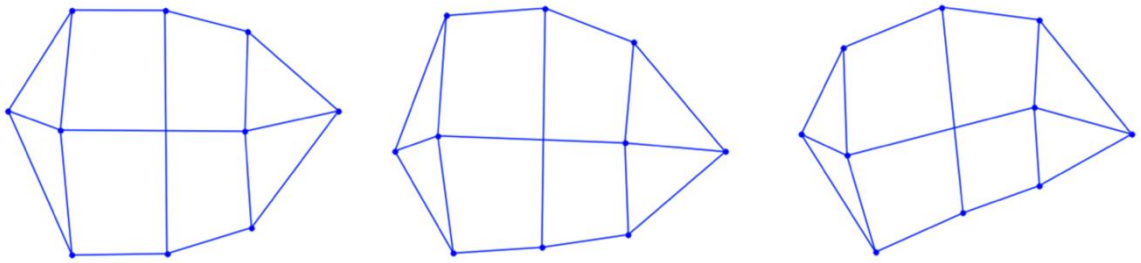

Figure 3.9. Examples of fake tracked points generated using variational autoencoders. These points were not from an actual vole.

3.5.3 Type of Autoencoders

There are two major types of autoencoders – the stacked autoencoder and the variational autoencoder. The stacked autoencoder is considered the vanilla (simple) kind of autoencoder, where all the neurons (this term will be fully explained later in section 3.5.6) within the autoencoder are connected. Its architecture is typically symmetrical around the latent layer (coding layer) (Figure 3.8A). In contrast, the variational autoencoder has a latent representation produced from the mean and standard deviation coding layer (Figure 3.8B). Therefore, instead of a single layer representing the encoded information, as seen in the stacked autoencoder, the encoder for the variational autoencoder generates values for two layers, the mean μ and standard deviation σ layers. The values from the mean and standard deviation layers are then randomly sampled to create coding outputs, which serve as input to the decoder part. One can imagine the coding as a Gaussian distribution, where samples are taken from it to train the decoder. Since the variational autoencoder has a mean and standard deviation layer, it is considered probabilistic and generative. It is defined to be probabilistic because, from the mean and standard, one can sample random values that would lead to indeterministic outputs. It is generative because a new instance of the data that never existed can be created. For example, figure 3.9 show the tracking of voles that were not taken from a real vole. They are fake.

3.5.4 The structure of the data input

In our autoencoder, the data input is the tracked points generated by animal tracking tools, like maDLC and SLEAP. We advise that the tracked points are ego-centered prior to using them as input. Ego-centering the data aligns all the tracked points to a reference point so that it can be imagined that the animal is always facing the same direction at every time, irrespective of its real-world coordinates. Although figure 3.9 is a set of fake tracked points, it can be observed that the animals are facing the same direction. Ego-centering can also be viewed as a way to standardize the data input since all the tracked points are centered on a reference point.

3.5.4 The number of layers

A layer of autoencoder, like any other deep neural network, consists of multiple units referred to as neurons (to be discussed shortly) that transform the data. For example, a layer is analogous to a brain region, like the nucleus accumbens, because it comprises neurons that receive projections of other neurons and send their axonal fibers to other neurons in different brain regions. Determining the number of layers for the autoencoder is arbitrary, but generally, the more layers (the deep) autoencoder, the better it performs (François Chollet, 2017). However, despite being arbitrary, testing the autoencoder on data and checking its validation loss is the practical way to know how many layers to have. The validation loss refers to the error between the prediction of the network and the actual data point. The network with the lowest validation loss is generally the best.

3.5.6 The number of neurons in each layer

The neurons are the units within the layers of the autoencoder. They are essentially functions that transform their inputs. Similar to the number of layers, determining the number of neurons is arbitrary, and more is better. In our design of the autoencoder, we chose a dense structure, meaning every neuron in a layer is fully connected to the neurons in the next layer but not to the other neurons within the same layer (Figure 3.6). In addition, we selected the number of neurons as powers of 2. It is because the power of 2s is computationally efficient and makes the neural networks train faster on the graphical processing units (GPUs) (François Chollet, 2017).

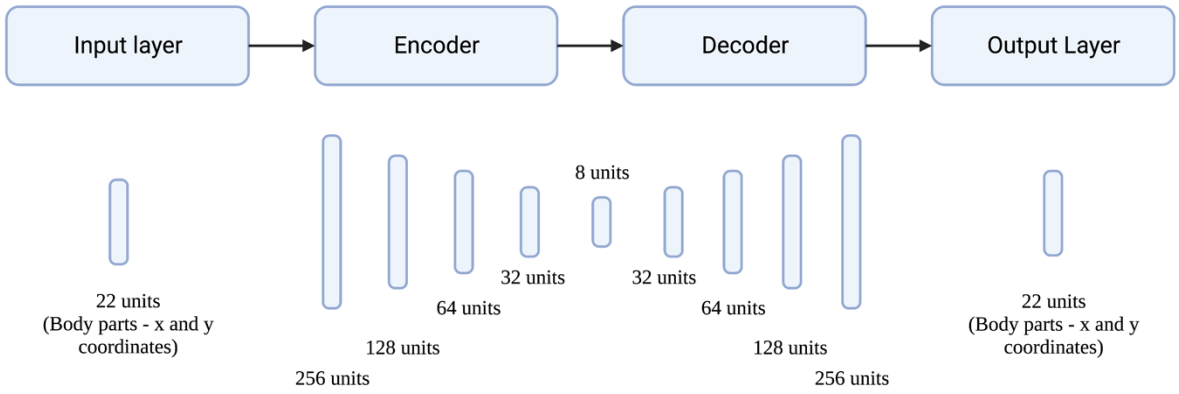

Figure 3.10. A schematic of the architecture of the primary autoencoder we used in the thesis

From testing a different number of neurons and layers, I found that the architecture presented in figure 3.10 performed the best. The performance was characterized based on obtaining the lowest value for the loss function during training and validation. The loss function was the mean squared error (to be discussed later in this section). I also evaluated the accuracy of the network based on its validation accuracy, where the network was tested on data it was not trained on.

3.5.7 The activation functions

The activation function is typically a nonlinear function that is applied to the hidden units of an artificial neural network to determine its outputs (Goodfellow lan, Bengio Yoshua, 2016). If one had a neuron unit with the function $h_i = g(x^T W_{:,i} + C_i)$, 'g' will be the activation function, e.g., a rectified linear unit (ReLU) that dedicates the output for a given range. There are several activation functions, such as sigmoid, tanh, rectified linear unit (ReLU), and exponential linear unit (ELU), that can be applied in deep learning networks given a task. In designing our network, we chose a scaled exponential linear unit (SELU) as the activation function. We selected this function because it has an internal normalization that can adjust the mean and variance from the previous layers. Its ability to scale the mean in the positive and negative direction is not available in ReLU, a commonly used activation function. The SELU function allows the network to converge faster and helps prevent vanishing gradients (when the gradients go to zero). Each layer of a neural network can have its unique activation function, but, given the properties of SELU to converge faster and prevent vanishing gradients, we chose it for every layer except for the last one, the output layer. The output layer is meant to have a different function that allows its results to match the input.

$$f(\alpha, x) = \lambda \begin{cases} \alpha(e^x - 1) & for\ x < 0 \\ x & for\ x \geq 0 \end{cases}$$

The alpha α (1.67) and lambda λ (1.05) hyperparameters are predefined (not learned from the training) for the activation function (Klambauer et al., 2017).

3.5.8 Regularizing the network

In general, it is always a good practice during the application of a learning algorithm to regularize it in the form of using a penalty (François Chollet, 2017; Géron, 2019). Regularizing

prevents the algorithm from over or under-learning the representation that makes up the data. One way to do so is through batch normalization.

3.5.8.1 Batch Normalization

Batch normalization is a form of regularizing artificial neural networks to prevent neurons' saturating and gradients from vanishing in the deep layers (Mehta et al., 2019). With saturating neurons and vanishing gradients, the weights of the neurons remain constant or go to zero, which is not ideal because one would want the weights to be adjusted as the network learns from the data. Therefore, the goal of batch normalization is to achieve a stable distribution of activation values throughout the training of the network (Ioffe and Szegedy, 2015). Although it is not fully understood in the field, batch normalization is thought to regularize the network by introducing some randomness into the training sample. In addition to acting as a regularizer, batch normalization increases the learning rate of the networks and accelerates the learning rate decay (Ioffe and Szegedy, 2015). Hence, we implemented it after every network layer.

3.5.8.2 Dropout

Dropout is another way to regularize a network by preventing it from overfitting on the data (Srivastava et al., 2014). In dropout, a set of units are randomly selected in each layer and are left out during a training epoch (Figure 3.11). Leaving out units is temporary and probabilistic because the dropped units might be added back to the network in the next run, and the process is random. In addition, applying dropouts is an alternative way of training several different networks on the data. It offers the least expensive way to do so because it is computationally costly to train several networks and find the correct hyperparameters. Adding

dropouts inherently creates a different network. It also introduces randomness into the network, which helps to prevent overfitting.

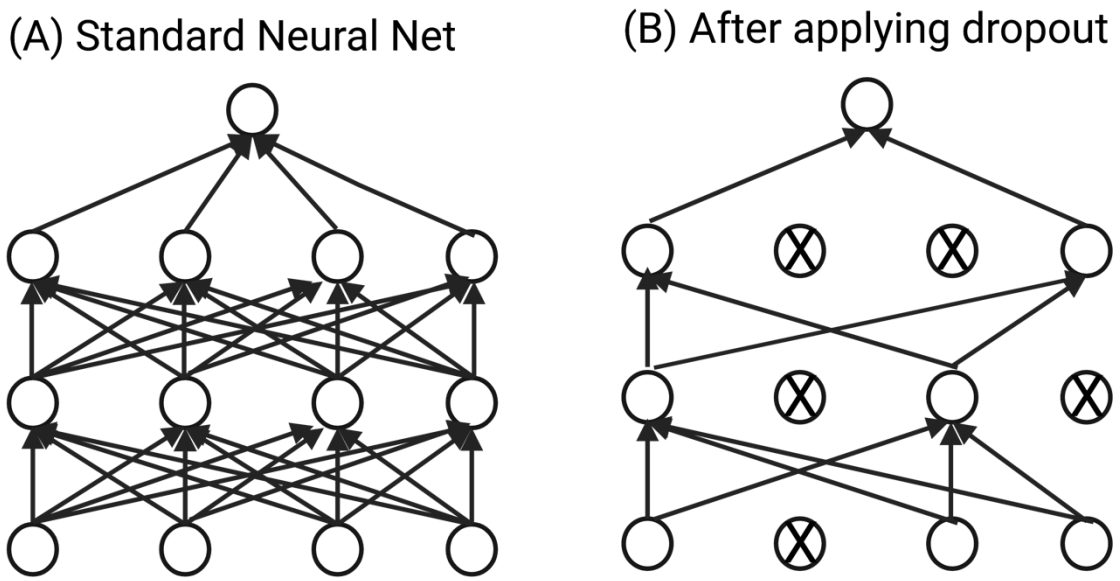

Figure 3.11. Dropout Neural Net Model. Left: A standard neural net with two hidden layers. Right: An example of a thinned net produced by applying dropout to the network on the left. Crossed units have been dropped.

The fraction of units that are dropped can range from 0 to 1. However, it is ideal that the fraction of left-out units is 0.2 to 0.5 (Srivastava et al., 2014). In our experiments, values between 0.2 and 0.5 produced similar results, so we used 0.2. Another essential advantage of having dropouts is that it allows a network to perform well on sparse data. Hence, if there are missing values in the data, which is likely due to untracked body points by maDLC or SLEAP, the network learns the underlying nature of the data and, therefore, can generate better predictions of those values. Thus, in our network, we applied dropout to every layer to increase the randomness.

3.5.9 Loss function

The loss function is used to evaluate a model's performance by calculating the deviation of its prediction from the actual data response (Mehta et al., 2019). It is sometimes referred to as the error, cost, and objective functions. In general, the closer the output of the loss function is to zero for continuous numerical data and the probability is near 0 or 1 for categorical data, the better the model is. For continuous data, the mean square and absolute errors are commonly used loss functions, and cross-entropy is a regularly used cost function for categorical data. Since our goal is to predict coordinates values for tracked points, we used mean square error for our model. It was possible to have used a regularized cost function with a Lasso regression penalty (L1 norm) or Ridge regression penalty (L2 norm). However, since we had already implemented batch normalization and dropout, we did not add those.

$$\boldsymbol{E(w) = \frac{1}{n}\sum_{i=1}^{n}(y_i - \hat{y}_i(w))^2}$$

3.5.10 Optimizers

Musstafa defines an optimizer as a learning algorithm used to minimize the loss function or maximize the accuracy of a model (Musstafa, 2021). It can be seen as a mathematical approach to adjusting the weight and biases of function with respect to the loss function. An example of an optimizer is gradient descent. Gradient descent is a standard optimization algorithm that iteratively changes the weight and biases of a model to attain the local minimum of a convex function. However, straightforward gradient descent is not applicable in most models due to certain factors, like having a complex convex and nonconvex function and a large dataset. Variations of the gradient descent, such as stochastic gradient descent with/ without momentum, and mini-batch gradient descent, introduce parameters like learning rate to help deal

with the large datasets issues and allow the functions to converge at their global minimum at a faster speed. The global minimum is the point at which the model has the lowest error. In our model, we chose adaptive moment estimation (Adam) as the optimizer. Adam is an efficient stochastic optimization that computes individual adaptive learning rates for different parameters from estimates of the first and second moments of the gradients (Kingma and Ba, 2015). Adam combines components of two optimizers, AdaGrad and RMSProp, to make it computationally efficient.

$$w_t = w_{t-1} - \frac{\eta}{\sqrt{S_{dw_t} - \varepsilon}} * V_{dw_t}$$

$$b_t = b_{t-1} - \frac{\eta}{\sqrt{S_{db_t} - \varepsilon}} * V_{db_t}$$

Where ‘w’ and ‘b’ are the weights and biases of a neuron, respectively.

3.6 Results and Discussion

Our pipeline for robustly tracking the postures of multiple animals is as follows:

(i) Given raw videos of prairie vole interaction, take random samples of images from them

(ii) Label the body parts of the animal that one is interested in.

(iii) Train maDLC or SLEAP on the labeled data

(iv) Use the trained network to make predictions on the raw videos

(v) Apply autoencoder on the tracked data generated by either maDLC or SLEAP

(vi) Manually correct swapped identities or wrongly tracked body points

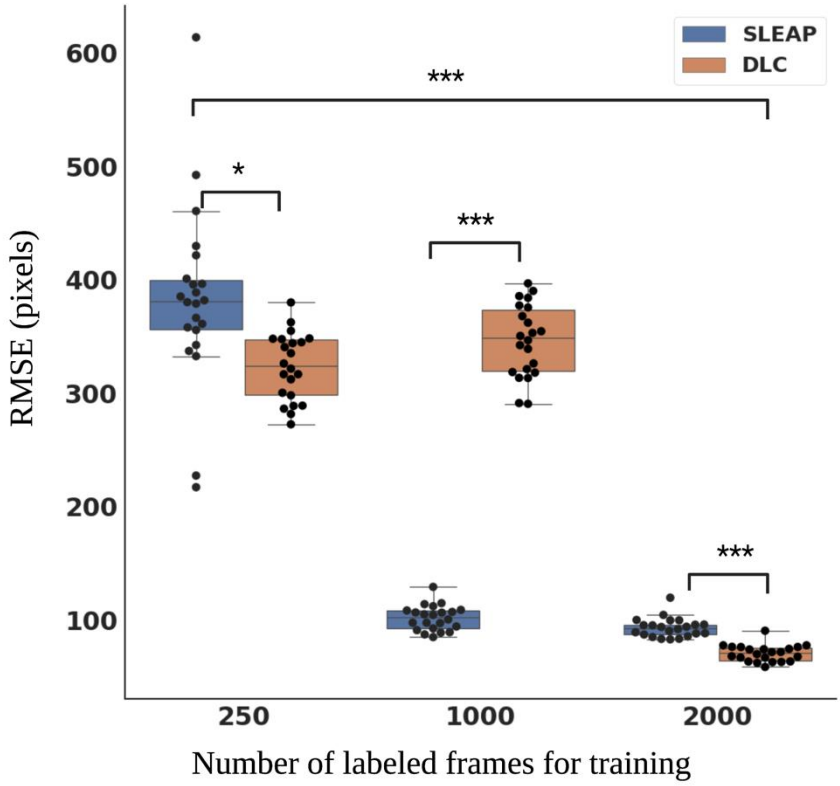

Figure 3.12. Performance of networks on different numbers of training datasets. The networks were tested on 500 frames that they were not trained on. Overall, both SLEAP and DLC performed better when trained with more labeled data. Each black point represents the average Euclidean distance (RMSE) for a body part of an individual

Following this pipeline, firstly, we had to decide on the number of annotated frames to train a maDLC or SLEAP network. Generally, the more labeled frames, the better the network's performance. Hence, to illustrate this point, we trained multiple networks on different numbers of labeled data and then tested the networks on data they had never seen before. We annotated 250, 1000, and 2000 frames with two prairie voles. Then, we trained both SLEAP and maDLC networks on the labeled data. Subsequently, we used the networks to predict a video of two voles from a different dataset, which they were not trained on. In this video, we generated 500 frames and manually annotated the body parts of the animals.

To test the accuracy of the networks, we measured the Euclidean distance (root mean square, RMSE) between the network-generated labels and those of the human scorer for the 500 frames. This metric is averaged over the set of images for each body part and each animal. In this accuracy test, the network had to correctly predict the body parts' locations and assign them to the right individual. Therefore, a high RMSE value means the network either predicted inaccurate body part location, labeled the wrong animal, or both. We observed that training the networks on 2000 frames generated significantly more accurate results than on 250 frames (had a lower RMSE value). An equivalent test of the networks on 2000 frames produced very similar results to Figure 3.12 (data not shown).

The next decision to be made regarding the pipeline is which animal tracker method should be used. We observed that with a low number of labeled (250) frames, both maDLC and SLEAP are comparably bad (SLEAP with a slight advantage). With 1000 annotated data, SLEAP significantly outperforms maDLC. However, with 2000 frames, both tracking tools produced similarly improved performances, with maDLC being a little better. At 8000 frames, the results remain comparable (data not shown). Therefore, when training with 2000 or more labeled frames, one can select SLEAP or maDLC and expect commensurable tracking results. However, as one starts to annotate more than 20,000 frames (like in our case, where we labeled 60,000 frames for the thesis work), there are rather practical considerations that need to be made. We have found that maDLC had an efficient implementation that allowed it to load and use all the labeled data to train its network. SLEAP, on the other hand, stopped working when we tried to use such a large dataset.

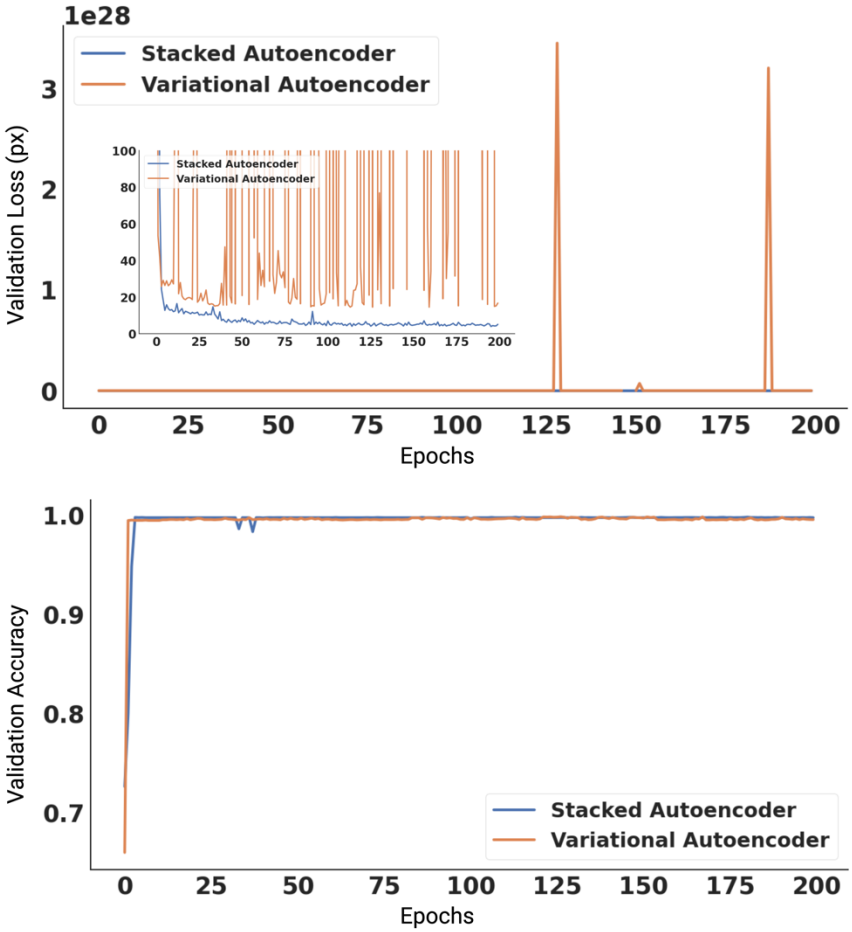

Figure 3.13. Comparison between the stacked and the variational autoencoder. The top figure shows the stacked autoencoder's lower mean squared error for the validation loss compared to the variational autoencoder. The bottom figure indicates no difference in the validation accuracy between the two models.

As we introduced at the beginning of the chapter, the tracked results generated by either SLEAP or maDLC are unreliable enough to create a behavioral space. Hence, one is likely to have a map with spurious tracking points. Therefore, we developed the autoencoder to fix the tracking issues.

Several choices were made in building the autoencoder, especially the autoencoder type. We found that the stacked autoencoder trained better on the data than the variational autoencoder (Figure 3.13). Although the variational autoencoder is generative and can create fake animal

postures (that look real) (Figure 3.9), which might be a good indication that the network has learned the representation, we observed that the stacked autoencoder had a lower validation loss (mean squared error) compared to it. The variational autoencoder is likely to have exploding gradients (unusually high values for the weights and biases of the neurons in the network), leading to generating unlikely values.

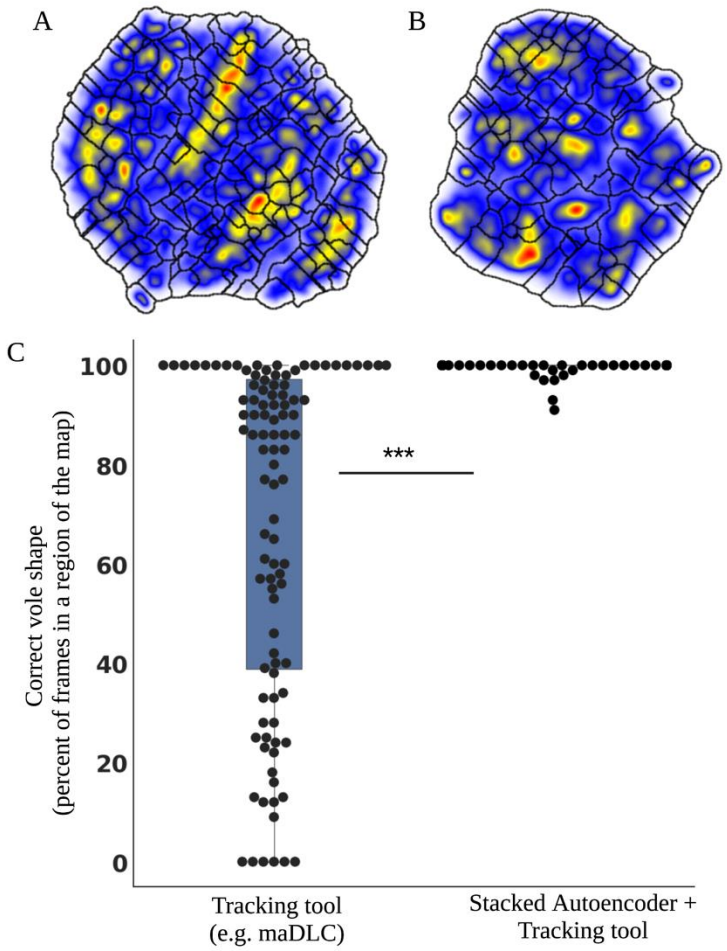

Figure 3.14. Comparing the behavioral map generated by the tracking tool and the autoencoder. A behavioral space created with only a tracking tool (e.g., maDLC) (A) and a combination of an autoencoder and tracking tool (B). C. Using GMM to if the tracked points in the behavioral regions had the correct vole shape in both A and B. The tracking improves by applying the Autoencoder to the tracked outputs from SLEAP. (***$p < 0.001$, Student t-test)

Decisions about the hyperparameters, such as the number of neurons in a layer, the number of layers, optimizers, and the activation and objective functions, are essential in designing the autoencoder's architecture. We would refer the reader to section 3.5 on the choice we made. The aim of building the autoencoder is to apply it to the trained points from either maDLC or SLEAP. However, before using it, the autoencoder must be trained similarly to the tracking tools. Therefore, we trained the stacked autoencoder to the data labeled for the tracking tools. This data is considered ground truth because it is user-curated from random frames in multiple videos where the animals assumed varying poses. This essential training process on randomly labeled frames from different videos teaches the autoencoder the postures that the animal is likely to adopt.

When we applied the trained autoencoder to the tracked data from the tracking tools, we observed a significant improvement in the accurate estimation of body points (see figure 3.7 and example videos: Bad Tracking and Good Tracking). For example, when tracking tools could not label body points on the voles (figure 3.7A), the autoencoder correctly annotated those points (figure 3.7B). In addition, when the tracking tools produced other tracking errors, such as incorrectly labeling a body point of one vole on the other (For example, tracking the left ear of vole one as that of vole two) (figure 3.7C), the autoencoder correctly assigned them to the individuals that belonged (figure 3.8D). We, therefore, see using the autoencoder as imposing an animal-like prior (in our case, a vole-like prior) on the pose estimations.

Given our primary goal to measure the social behavior of animals by creating a behavioral representation of their movement, we created maps using the tracked points with and without the autoencoder applied to them. We observed that when we quantified the regions in the behavioral map that had tracks with the correct vole shape, the map generated from the

combination of the tracking tools and autoencoder had a significantly higher percentage of the vole-like body (figure 3.14B) than the other map created with only the tracking methods (figure 3.14A). We measured the accuracy of having a vole-like shape using a Gaussian-mixture model (GMM). The GMM was initially trained to the ground truth data used to train the tracking tools and the autoencoder.

3.11 Conclusion

In this chapter, we have shown that despite the advancement in the methods to estimate the poses of multiple animals, the tools cannot robustly track the animals when they are close to each other. In addition, they are likely to swap the identities of the annotated animals. Therefore, we developed a pipeline that combines an autoencoder with multi-animal tracking tools to resolve the labeling issues. We saw a significant improvement in the tracking, which led to building a reliable behavioral map of the social interactions of the animals.

Despite the autoencoder's performance, it relies on the output of the maDLC or SLEAP as its input. This can be a significant problem when the predictions of maDLC or SLEAP are consistently wrong, i.e., the coordinates of body points are far from their desired position for a sequence of video frames. Such an instance can be seen as providing a weak or negative prior to the autoencoder model. Since our autoencoder has no image of the animal to rely on, its predictions would be wrong.

An alternative way is to build a convolutional neural network (CNN) to take the image data as input. The CNN would predict the centers of masses in the image. These centers of masses will then be used as additional input for the autoencoder. So, for the current frame, the autoencoder will compare how the predicted points are close to those values. If the centers of masses are close (in terms of Euclidean distance) to the prior predicted points for the previous frames, it would indicate that the tracking generated by maDLC or SLEAP is unreliable. The autoencoder would generate an animal-like shape guided by the earlier prediction and adjusted based on the centers of masses.

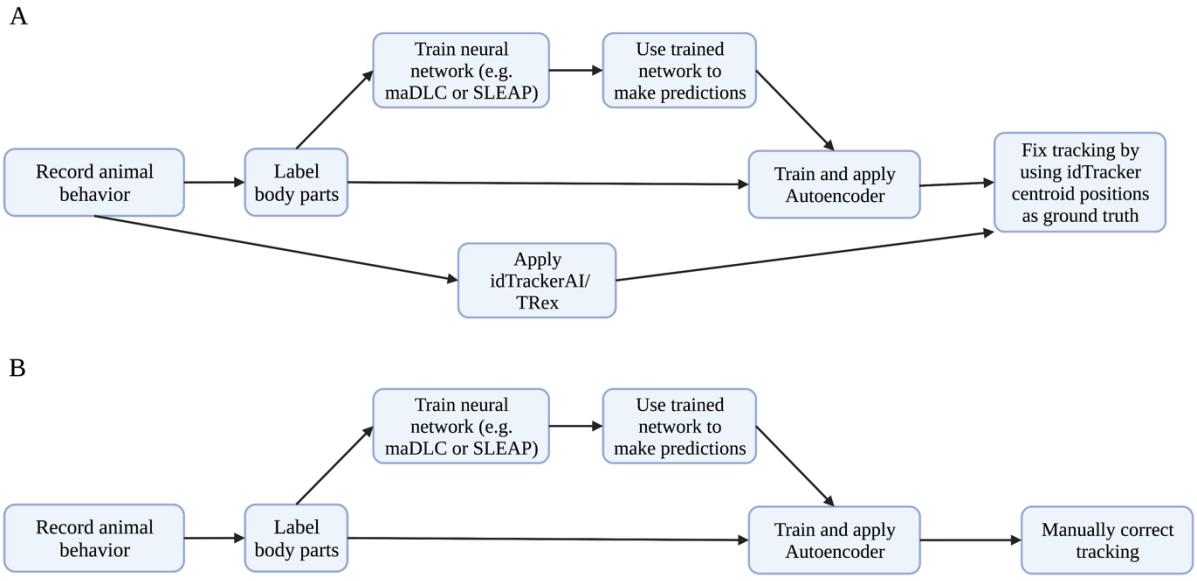

Figure 3.15. Pipeline for robustly tracking multi-animal poses. A schematic of the pipelines for fixing tracking errors using Autoencoder combined with idTracker/TRex (A) or manual correction (B).

One lingering issue that is a significant drawback for all the methods, including the autoencoder, is the swapping of animal identities. Similar to switching individual body points, swapping of tracked identities is likely to happen when animals huddle, are involved in a prolonged fight, and frequently cross each other's path. We tried using idTracker Field (Romero-

Ferrero et al., 2019) and TRex Field (Walter and Couzin, 2020) to resolve this problem. TRex is another multi-animal centroid tracking tool that works similarly to idTracker. idTracker and TRex are highly optimized to maintain the identities of multiple animals (up to a hundred). Therefore, the approach we adopted (as illustrated in Figure 2.15) was to track the video data with either idTracker or TRex and use the centroid positions they generated as ground truth to adjust the tracking after applying the autoencoder. However, we noticed that idTracker and TRex still struggled to correctly identify and maintain the animals' identities.

Thus, the ultimate approach we used in this thesis work was manually correcting the missed tracking and the swapping identities. Therefore, after applying the autoencoder, we manually stepped through each frame of tracked points and fixed those instances where swapping occurred. Although it was prohibitively time-consuming, it was guaranteed to ensure accurate tracking over time.

In the next chapter, I will show how we use this pipeline to quantify the social behavior of prairie voles as they form pair bonds.

Chapter 4. QUANTIFYING THE REPERTOIRE OF BEHAVIORS INVOLVED IN PRAIRIE VOLE SOCIAL BOND FORMATION

4.1 Introduction

In this chapter, I leverage the pipeline discussed in chapter 3 to track the social behavior of prairie voles as they form social bonds. Using the tracked postures, I apply both unsupervised and supervised machine learning approaches to investigate the behavioral repertoire of prairie voles with genetically modified oxytocin receptors (OTRs). Specifically, I study voles with OTRs globally knocked out (both centrally and peripherally) using clustered regularly interspaced short palindromic repeats (CRISPR). With the CRISPR knockout (CRISPR KO) voles, I first replicate a recent finding about the role of OTRs in social bond formation. Then applying an unsupervised behavioral mapping approach, I extract the behaviors of the voles as they form pair bonds. In comparing CRISPR KO voles to wild-type control animals, I examine the subtle behavioral differences that are likely to emerge between the two groups. Finally, I take advantage of a supervised machine learning classifier to identify the subtle behavioral differences between the CRISPR KO and wild types as they form pair bonds.

4.2 Background

Pair bonding is a complex social process that involves behavioral changes across contexts during sociosexual interactions. During the formation of a pair bond, animals perform many different actions, such as chasing, fighting, allogrooming, mating, and huddling, with the repertoire of these behaviors evolving over time as the nature of the social bond changes. These changes can be thought of as alterations in an animal's underlying "hidden state" of social

engagement (Tinbergen, 1952; Dawkins, 1976) (e.g., when one shifts from being unfamiliar to familiar to being closely bonded with another).

The formation of these pair bonds in animals is thought to be modulated by neurochemical systems acting within the brain to influence the behaviors of the animals to move towards a state of pair-bondedness. One of these neurochemical systems is the oxytocin system (OT), among several others, like arginine vasopressin, dopamine, and serotonin. The OT system is thought to act within the social brain network to promote social bond formation, maternal care, empathy-related behaviors, and parturition and lactation (Sue Carter et al., 1995; Insel and Young, 2001; Numan and Young, 2016; Walum and Young, 2018). The activity of OT is mediated by its highly selective receptors, OTRs. Although recent evidence indicates that there is a cross-talk, where the OT molecule can bind to vasopressin receptors (Kimura et al., 1994; Hawtin et al., 2000; Song et al., 2014).

The OTRs are G protein-coupled receptors widely expressed throughout the body and brain; they can be found in the uterus, kidney, heart, mammary gland, and brain (Gimpl and Fahrenholz, 2001). In the periphery, the binding of OT to the OTRs is implicated in mediating reproductive functions in both females and males, like parturition and lactation and erectile function and copulation, respectively (Dale, 1906; Summerlee and Lincoln, 1981; Swaney et al., 2012). In the brain, they are densely expressed in the social brain areas, like the nucleus accumbens, the amygdala, the prefrontal cortex, and the olfactory bulb, and are implicated in mediating social behavior, specifically pair bonding (Shapiro and Insel, 1992; Olazábal and Young, 2006).

Early work with OTRs shows that intracerebroventricular (ICV) injection of oxytocin receptor antagonist (OTA) inhibits pair bond formation (Williams et al., 1994). Even after

mating (since mating is thought to facilitate bond formation), when an OTA is centrally infused into the brain, it reduces the preference for a partner (Insel and Hulihan, 1995). Using viral techniques such as RNA interference to knock down the OTR in the accumbens, thereby reducing its density, inhibits pair bond formation (Keebaugh et al., 2015). Conversely, taking advantage of this viral technique to overexpress the OTRs within the accumbens via viral-mediated gene transfer also facilitates the formation of partner preference in the prairie voles (Keebaugh and Young, 2011). Related to the individual genetic variation of the OTRs in the accumbens, voles that have a high expression of OTR show a significant preference for the partners compared to voles with a low expression (King et al., 2016).

Most of these studies revealing the role of OTRs in pair bonding were performed in prairie voles (*Microtus ochrogaster*). The prairie voles have emerged as a premier animal model for studying pair bonding. They are among the few percentages of mammals that are capable of forming pair bonds that involve biparental care, where both sexes contribute equally to naturing the young and defending their territory against intruders. In addition, the pair bonds formed by the voles are robust because it is observed both in the field and the lab (Getz et al., 1981). When prairie voles are tested in a partner preference test, a simple behavioral paradigm to assess the choices of the animal (Williams et al., 1992), the paired individuals spend most of the time in side-by-side physical contact with their partners compared to strangers, animals that are novel to the pair (Gavish et al., 1983; Carter et al., 1988). In addition to the selective preference for their partners, paired males and females that have had sexual contact show highly aggressive behaviors toward unfamiliar conspecifics as a way to guard their mates compared to sexually naïve individuals (Getz and Carter, 1980; Gavish et al., 1983).

Contrary to what was previously thought of as the role of OTR in pair bond formation, a recent publication tells a different story. Berendzen and colleagues show that OTRs are not necessary for pair bond formation (Berendzen et al., 2022). Using a viral technology, CRISPR-Cas9, they selectively knocked out the OTRs in the prairie voles, creating a mutant CRISPR knockout (CRISPR KO) voles null for the receptor. Their results indicate that the CRISPR KO voles, both males and females, show a strong preference for the partners when assayed with the pair preference test after seven days of pairing the mutant voles with opposite-sex wild types. In addition to being able to form pair bonds, the mutant voles displayed aggressive behaviors towards unfamiliar animals in the partner preference paradigm. They also found that the mutant voles showed bi-parental care and could bear viable pups similar to wild types. Before this work, Horie and colleagues, who developed mutant voles with the same viral technology, showed that the CRISPR KO voles exhibited alloparental behavior, as observed in wild-type animals, and were likely to spend significantly more time with another vole rather than an empty cup (Horie et al., 2019).

In light of these results, several questions arise: what is the role of the OTRs in pair bonding if the end state of forming a bond is still achieved without them? Do the OTRs play a role in the overall social behaviors of animals? It is challenging to imagine that the OTRs highly expressed in areas of the nucleus accumbens, amygdala, prefrontal cortex, and brain regions considered part of the social centers do not have an adaptive benefit. In addition, OTR's expression in the brain varies widely from one species to another. For example, even within closely related species like prairie voles and meadow voles, there is a higher concentration of OTRs in the nucleus accumbens and amygdala in the prairie voles than in the promiscuous meadow and montane voles (Shapiro and Insel, 1992; Olazábal and Young, 2006). Even within

the same species, there is a natural variation of the OTR expression in the brain. Due to a single nucleotide polymorphism in the gene, some prairie voles have a high expression of OTR in the nucleus accumbens than others with low expression in the same brain region (King et al., 2016).

Given our decades of knowledge about OTRs, and that the publication by Berendzen et al., was only the recent work to show the counterevidence, we wanted to replicate their (Berendzen and colleagues) work to observe whether knocking the OTR with CRISPR-cas9 does not prevent the prairie voles from showing a preference for the partners. Secondly, much of the work involving the role of OTR in pair bond formation has primarily been centered on the end state of it, measuring the preference of vole for its conspecific partner using the partner preference assay(Williams et al., 1992; Keebaugh et al., 2015; King et al., 2016; Berendzen et al., 2022). There has been less work looking at the behavioral repertoire of the animals as they form pair bonds. For example, although Horie et al. measured social novelty, a test to detect the preference for investigating an unfamiliar conspecific compared to a familiar one, they did not analyze the behaviors performed during the familiarization process (Horie et al., 2019).

Given that the OT system is thought to modulate the behavior of animals during social interactions by mediating the social recognition and identity of a conspecific individual and developing an association of a rewarding encounter with that animal (Ferguson et al., 2001; Okuyama et al., 2016; Shamay-Tsoory and Abu-Akel, 2016; Walum and Young, 2018), we hypothesized that the OTRs modulate the social dynamics of between prairie voles as they form pair bonds. By leveraging our ability to knock out the OTRs specifically, we could investigate how the behaviors of the mutants differed from the wild-type animals during bond formation but not only at the end state. Moreover, Berendzen and colleagues measured the end state of the pair bonds by performing the partner preference test assay and did not quantify the behavioral

interaction of the voles as they formed the pair bond. Therefore, we wanted to measure the behavior of the prairie voles as they formed pair bonds.

4.3 Materials and Methods

4.3.1 Experimental Model and Subject Details

The prairie voles (Microtus ochrogaster) laboratory-bred at Emory University were initially caught from the field in Illinois, USA. After weaning at postnatal day P20-23, the animals were housed in groups of two to three voles of same-sex siblings per cage.
The animals were maintained on a 14:10 light/dark cycle with a temperature of 68 – 72 degrees Fahrenheit and humidity at 40-60%. They had ad libitum access to food (lab rabbit diet HF #5326) and water. Their cages were enriched with cotton pieces so that they could build nests. The experiments were conducted in accordance with the guidelines of the National Institutes of Health Guide for the Care and Use of Laboratory Animals and were approved by the Emory University Institutional Animal Care and Use Committee.

4.3.2 CRISPR/Cas9 knockout prairie voles

The CRISPR-Cas9 knockout prairie voles were made according to the protocol developed by Horie (Horie et al., 2019; Horie and Nishimori, 2022), who specifically created the animals that were used in this experiment. In summary, an embryo taken from an ovulating female prairie vole is injected with Cas9-sgRNA ribonucleoprotein. The single guide RNA is a type of RNA molecule that binds to Cas9, an endonuclease, and directs it (Cas9) to the target DNA. The Cas9 acts as molecular scissors to cut DNA at the location specified by the guide RNA. The infected embryos are then transferred into pseudo-pregnant recipient females who

carry them until they deliver newborns. Tissues from the fingertips of the pups at P5 or ear punches at p21 are genotyped to check for the deletion of OTRs. To expand the colony, the founder voles, the first genetic line with knocked-out OTRs, are mated with wild-type partners to yield more knockouts.

4.3.3 Animal Types

We used only female prairie voles as the subject animals. We used 16 CRISPR KO and 12 wild types (WT) females. The WT females were siblings of the CRISPR KO voles. Their male conspecifics used in either the pairing or the other experimental recordings were WT animals. Both the female and male animals were sexually naïve, and also, the females were not ovariectomized or estrogen-primed for the experiments.

4.3.4 Behavioral Paradigm

Once the voles were of adult age, after 60 days, they were used in the experiments. The behavior of the voles was recorded as illustrated in the figure 4.1. We initially placed the subject vole (a CRISPR KO or WT animal) in a chamber (24 inches wide by 12 inches high and breadth of 12 inches) separated by a Plexiglas with a novel (WT) or the partner-to-be (WT) animal for 30 minutes. It was done to get an idea of the behavior of voles when they are alone but in the presence of another individual separated by a divider. To allow social stimulus transmission between the separated voles, we used transparent Plexiglas with multiple holes (1/16 inches in diameter) drilled in them so that the animals could see and smell the other conspecifics. We randomly alternated the individual recorded with the subject. If the subject was recorded with a novel animal in the first session, then in the second session, they were recorded with their

partner-to-be. Vice versa, the subject could have been recorded with the partner-to-be in the first session, then with the novel animal in the second session.

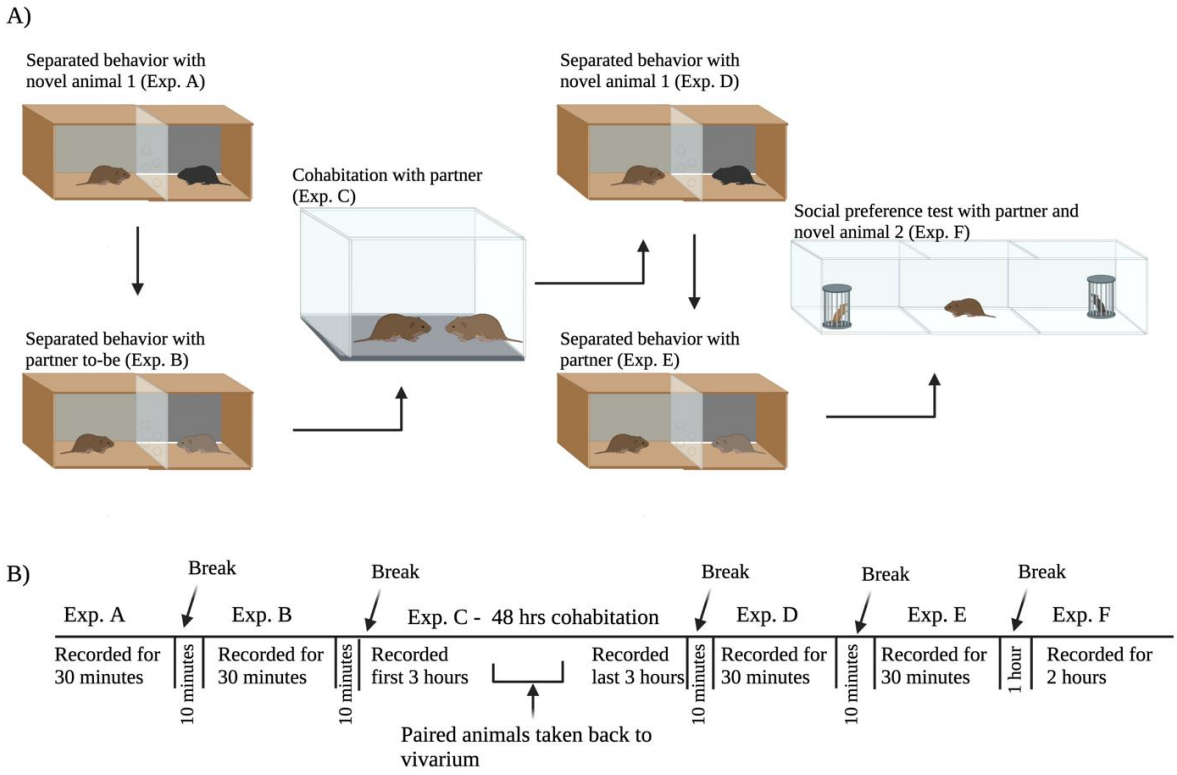

Figure 4.1. The experimental paradigm with its timeline. The subject voles were initially recorded with a novel animal or the future partner (Exp. A) in a chamber separated by a transparent divider. If they were recorded with a novel animal in Exp. A, then in Exp. B they were paired with the future partner animal or vice versa. The subject animal was paired with their partner for 48 hours. Following the cohabitation, the solo separated behavior was repeated in the same order as before the cohabitation. Therefore, Exp. A == Exp. D and Exp. B == Exp. E. After it, we performed a social preference test for 2 hours.

Following the modified open field test, a solo separated session, we paired the subject animals with their partners for 48 hours. Previous studies have shown that at least 24 hours of cohabitation is sufficient to induce a partner preference, where individuals spend more time huddling with their partner compared to a stranger in a partner preference test (Williams et al., 1992). We recorded the first and the last 3 hours of the cohabitation. When they were not being

recorded, the paired animals were placed in their home cage and taken back to the vivarium. After cohabitation, we repeated the solo separated experiments in the same order as before the pairing. We did this experiment to see if the animals altered their behaviors after they were paired with their partner.

Following this experiment, we performed a social preference test (SPT). The SPT is slightly different from the partner preference test, with the difference being that the partner and stranger are placed under a cup instead of being tethered in the SPT. The stranger in the SPT differs from the animal used in solo separated behavior recordings. We used a rectangular arena (30 x 8 inches) and put the partner and stranger under rectangular metallic cups (7 inches wide by 4 inches high and breadth of 4 inches). The mesh-like metallic cups were placed at the ends of the arena. The WT male animals were placed under the cups before the female CRISPR KO or WT animals were introduced into the middle of the chamber. We allowed the females to explore the arena for 2 hours and recorded the session.

4.3.5 Tracking animals

As discussed in chapter 3, we developed a custom pipeline that combines multi-animal deep learning pose estimation technology, such as maDLC (Lauer et al., 2022) and SLEAP (Pereira et al., 2022), with an autoencoder to robustly track multiple animals (Figure 4.2). By adding the autoencoder, we can obtain detailed and high-accuracy postural trajectories of various animals. The pipeline helped us track instances, like when the animals spend more time with each other during behaviors such as huddling, mutual grooming, and mating, that are key to the social behavior of the voles. Although we had significant improvements in the tracking (please refer to chapter 3), there are times when the tracked points swap identities between animals. It is

a worrying limitation because it is ideal that we know the identity of the animals throughout the entire recording.

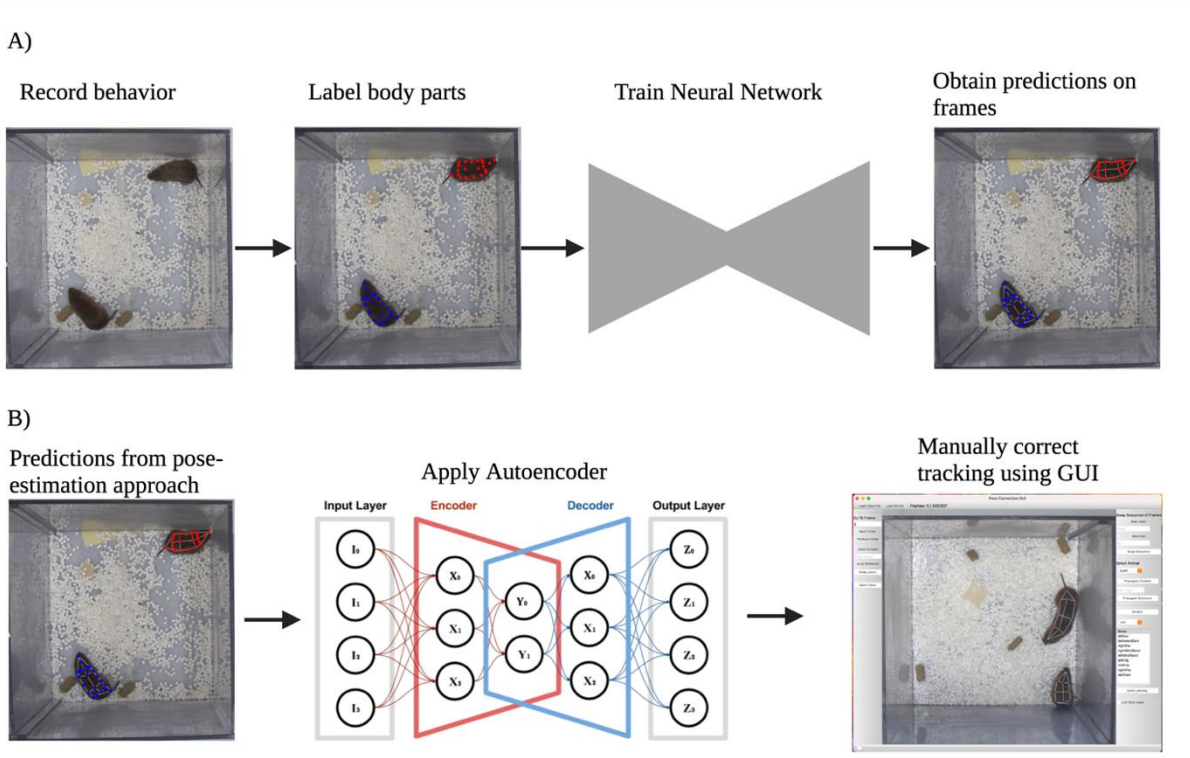

Figure 4.2. Pipeline for robustly tracking animals. A) The pipeline to implement a multi-animal pose-estimation deep learning method to track the posture of the animals. B) Adding an autoencoder to improve tracking and manually correct the swapped animal identities with the aid of a GUI

To address this issue, we initially added a step to the pipeline by using idTracker (Romero-Ferrero et al., 2019), another deep-learning approach, to track the identities of animals. However, we realized that idTracker wasn't robust enough to maintain the animal's identities in every instance. Hence, we manually corrected the swapped identity by stepping through the video frames. I built a graphical user interface (GUI) to make it easier to fix the identities (https://github.com/senakoko/poseCorrectionGUI). For the analysis in this dissertation, I used

maDLC and trained the network on approximately 60,000 frames, although the creators suggest using 500 frames. I found that even 8000 frames could not generate a well-trained network. Given such a large training dataset, I discovered that the maDLC was better at handling the data than SLEAP. maDLC had a better algorithm for loading the data into the computer's memory and graphical processing unit (GPU), which is used to train the network, than SLEAP. I tracked 11 body points on each animal, which included points from the nose to the ears and along the body trunk to their tails.

4.3.6 Unsupervised mapping of behaviors

Given our accurate and detailed frame-by-frame tracking of the posture of animals, we proceeded to measure their behaviors. One approach to quantify the behavior of the voles is to use the tracked x and y coordinates of the animal's center of mass to extract the trajectory and other metrics like the distance traveled and the animal's speed. Although such metrics help determine the locomotory behavior of the animals, they provide limited information about the animal's behavioral repertoire, such as huddling and mating. We decided to use an unsupervised behavioral mapping approach, MotionMapper, (Berman et al., 2014), to measure the behavioral repertoire of the animals. This method takes an unbiased approach to extract stereotyped behaviors (where stereotyped behaviors refer to repeatable behavioral actions). Therefore, instead of a supervised machine learning approach (to be discussed later), where behaviors, such as huddling and escape, are predefined, the unsupervised MotionMapper helps avoid the human bias in scoring behavior and allows the revelation of the unknown subtle behaviors. In this analysis, we only applied the MotionMapper to only the first three hours of cohabitation data, not the last three hours, or the solo-separated behavior and SPT. We did this to avoid the behavioral

map being heavily skewed to stationary-like behaviors like huddling and sitting idle since they are common during solo and SPT periods.

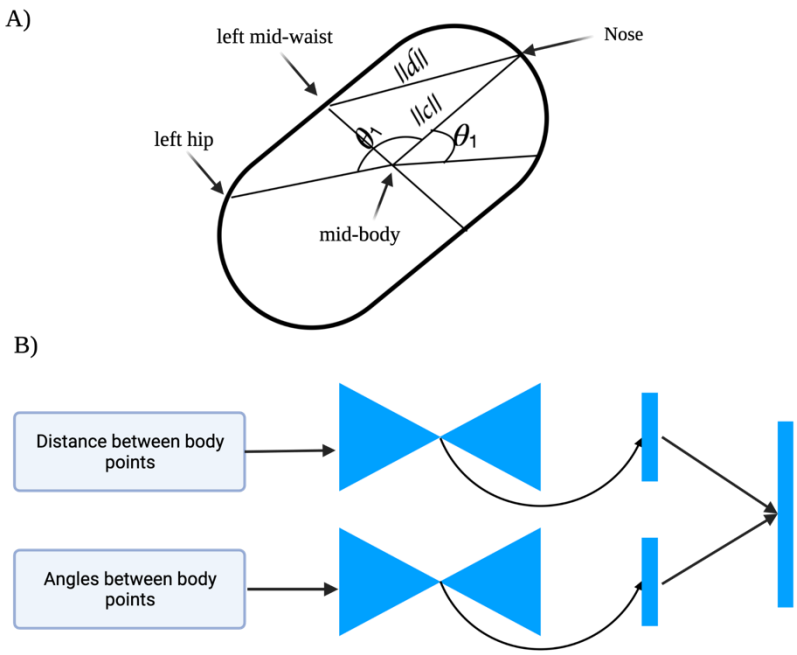

Figure 4.3. Calculating the metrics for MotionMapper. A) Schematic for calculating the Euclidean distances and 'Joint' angles between body points. B) Pipeline for generating a low-dimensional set of time series for MotionMapper.

4.3.6.1 Transforming input data for MotionMapper

To implement MotionMapper, we modified the pipeline and parameters used in the original method to extract the behavior of animals. Since we tracked the body points of the animals, instead of an image as used in the initial approach, we calculated the Euclidean distances between these points on the vole (Figure 4.3). Therefore, for each body point, e.g., the nose, I measured its distance to all other tracked points, like the animal's left and right ears, hips, and tail. Since the voles were of different sizes, I normalized the distance by the area of the animal. I assumed the shape of the vole to be an ellipsoid, so I calculated its area.

$$A = \pi * a * b.$$

a – the distance between the nose and mid-body

b – the distance between the mid-body and the left/right end of the mid-waist of the body

Since the area of the vole would vary at different times based on the animal's posture, I calculated its area at 1000 random time points and found the median value. That median value was used to normalize the distances. In addition to finding the distances, I found the "joint" angles between body points, for example, between the nose, mid-body, and left ear. However, unlike the distance, I did not need to normalize the angles since that would not be affected by the size of the vole. Therefore, by measuring the Euclidean distances and "joint" angles, when the animals performed a movement like running, grooming, rearing, and turning left or right, those actions were captured by a change in the magnitude of those values.

By measuring those metrics, we created a high-dimensional time series with 55 and 16 features for the distances and angles, respectively. Since some of the features are highly correlated and it is computationally expensive to work with 71 features, we decided to reduce the dimensions of the data using an autoencoder. As discussed in chapter 3, the autoencoder functions like a non-linear principal component analysis (PCA). We decided that instead of combining the distance and angles into one data unit, we would treat them separately since they are different units. Therefore, we applied a separate autoencoder to the distance and angles (Figure 4.3). While there is no rigorous manner to determine the number of features for the reduced dimension, we used a PCA to determine the lower bound of dimensionality reduction, given that 95% of the variance is explained. We found that a lower dimension of 8 for each metric was ideal. Therefore, combining the latent representation from both autoencoders, we

have 16 features represented in the same unit. We then standardize each feature by centering it to its mean and scaling it to the unit standard deviation.

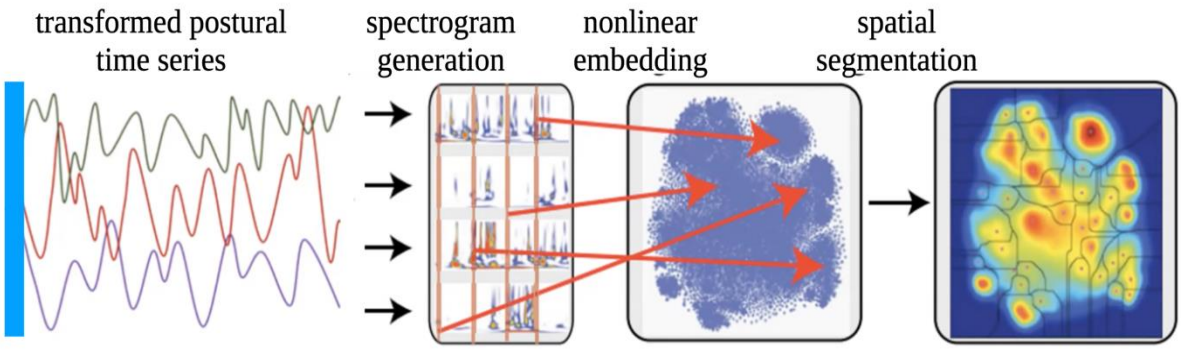

Figure 4.4. Pipeline for MotionMapper. A Morlet wavelet transform is applied to the transformed postural time series to create a spectrogram for each feature. Subsequently, t-SNE is used to map each point in time into a two-dimensional plane, and that is then clustered into 'behavioral' regions by a watershed transform. (Adapted from Berman et. al., 2014)

4.3.6.2 Overview of modified MotionMapper pipeline

As performed in previous studies (Berman et al., 2014; Klibaite and Shaevitz, 2020; Overman et al., 2022), we applied a Morlet wavelet transform on the latent postural time series data to generate a spectrogram. This wavelet transformation creates a multi-scale time and frequency resolution allowing for the representation of the postural dynamics at different time scales. This idea of transforming the data from the time to frequency domain is critical to quantifying the stereotypy of behavior. We sampled 50 points dyadically spaced between a minimum frequency of 0.5 Hz and a maximum of 15 Hz (determined by the Nyquist frequency of sampling frequency data, which was 30 Hz) from the spectrogram generated by the Morlet wavelet transform. Therefore, for each feature in the latent representation (16 in total) from the transformed postural time series, we have 50 frequency channels, resulting in 800 (16*50) dimensional feature vectors encoding the postural dynamics.

Given that most of these features are strongly correlated, we applied a non-linear dimensionality reduction technique, t-distributed stochastic neighbor embedding, t-SNE, to reduce the dimensions. Maintaining the same parameters (like the perplexity) as used in the original method (since changing them did not alter our results), we used t-SNE to create a two-dimensional (2-D) probability density function (PDF) across the map of the postural dynamic.

We then applied a watershed transform to a gaussian smoothed 2-D transform from the t-SNE. The watershed algorithm captures repeated motifs as stereotyped behaviors by assigning data points to the same cluster that reach the same local maximum by ascending a local gradient.

4.3.7 Supervised extraction of behavior

The results obtained from the unsupervised mapping of behavior can sometimes be a bird-eye view of behaviors and, as we shall see later in the results section, behaviors that occur less often but share a similar frequency pattern with those that occur frequently can be lost in the classification of behaviors extracted. Therefore, we decided to implement a supervised machine-learning approach to classify behaviors, such as oral and anogenital investigation, approach, attack, and escape, usually observed during a social interaction between animals. We leveraged the metrics, like the Euclidean distances and angles, computed from the unsupervised approach and included additional calculations to create a feature space. We calculated the distances between the nose and mid-body of one animal to the other body points of the second animal. We also found an individual's orientation (angle from -180 to 180 degrees) relative to the other and computed each animal's speed at different time lags (from 1 to 10). We proceeded to score the cohabitation videos for behaviors, like oral and anogenital investigations, investigating the side of an individual, approach, attack, escape, and huddling, by marking the video frame at which

they start and stop. I have uploaded samples of the classified videos to Git Hub (https://github.com/senakoko/Thesis_Videos). To aid the process of marking the start and stop frames, I built a GUI (https://github.com/senakoko/behaviorMarker). Given the features and the marked frames associated with the behaviors, we trained a support vector machine (SVM) to classify them.

4.3.8 Statistical analysis

We performed a non-parametric analysis in all cases when we evaluated for statistical significance. We chose an alpha value of 0.05. When we were comparing repeated measures of the samples, we performed a Wilcoxon signed rank test and did Mann-Whitney test for the independent group analysis. We used factorial analysis of variance (ANOVA) to compare multiple groups, followed by post hoc comparisons with Mann-Whitney. The data were shown as mean ± standard error of the mean (SEM). All statistical analysis was performed using Scipy (version 1.10. 0) and Statsmodel (version 0.13.5) in Python.

4.4 Results

4.4.1 Oxytocin Receptor Knockout voles can form social bonds

We sought to investigate whether the CRISPR KO voles could form social bonds and, in a way, replicate the results published by Berendzen and colleagues. We paired sexually naïve CRISPR KO female voles with wild-type (WT) males for 48 hours. Similarly, as controls, we paired naïve WT female voles with WT males. After the cohabitation, we performed modified partner preference tests – social preference tests (SPTs) to evaluate the preference for a partner over a novel stranger. The WT males (both partner and stranger) were placed under cups,

restricting them from initiating the approach toward the experimental females and making physical contact with them.

We evaluated the time the experimental females spent in the partner and stranger zones (within 3 inches from the edge of the cup) (Figure 4.5.A). We observed that CRISPR KO voles spent significantly more time in their partner zone than in the stranger zone, and similarly seen for the WT animals (Figure 4.5.B). When we broke the time spent in the zones into 10-minute time blocks, the CRISPR KO spent a considerable amount of time in their partner's zone after the first 20 minutes, similar to the WT animals (Figure 4.5.C). We decided to investigate the total distance traveled by subject animals to identify if there were any locomotory differences. Although we observed that in the 2 hours of SPT, the CRISPR KO and WT animals traveled more within their partner's zone, we did not see any difference between them (Figure 4.5.D). However, when we broke the distance traveled into 10-minute blocks, the WTs traveled more in their partner's zone within the first 20 minutes than the CRISPR KO voles. This increase in the distance traveled observed in the WTs is due to them moving around more in their partner's zone. The increased movement might be necessitated by their partner's activity under the cup. However, since we cannot track the partners due to the occlusion by cup, we are unable to completely ascertain how much of their behavior influences the behavior of the subject animals. From the overall results of the time spent and distance traveled, we observe similar outcomes as Berendzen and colleagues in that CRISPR KO animals show a strong preference for their partners.

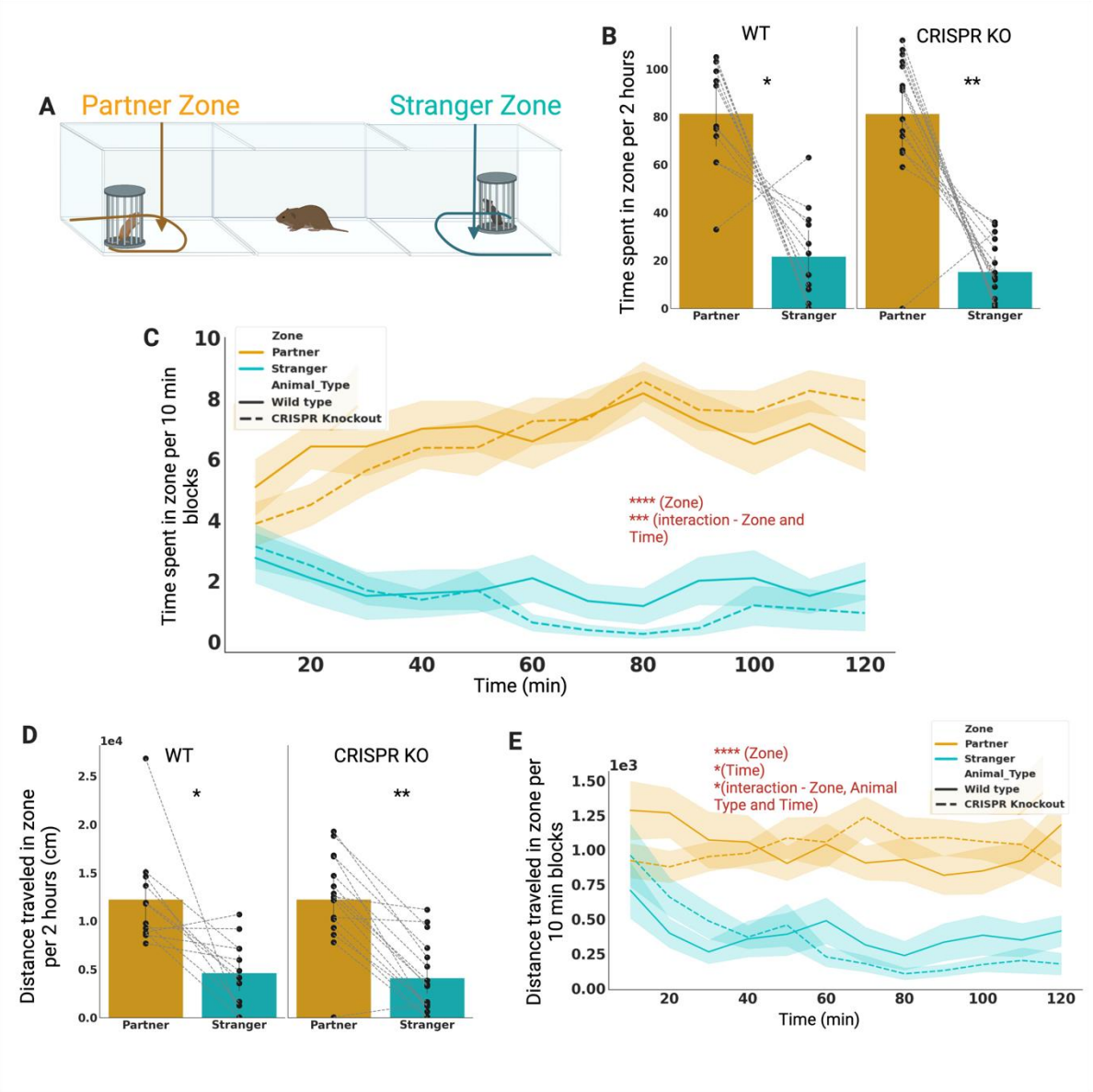

Figure 4.5. Female CRISPR KO shows pair bonding behaviors. A. Schematic of social preference test. B-C. CRISPR KO, like WT, animals spend more time in their partner's and stranger's zone for 2 hours (B) and within 10-minute blocks (C). D-E. CRISPR KO and WT travel more in their partner's zone than in the stranger's. Mean ± SEM, n= 12 WT and 16 CRISPR KO; *p<0.05, **p<0.01, ***p<0.0001; N.S., not significant

4.4.2 Knocking out OTRs does not impair social curiosity and locomotory behavior

Given that the OTRs have been implicated in social behavior, we wondered if they modulated the behaviors of the animals during social interactions. Therefore, we wanted to

quantify the behavior of the voles as they formed a pair bond. However, before analyzing the social interaction during cohabitation, we sought to identify whether, by knocking out the OTRs, the behavioral activity of the voles, such as locomotion, would be altered.

We performed a modified open field test where voles were placed in a chamber separated from a conspecific who could be a potential partner or a stranger (Figure 4.6.A). Hence, this modified open field had a social component, which is different from the traditional open field test - a solo animal behavioral measure without any other individual in the vicinity of the chamber. In this separation, the subject vole could see and smell the to-be partner or novel animal because we used a transparent Plexiglass and drilled several holes in it to allow the flow of scent. Since the OT system is implicated as a critical regulator of anxiety-like behavior and

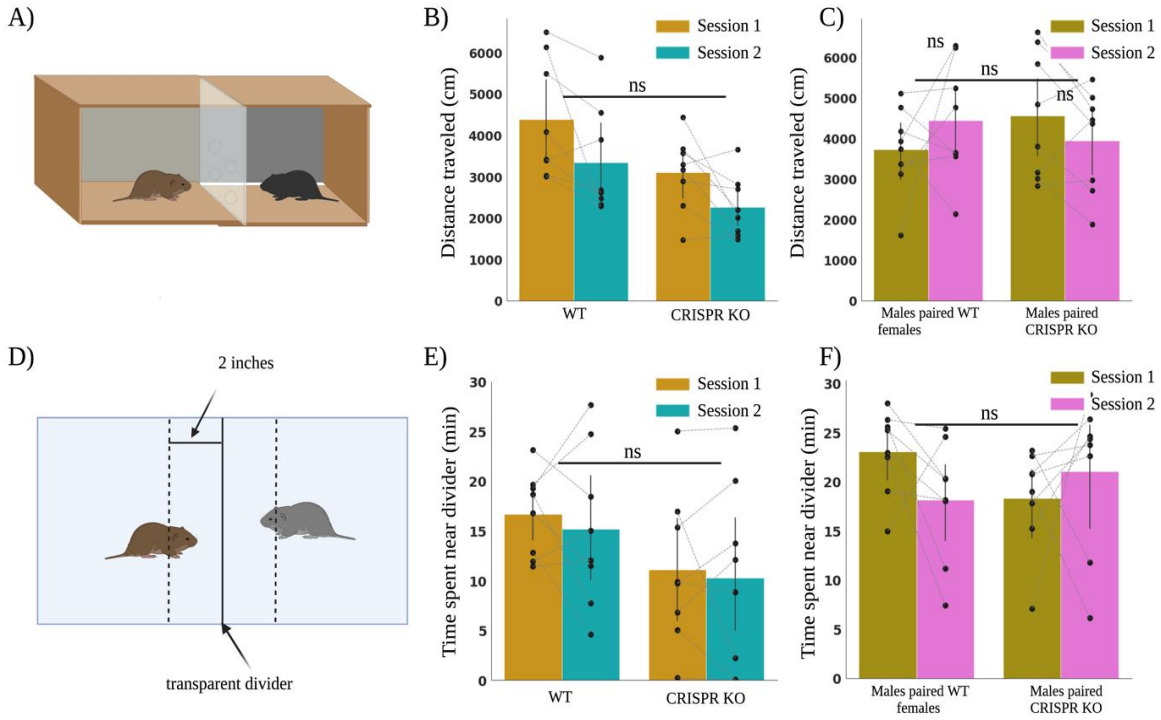

Figure 4.6. CRISPR KO female prairie voles do not show any deficit in locomotor activity. A. Schematic of the behavioral paradigm. A transparent divider with holes is used to separate animals. B – C. The total distance traveled by animals in both the first and second sessions. D. Schematic showing distance threshold to consider an animal near the divider. E-F. Time spent near the divider by the animals. *p<0.05, **p<0.01, ***p<0.0001; ns, not significant

social curiosity (Pisansky et al., 2017; Cohen and Shamay-Tsoory, 2018), would the knockout voles move around less frequently and spend less time near the divider that separates them?

We quantified the locomotor activity of the animals in both sessions when recorded with a future partner and a novel. We observed that CRISPR KO significantly moved around less when compared to the WTs (ANOVA, p-value = 0.007) when the results of both sessions were combined, and it was significantly less in the second session than in the first (ANOVA, p-value = 0.03). However, when considering it as two separate experimental sessions, although the CRISPR KO animals were less likely to move around, we did not see any significant difference between them and the WT animals (p-value = 0.12 in session 1 and p-value = 0.08 in session 2, calculated using Posthoc Mann-Whitney non-parametric test) (Figure 4.6.B, Appendix A.2.1). When we looked at the time spent near the divider, which is a reflection of social curiosity and novelty – the interest to investigate another animal that can be sensed, we did not see a significant difference between the CRISPR KO and WT animals (p-value > 0.05 in both sessions 2, calculated using Posthoc Mann-Whitney non-parametric test) (Figure 4.6.E, Appendix A.2.2). However, we did notice that WT males were likely to move around more and spend a significant amount of time near the partition than the female CRISPR KO animals. Taken together, the OTR does not influence the anxiety-like, and social curiosity-like behavior in female prairie voles. However, there is some activity-like difference between the female CRISPR KO animals and WT animals. This activity-like result is different from what was observed by Horie and colleagues (Horie et al., 2019). The difference is likely due to a behavioral setup. In Horie et al., they performed a traditional open-field test; hence the presence of another individual cannot influence the behavior of the subject animal.

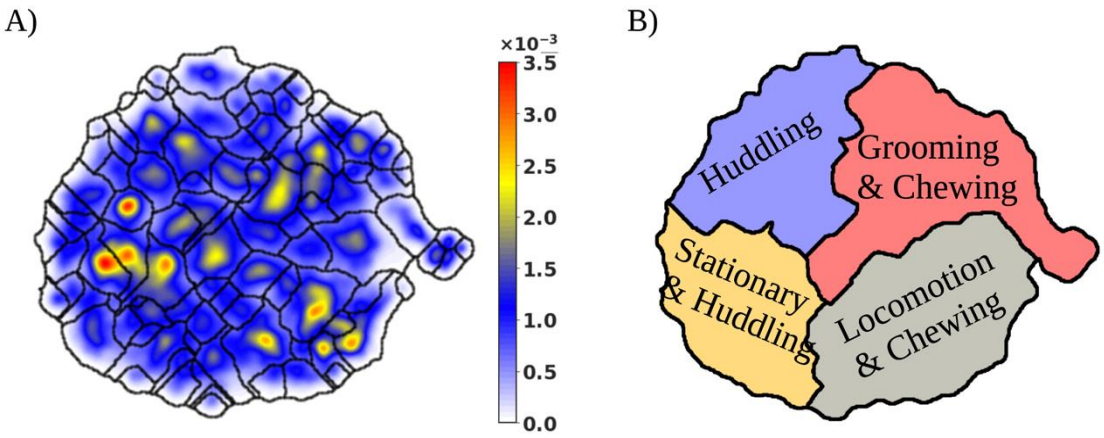

Figure 4.7. Behavioral map of the voles during the early phase (first 3 hours) of cohabitation. A) A PDF of the stereotyped behaviors marked by boundary lines from the watershed transform B) Hierarchical cluster of behaviors into coarse-grained regions

4.4.3 Examining the behavioral repertoire of prairie voles during the early phase of cohabitation

Since we did not find any substantial difference (except for a likely increased locomotor activity) in CRISPR KO and WT animals in the social preference test and modified open field test, we sought to investigate the role of OTR in pair bond formation. We recorded the first three hours of cohabitation between opposite-sex prairie voles. The females were either CRISPR KO (n=16) or WT (n=12), and the males were always WT voles. Using our unsupervised behavioral mapping pipeline, we measured the behavioral repertoire of the voles during the early phase of cohabitation by creating a behavioral space, a two-dimensional probability density representation (Figure 4.7.A). To ensure that we can compare the behavioral repertoire between the female and male voles across the different groups of CRISPR KOs and WTs, we embedded all the animals into the same space. The behavioral map consisted of 19,323,150 frames across the data for the female and male voles. Using the watershed algorithm, we segmented the PDF into 99

discretized behavioral regions, with nearby regions corresponding to similar behaviors (Figure 4.7.A). The 2D space revealed behavioral actions like rearing, oral investigation, grooming, chewing, locomotory behavior, and huddling, represented as distinct peaks in the behavioral map. Videos of these behaviors are uploaded to the GitHub repository (https://github.com/senakoko/Thesis_Videos). – use the behavioral map with the numbers to identify the specific regions.

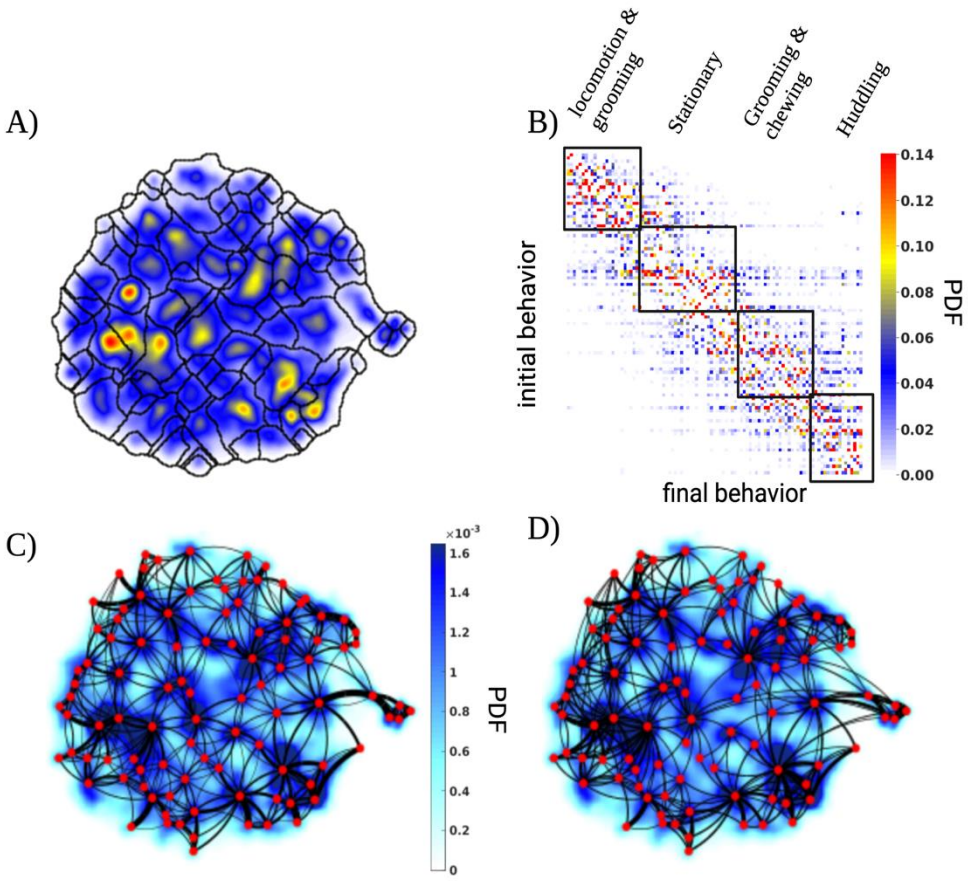

Figure 4.8. Transition probabilities and behavioral modularity. (A) Behavioral space probability density function (PDF). B) One-step Markov transition probability matrix τ=1, overlayed with the behavioral clusters from the information bottleneck calculation. (C-D) Transitions rates are plotted on the behavioral map with τ=1 (C) and τ=5 (D).

Using a hierarchical approach, an information-bottleneck method (Tishby et al., 2000), we combined the fine-grained behavioral clusters into large segments (Figure 4.7.B). The information bottleneck method is a non-Markovian approach that maximizes the information about a future behavioral state while holding the information about the past states fixed. Therefore, coarser representations of behaviors are made of fine-grained behaviors that are closely similar in actions. We identified four prominent coarse-grained behavioral labels - grooming, chewing, locomotion, and idle-like behaviors. This identification was based on viewing randomly selected clips of behaviors from the regions within those clusters. While we note that several hierarchical coarse-grained could have been generated from the information-bottleneck approach, we found these four clusters were representative of the voles' behavior after qualitatively examining them.

To investigate the temporal pattern of the behaviors at different time scales, we computed the behavioral transition matrix. We calculated the probability that an individual moves a behavioral region '*i'* to region '*j'* after τ transition steps. For a given τ=1, where the behavior transitions from one state to the next immediate state, we observed a local behavior transition; behaviors moving to the next ones that are closely associated with it (Figure 4.8B). When we organize the behavioral states by cluster generated from the information bottleneck method, we see a modular structure (Figure 4.8B-C). This modular structure is more pronounced when we plot the transition matrix at longer time scales (Figure 4.8.D). At longer time scales, we start to see that behavioral transition is non-Markovian, indicating that there is an underlying memory to its transition rather than only being Markovian. In plotting the transitions at longer time scales, we selected the Markov time (τ=5) that characterizes the decay time in the Markovian structure. The decay time was calculated with this equation:

$$t_2 = -\frac{1}{log\ |\lambda_2(1)|}$$

Where $\lambda_2(1)$ is the second largest eigenvalue describing the transition matrix (τ=1).

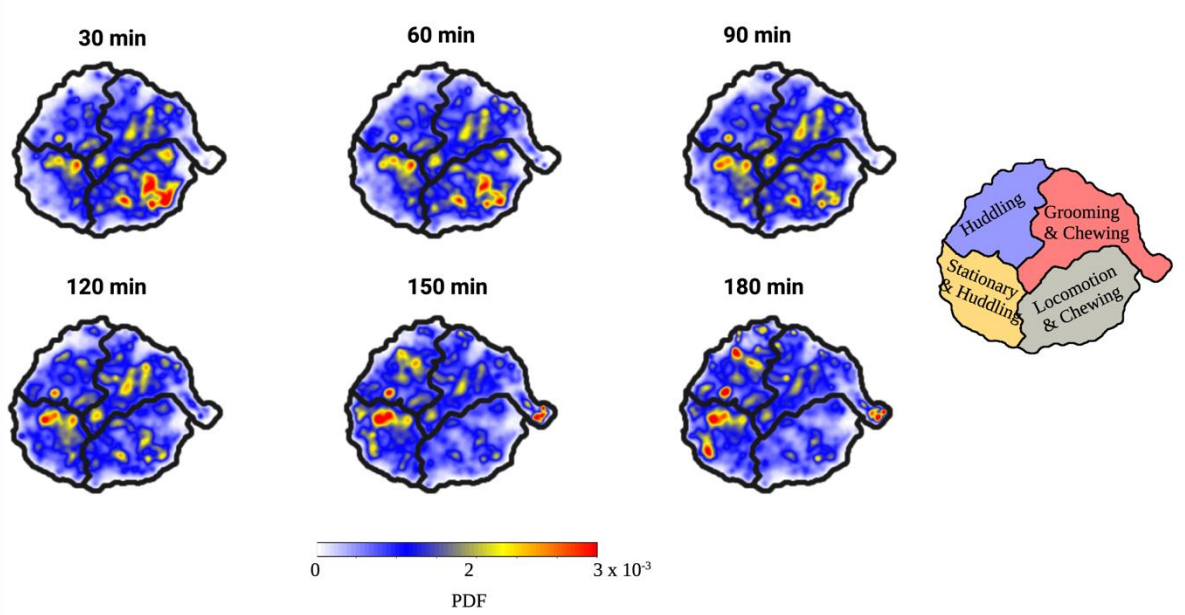

Figure 4.9. Behavioral densities as a function of time. We split the behavioral repertoire into 30 minutes time bins. We see a gradual evolution from locomotion-like behavior in the early cohabitation period to more stationary-like behavior in the later hour.

We then sought to investigate how the behavioral repertoire of the voles changes over time. Dividing the behaviors into 30 minutes bins over the 3 hours, we observed that voles' behavior transitioned from activity- and locomotory-like behaviors to more stationery-like behaviors such as huddling (Figure 4.9). An indication of the natural behavior of animals to explore new places, investigate and be wary of strangers before gradually settling down to non-active behaviors when they have familiarized themselves with the area and the novel animals.

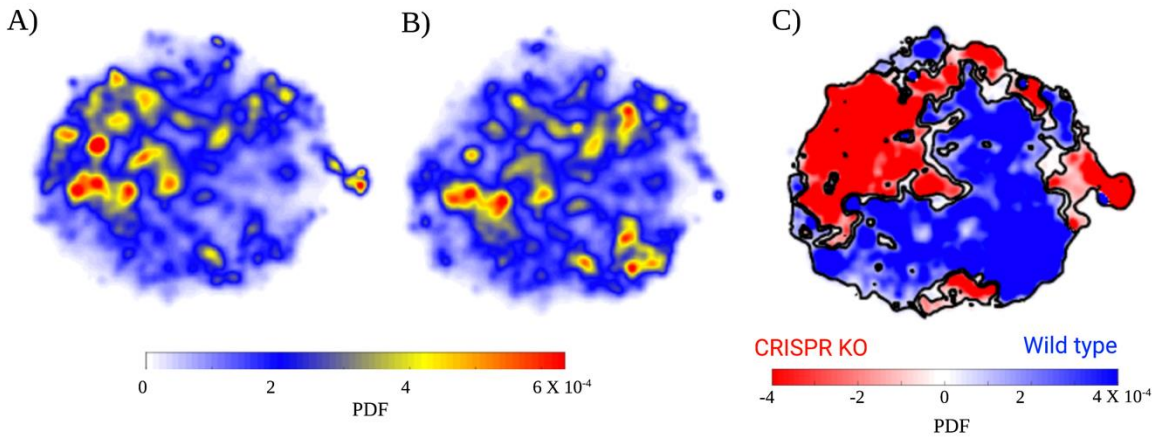

Figure 4.10. Differences in behavior between CRISPR KO and WT female animals. A) Behavioral PDF map of recordings of all the CRISPR KO females B) Behavioral PDF map of recordings of all the WT females. C) Difference between the two PDFs in A) and B). Outlined areas are statistically significantly different regions across the two maps.

4.4.4 CRISPR KO animals show subtle behavioral differences as compared to WT animals

Given that we can measure the prairie voles' behavioral repertoire and how they change over time, we were interested in how OTR would modulate them since it is implicated in regulating the social behavior of animals. In creating the behavioral map, we combined the data from the CRISPR KO females, WT females, and WT males and projected them into one space that allowed us to compare animal behaviors. Using a hierarchical bootstrapping approach, where we took 1000 random samples while correcting for multiple hypotheses, we compared the difference between the behavioral maps of the CRISPR females and WT females. We observed that CRISPR females were significantly more likely to engage in stationary- and huddling-like behavior than the WT females, who performed more active and locomotion-like behaviors (Figure 10).

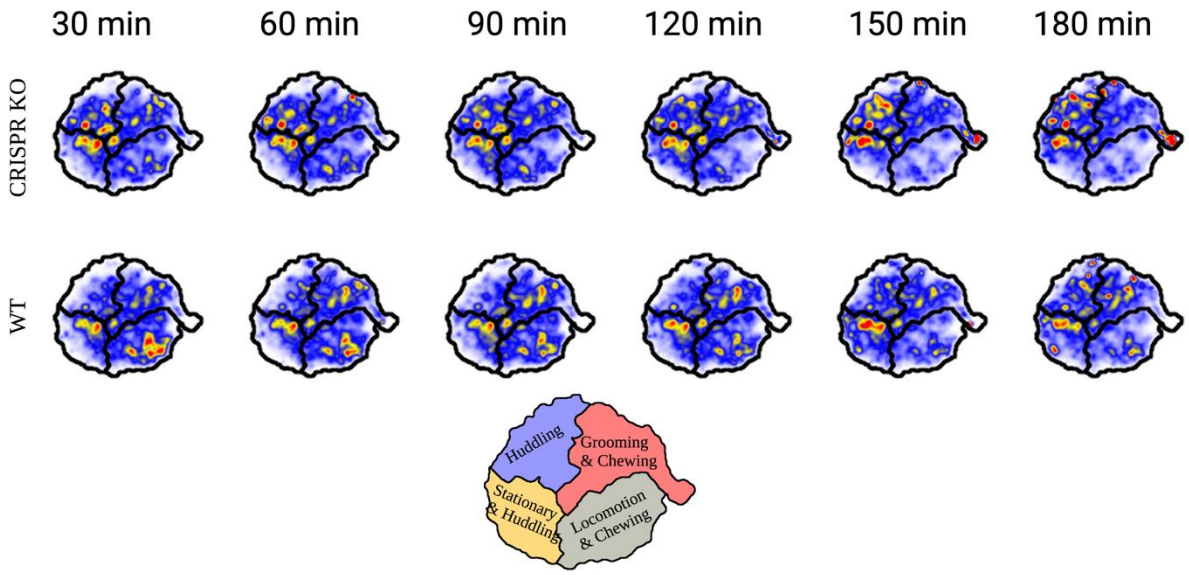

Figure 4.11. Behavioral densities as a function of time. Behavioral densities for CRISPR KO and WT female voles are broken down into 30-minute intervals. WT females perform very active-like behavior during the early part of cohabitation and gradually transition to idle-like behavior later. In contrast, CRISPR KO females are more idle-like during the entire period

4.4.5 Subtle differences between CRISPR KO and WT animals show up in the early stages of bonding

From observing the subtle differences in the behavioral repertoire between CRISPR KO and WT animals, we were interested in identifying whether there was a time component to the difference. Since we observed that the behavioral repertoire changes over time, we asked whether OTR similarly modulates the behavior differently at specific time points during cohabitation. Taking a similar approach as done earlier, we separated the maps for the CRISPR KO and WT female animals and divided them into 30-minute intervals. We identified that the WT animals engaged in locomotory-like behaviors in the first hour and thirty minutes and moved to more stationary-like behaviors (Figure 4.11). Although the CRISPR KO performed locomotory-like actions, the behaviors of the CRISPR KO were predominately more stationary-like behaviors throughout the recorded period. In addition, we saw that the behavior of the WT

males paired with either the CRISPR KO or WT females transitioned from locomotory-like actions to stationary-like behaviors over the course of the 3 hours (Appendix A.2.5.)

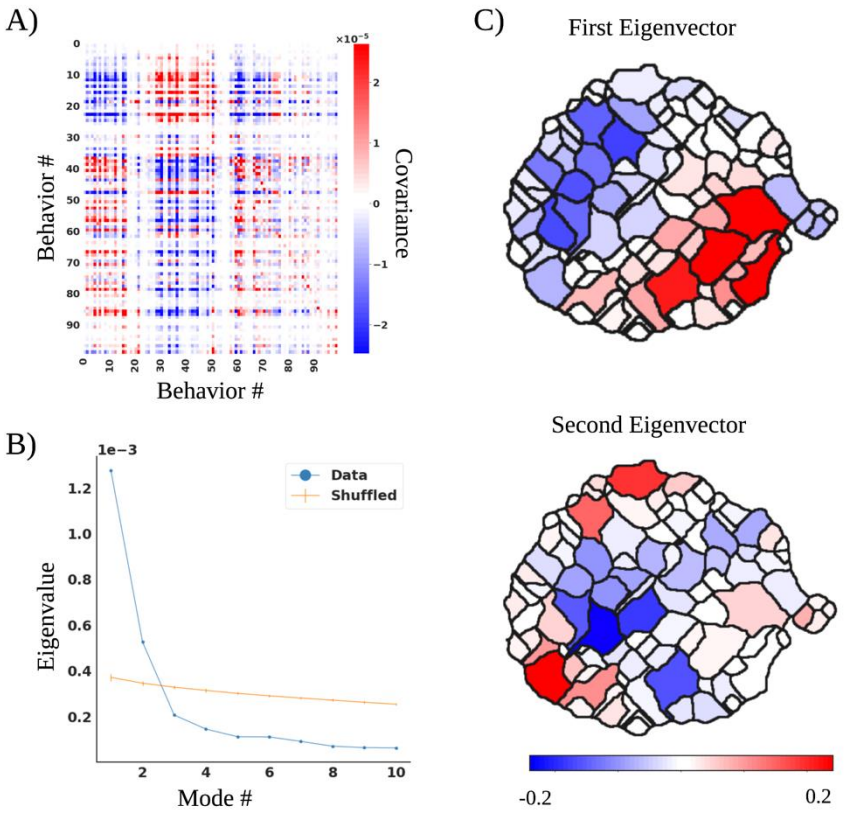

Figure 4.12. Examining the behavioral covariances. (A) The covariance matrix of the mean behaviors is sorted according to the information bottleneck clusters. (B) The eigenvalues of the covariance matrix. The first two eigenvalues (blue) are larger than the eigenvalues returned from shuffling the behavioral density matrix (the error bars are the standard deviation of the shuffled data) (C) The eigenvectors corresponding to the first (top) and second (bottom) eigenvalues plotted on the behavioral map.

One could have analyzed the total distance and speed based on the center-of-mass tracking and observed that the WTs moved more than CRISPR KO animals. However, you would have missed the subtle transition in the behavioral repertoire of the animals over time. The behavioral repertoire captures actions, such as escaping, approaching, and chewing, which cannot be represented in the quantification of the total distance. To further dissociate the

variance in the behavioral repertoire between the two groups, we measured the behavioral covariance matrix across all the animal types over time (Overman et al., 2022). Like the approach taken by Overman, we found a vector of probabilities $P^{(i)}$ based on the regions from the watershed transform (Figure 4.12A). $P_j^{(i)}$ is the time-average probability that vole (*i)* performs behavior (*j)* during 3 hours of recording. To obtain a trajectory of the behavioral vector, we calculated $P^{(i)}$ for every 5 minutes within 3 hours. We then calculated the average behavioral vector for the animal groups (CRISPR KO females, WT females, and the respective conspecific WT male partners for the CRISPR KO and WT females).

We then computed the covariance matrix of the set of mean behavioral vectors, $M \equiv [\mu_1^{(\text{CRISPR KO})} \ldots \mu_{36}^{(\text{CRISPR KO})} \mu_1^{(\text{WT})} \ldots \mu_{36}^{(\text{WT})} \mu_1^{(\text{WT paired with CRISPR KO})} \ldots \mu_{36}^{(\text{WT paired with CRISPR KO})} \mu_1^{(\text{WT paired with WT})} \ldots \mu_{36}^{(\text{WT paired with WT})}] \in \Re^{100 \text{ x } 144}$.

The covariance matrix ($C(M) \equiv \text{Cov}(M)$) reveals behaviors that are likely to increase or decrease with respect to each other in the animal groups (Figure 4.12A). We then performed an eigendecomposition on the covariance matrix to project it into a lower dimensional space to evaluate the modes that would likely explain the trajectories of the behavioral vectors. We observed that the first and second modes captured the behavioral vector above the eigenvector and eigenvalues from the covariance matrix of the independently shuffled columns of the behavioral vector M (Figure 4.12B). The modes, especially the first, seem to capture the locomotory-like and stationary-like behaviors of the voles (Figure 4.12B).

To observe how the lower dimensional representation of the voles changes with time, we projected each animal's behavioral vector onto the eigenvalues (only focused on the first and second). The first eigenmode isolated behavior differences between the CRISPR KO and WT females (Figure 4.13). It confirmed our earlier observation from Figure 4.11, which showed the transition from locomotory-like behavior to a more stationary one, especially in WT animals, compared to predominantly stationary-like behavior in CRISPR KO animals. We also observed an evident sexual dimorphism in the projection of behavior between the CRISPR female and WT males, but not seen in the pairing between WT females and males (Figure 4.13).

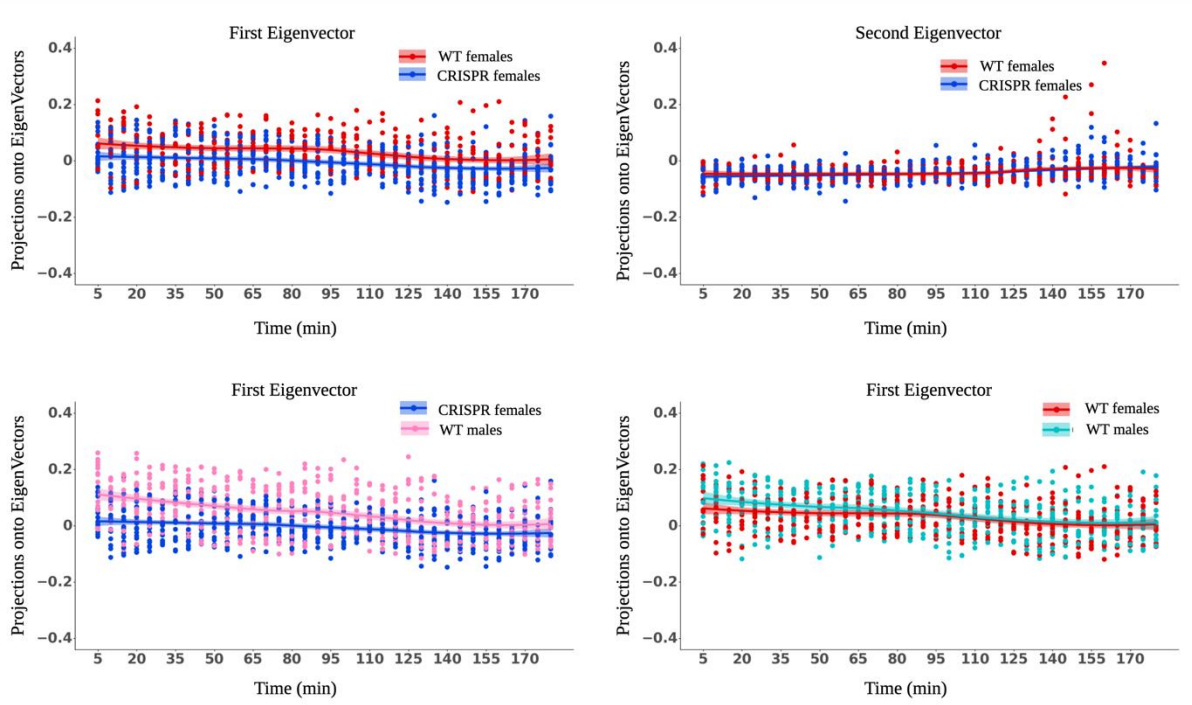

Figure 4.13. Projections of the CRISPR and WT females' data onto the first eigenvector (A) and the second eigenvector (B) plotted as a function of time. Projections of the CRISPR and WT pair data onto the first eigenvector (C) and WT female and male pair onto the first eigenvector (D). The dots are values for individual animals. Mean and SEM plot for the line and error bars.

4.4.6 The subtle behavioral difference between CRISPR KO and WT associated with oral investigation and movement activities

In creating the map of the voles' behavioral repertoire, one inherently assumes that behavior is stereotyped. However, behavior is not always stereotyped, and movement actions with similar frequency patterns can easily be clustered under one highly dominating behavior. When the postural time series is transformed into the frequency domain by applying the wavelet transformation, a crucial step in creating the behavioral map, we assume that all behaviors would have unique frequency dynamics that would allow us to cluster them separately. Our analyses show that certain behaviors have similar frequency patterns, as illustrated by their spectrograms (Figure 4.14). For example, a behavior like escape shares a frequency pattern similar to an oral investigation, and also, when you look at the spectrogram for stationary-like behavior, such as huddling and defensive upright, they have identical properties. Consequently, those comparable behaviors are likely to be clustered together, leading to that behavior that often happens during the social interaction between animals being identified as the primary behavior over the less frequent ones. A solution to this challenge is to perform a frequency template matching where templates based on specified behaviors are used to extract those behaviors from the wavelet transformation. Although there is an advantage of obtaining the desired behaviors, this approach is limited by having to know all desired behaviors that an animal is likely to perform. It removes the ability to identify subtle and unknown behaviors in the animal’s repertoire.

However, since we took advantage of the unsupervised approach to identify subtle differences between CRISPR KO and WT females, we can narrow down to the time points where they occurred. Leveraging the features (the Euclidean distances and angles between body points on an animal - see methods and materials for details) extracted to create the modified

postural time series and other calculated metrics like the animals' speed, we trained a supervised machine classifier, a support vector machine, to classify a set of predefined behaviors like oral and anogenital investigation, escape, and approach. We adopted the approach of using a classifier instead of manual scoring because the classifier allowed for higher throughput of labeling more behaviors compared to the human annotation.

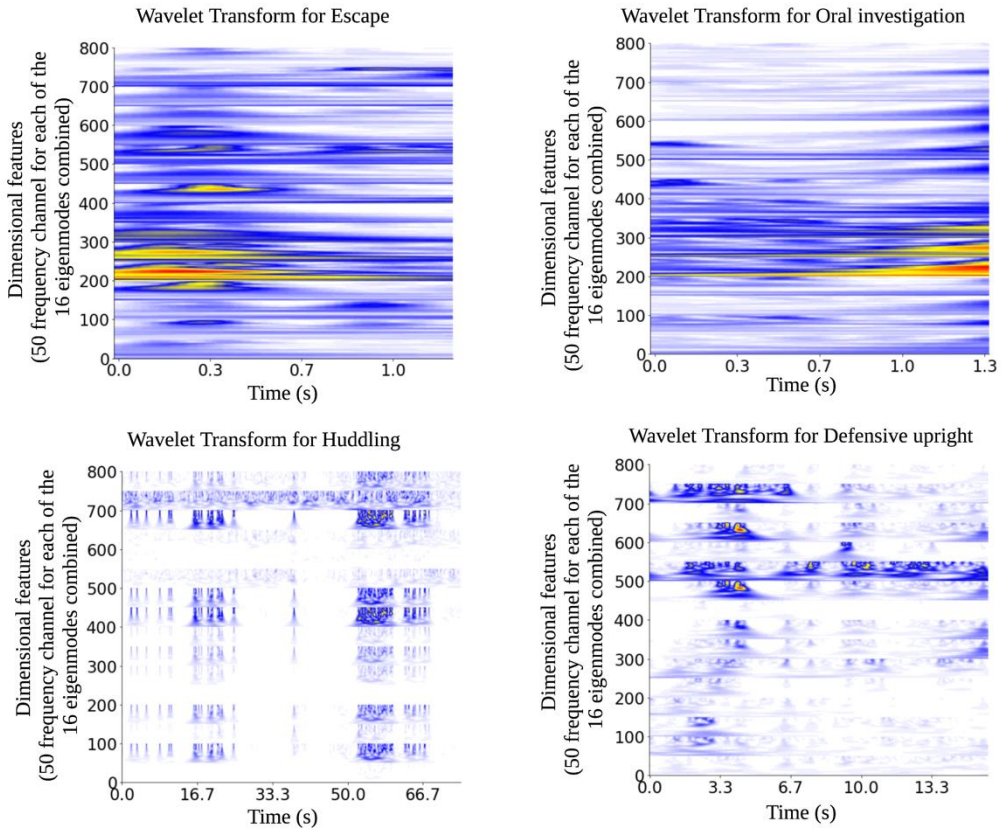

Figure 4.14. Spectrograms of the wavelet transformation of behaviors. Certain behaviors like escape (top left) and oral investigation (top right) show similar frequency patterns which could lead them being clustered together as the same behavior. Also, the behaviors like huddling (bottom left) would be selected over defensive upright (bottom right) when clustered together because the y occur more

We focused on the first 30 minutes of social interaction to investigate the differences in behaviors. We observed that WT female animals were significantly more likely to perform an

oral investigation of their conspecific partner than the CRISPR KO females (Figure 4.15). We did not see any difference between the two groups in behaviors like defensive upright, anogenital sniffing, and investigating other body sides of the animal. Considering that from our earlier observation with the unsupervised approach, we saw that WT females performed locomotion-like behaviors more than CRISPR females, we wanted to find what were those active behaviors. Applying the classifier to extract locomotion behaviors like approaching or escaping from a partner, we found that WT females were likelier to perform those behaviors (although not significant). When all locomotion-like behaviors were combined, we saw a significant increase in the WT compared to the CRISPR KO. Taken together, these results confirm our earlier observation based on the unsupervised approach and implicating OTRs in possible active-like behaviors.

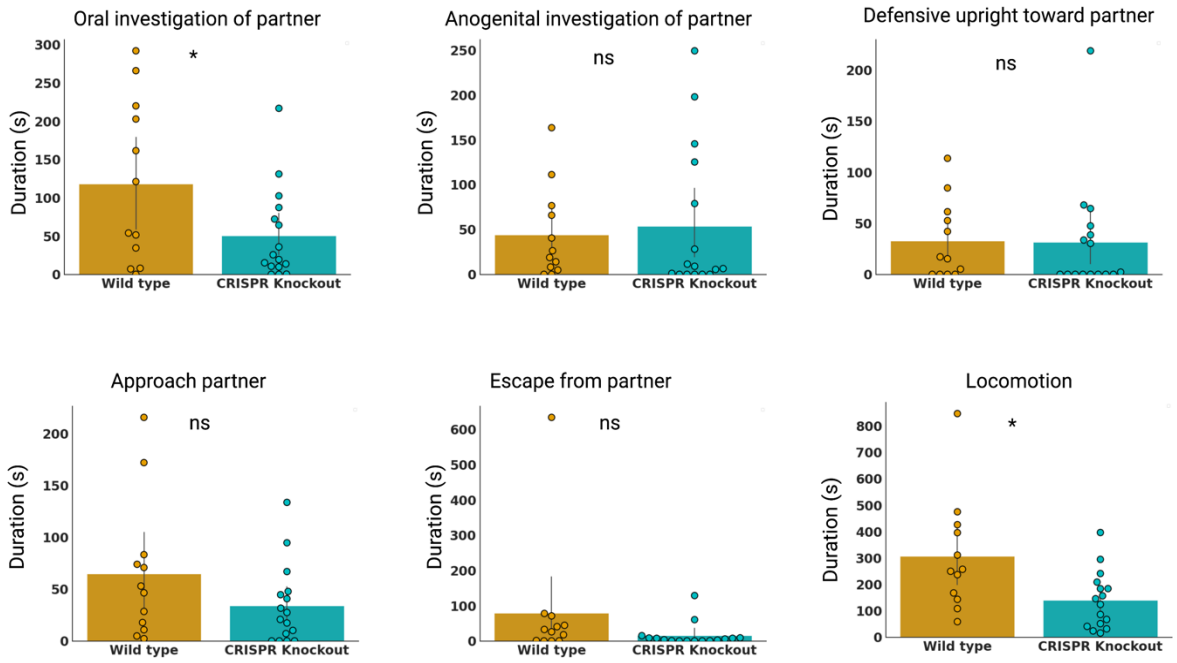

Figure 4.15. CRISPR KO animals move less compared to WT. Examined the durations of investigatory (oral, anogenital investigation and approach) and aggressive (escape and defensive upright) behaviors displayed toward a partner. *p<0.05, **p<0.01, ***p<0.0001; ns, not significant

4.5 DISCUSSION

In this chapter, we investigate the social behavior of prairie voles as they form pair bonds. We find that mutant voles with OTR knocked out show a subtle behavioral difference from WT animals. Given recent evidence by Berendzen and colleagues (Berendzen et al., 2022) showing that mutant voles with OTR knocked out can form pair bonds, which contradicted previous studies that indicated pharmacologically blocking or virally interfering with the OTRs prevents prairie voles from showing a preference for the partner, we wanted to investigate if OTR influences the behaviors of at some point during their interactions. Interestingly, by employing the same viral technique as Berendzen et al., using CRISPR-Cas9 to knock out the OTR globally in the voles, we show that voles can still form pair bonds (Figure 4.5). There are a few possibilities as to why our results (including that of Berendzen et al.) contrast with the previous studies. One possible reason is that although the OTRs are knocked out, the OT neurochemical binds to AVP receptors. Studies have shown that there is crosstalk between the OT and AVP systems, where OT binds to OTRs and AVP receptors, V1aR, and V1bR, and the AVP has an affinity for its three receptors, V1aR, V1bR, and V2R and OTR (Kimura et al., 1994; Chini et al., 1995; Hawtin et al., 2000; Song et al., 2014). Hence, even though the OTR pathway might be eliminated, the AVP receptor pathways are sufficient to allow pair bonding in the prairie voles. The AVP system is implicated in pair bond formation in prairie voles (Liu et al., 2001; Lim and Young, 2004). Secondly, even if there was no strong binding between OT and AVP receptors, there is a chance of brain plasticity where the AVP pathway becomes the dominant channel for bonding. After the voles are weaned, they are placed together with same-sex siblings. Therefore, it is probable that since the animals have to form a familial bonding to

coexist with one another, given that voles are very territorial and aggressive towards strangers, the AVP system becomes the main pathway through which the animals form social bonds.

To rule out the possibility of the brain developing a compensatory mechanism via the AVP system, future studies can leverage the CRISPR-Cas9 viral technique to knock out either only the AVP receptors or both AVP and OT receptors. In creating mutant voles with only AVP receptors knocked out, its role in modulating pair bond formation can be established, similar to the experiments in this research. If the voles do not form a pair bond by eliminating only the AVP receptors, we can attribute the AVP system as the primary pathway via which the animals form pair bonds. However, if they still form pair bonds, as we have seen here, one could then knock out both systems. Eliminating both the OT and AVP receptors takes away the chance of crosstalk, and hence it might provide a conclusive study of their roles in pair bonding.

A third reason why our results contradict previous studies could be because the pharmacological and viral approaches were not specific in targeting only OTRs. The OTR antagonists might have blocked other receptors, specifically AVP receptors, preventing the prairie voles from showing a preference for their partners.

Since there are genetic variations of OTRs within the same species (King et al., 2016) and varying OTR expressions in different brain areas and species (Shapiro and Insel, 1992; Olazábal and Young, 2006), we hypothesized that for adaptive reasons OTR might still influence the social behavior of animals during pair bond formation. We applied unsupervised behavioral mapping to extract the behaviors of the prairie voles during the early phase of cohabitation (first 3 hours). Using this method, we were able to measure the behavioral repertoire for a large number of voles for a long duration, which would have been time-consuming and biased if done by a human annotator (Figure 4.7). We saw a gradual shift from locomotory and active-like

behavior to stationary and huddling behavior (Figure 4.9). In this behavioral repertoire transition, we observed that CRISPR KO females were likely to spend more time in a stationary mode than WT, which showed more active to idle-like behaviors (Figure 4.11). The Oxytocin system is implicated in regulating social approaches and escape behavior of animals (Pisansky et al., 2017; Cohen and Shamay-Tsoory, 2018; Terburg et al., 2018), and hence the WT animals, with intact OTR, were likely to move around more compared to the CRISPR KO voles.

Although the unsupervised approach reveals the behavior repertoire of the animals, it does not cluster every possible animal behavior into its unique group. Some behaviors, like an escape and oral investigation, might be clustered together. Hence, we are likely to miss certain behaviors that are uniquely and differently performed by either the CRISPR KO or WT females. Since the spectrogram of some behaviors, as seen in figure 4.14, might have similar patterns, an approach that can be implemented is to perform wavelet matching, commonly used in spiking sorting in electrophysiological analysis (Ekanadham et al., 2014; Pachitariu et al., 2016). However, trying to perform a wavelet template-matching approach could become supervised, requiring the experimenter to have a foreknowledge of all behaviors they are interested in. It has the advantage of classifying the desired behaviors but would be limited to extracting other actions that are not predefined.

In addition, in adopting the unsupervised method, we assume that behavior is stereotyped and create a behavioral representation that primarily clusters those stereotyped behaviors. However, there are non-stereotyped behaviors that might dictate the animals' movements. For example, as observed in fruit flies, they perform non-stereotyped behaviors approximately half the time (Berman et al., 2014; Todd et al., 2017). Therefore, we might not have wholly represented the entire behavioral repertoire of the prairie voles during pair bond formation.

Taking advantage of a supervised machine learning classifier, we looked at the first 30 minutes of cohabitation and saw that CRISPR KO voles were less likely to investigate their partners orally and both approach and escape from them compared to the WT animals (Figure 4.15). Therefore, although the OTR might not alter the end state of pair bondedness, it is likely to induce subtle behavioral differences in the voles as they form their bonds.

Although we recorded and analyzed the behavioral repertoire of prairie voles during the first 3 hours of the pair bond formation, a pair bond is a complex state that manifests over long periods. Hence, the 3 hours of recording provide a limited picture of the bond formation. Analyzing a 48-hour (or at least 24 hours of recording, since 24 hours of cohabitation is sufficient for pair bond formation (Williams et al., 1992)) cohabitation of prairie voles social interaction will provide an extensive overview of the behavioral dynamics involved in pair bond formation. In addition to the videography, a recording of the vocalization of the voles will give extra information about their behavioral dynamics (we will further discuss this topic in the next Chapter).

In conclusion, this work lays a foundation for applying quantitative methods to measure the social behavior of prairie voles and to encourage further investigation of the role of both OT and AVP receptors during pair bond formation.

Chapter 5. CONCLUSION AND FUTURE DIRECTIONS

5.1 Thesis Contribution

The objective of this thesis is to quantify the social behavior of prairie voles during pair bond formation and the role of oxytocin receptors during the process. It has been a long-held view that oxytocin receptors are necessary for pair bond formation in prairie voles. However, recent studies (Berendzen et al., 2022) and our work here show the contrary. Thus, by quantifying prairie vole's social behavior, this work addresses the role of the oxytocin receptors during pair bond formation.

We leveraged varying technological advancements, from using prairie voles with oxytocin receptors knocked out with CRISPR/Cas-9 to utilizing deep-learning approaches to quantify the animals' social behaviors. Using the CRISPR/Cas-9 knocked-out voles, we have a mutant animal model where we know the oxytocin receptors are absent globally, both centrally and peripherally. With these mutant animals, we could investigate whether the oxytocin receptors influence pair bond formation in prairie voles.

We developed a pipeline that enabled us to robustly track the postures of the prairie voles during pair bond formation (See Chapter 3). Thus, with these postures, we can build a detailed behavioral representation of the animals' social behavior. Previous studies have only quantified a subset of behaviors like huddling and mating, but not the entire behavioral repertoire of the animals. Hence, to our knowledge, no work has shown the detailed mapping of the vole behavior during the early phase (first 3 hours) of cohabitation.

From our work, we find that although oxytocin receptors might alter some behaviors, like the activity level of the prairie voles, during pair bond formation, they are not necessary for bond formation.

5.2 Summaries of Chapters

5.2.1 Chapter 1 summary

In chapter 1, I introduced the oxytocin system and its purported role in facilitating social behavior, specifically pair bond formation. This chapter is primarily a review of studies about what is known regarding the neurochemical oxytocin and its canonical receptors, oxytocin receptors. The oxytocin system is thought to act both centrally in the brain and peripherally in the body. It is implicated in pair bond formation, parental care, uterine contraction, and lactation. Our knowledge of its role in facilitating pair bond formation comes from extensive studies in a premier animal model, prairie voles. The prairie voles, a socially monogamous rodent, have a dense expression of the oxytocin receptors in brain regions such as the nucleus accumbens, prefrontal cortex, and amygdala, considered social brain centers. And by manipulating the oxytocin system in these brain regions, we have observed alterations in the social behaviors of the prairie voles, from parental care and empathy to their preference for a partner.

Through studies in the voles and other animals like mice and primates, we have developed a working hypothesis about the role of oxytocin in social behavior. The hypothesis postulates that the oxytocin system facilitates the salience of the social information received from a conspecific partner, such that the animal develops a memory of the other individual and associates a rewarding value to the interaction. In addition, we also highlight the role of arginine vasopressin, a closely related molecule to oxytocin, dopamine, opioids, and endocannabinoids.

5.2.2 Chapter 2 summary

This chapter focuses on why it is essential to quantify social behavior and its difficulty. Contrary to measuring behavior in a single animal or collective behaviors of large groups, like a swarm of insects or birds or a gang of meerkats, quantifying social behavior in 2-3 animals remains under-explored. We lack the same level of detailed language in quantification and tools for measuring the social interaction of a couple of animals. Hence, I provide a perspective on how to address this gap. I propose a framework to measure the moment-by-moment classification of behaviors of the animals during social interactions and project the behavioral repertoire of the animals into a space based on their stereotypy. With the ethogram of the animals' behaviors and two or three-dimensional space representation of their stereotyped behavior, we can better understand the complex dynamic nature of social behavior.

Additionally, through this framework, we can investigate the hierarchical organization of behavior during social interactions. We can look at if future behaviors are only dependent on the current state of movement, a Markovian principle, or if there is memory in behavior, a non-Markovian rule, where a current behavior is dependent on an action that happened sometime in the past (some distant behavioral state). Investigating social behavior is a lens to understanding the brain; therefore, by measuring social behavior, we can gain insights into how the brain processes input signals from the environment, including social cues, and couples that with its internal state to dictate actions.

5.2.3 Chapter 3 summary

In this chapter, I talked about the pipeline I developed to robustly track the social behavior of prairie voles during pair bond formation. Although there have been technological

advancements in annotating several body points on multiple animals in the last few years using deep-learning approaches, these tools struggle to accurately track the body points when the animals are in close contact. They either label a body part on the wrong individual or swap the animals' identities. Therefore, I developed an Autoencoder, a deep-learning network, combined with the output of tracking tools, like maDLC and SLEAP, to fix the swapping issues. The Autoencoder learns the postures of the voles and imposes a vole-like prior on the tracked body points. Therefore, whenever there is a significant deviation from a possible vole-like shape, the Autoencoder impugns a fix on it. In such a manner that when the tracking tools don't even label body points in some video frames, the Autoencoder makes a considerably good estimation of where they should be, based on its memory of the previous point and other current labeled ones.

With the improved tracking, we can implement the framework discussed in chapter 2 to create a representation of the behavioral repertoire of the animals instead of having maps built from spurious body postures.

5.2.3 Chapter 4 summary

This chapter investigates the role of oxytocin receptors during pair bond formation. I combine the framework proposed in chapter 2 and the pipeline developed in chapter 3 to measure the social behavior in mutant and wild-type voles during the first 3 hours of cohabitation. By robustly tracking the postures of the paired voles and using an unsupervised method to project the behavior into 2D representation, I observed the temporal evolution of the vole behavior from locomotory-like movements to stationary-like actions like huddling. When the CRISPR-Cas9 mutant voles are compared to wild-type animals, the oxytocin receptor knockout animals exhibited more stationary-like behaviors than wild-type animals. To confirm

the presence of this subtle behavioral repertoire difference, I applied a supervised machine learning classifier to classify behaviors such as oral and anogenital investigation, attack, and locomotion behaviors like approaching and escaping. CRISPR/Cas-9 voles performed less of these behaviors compared to wild-type animals. However, despite subtle behavioral differences, we concluded oxytocin receptors were not necessary for pair bond formation in prairie voles.

5.3 Future Directions

This thesis work proposes a framework to measure social behavior in prairie voles during social behavior and contributes to understanding the possible role of the oxytocin receptors. However, it opens several questions that need to be addressed and further improvements that need to be made. These questions and improvements will be the focus of my discussion below.

5.3.1 Beyond Videography

In chapter 2, I proposed a framework for measuring the social behavior of 2-3 animals. However, it is reliant on taking a video recording of the social interactions of the animals, and this inherently excludes external sensory cues, like vocalizations, that cannot be captured with a camera. To fully understand the social behavior of animals, one must measure all the information that is likely to influence social interactions. Given that behavior is both spontaneous (driven by the animal's internal state) and reactive (dictated by external cues), it is essential that communication via auditory or odorant cues is integrated into quantifying the social behavior. For example, studies in mice show that they emit ultrasonic vocalizations in different social contexts and that there is associated sexual dimorphism to it (White et al., 1998; D'Amato and Moles, 2001; Hanson and Hurley, 2012). Sangiamo and colleagues show that mice were likely

to decrease the pitch of vocal signals during courting and aggressive behaviors and conversely increase them during non-dominant behaviors like fleeing from another animal (Sangiamo et al., 2020). Therefore, by considering the communication information, one is likely to understand better why behavior captured with videography is performed at different frequencies or times during an interaction. A female animal might be receptive to a male that vocalizes more, hence more mating behavior between them, than a less vocal male, who might have fewer mating bouts (White et al., 1998; Hammerschmidt et al., 2009).

5.3.2 What about non-stereotyped behaviors?

In our framework, we discussed projecting the behavioral repertoire of animals in 2D representations that maps their stereotyped behaviors. Hence, we make this assumption of stereotypy. So, if a behavior happens to be non-stereotyped, we don't group it by itself, or it is naively clustered next to a stereotyped action. Behavior is not always stereotyped, and animals perform non-stereotyped behaviors a considerable amount of time (Berman et al., 2014; Todd et al., 2017). Therefore, a behavioral mapping framework must carefully consider how to include those behaviors in the measurements.

5.3.3 Extending from 2D to a 3D recording of social behavior

In collecting the video data for measuring the social behavior of voles, we used a single camera mounted onto the chamber to record a 2D top view. This view limits the ability of the experimenter to quantify certain behaviors, like defensive upright and mounting, which are better identified with a side-view camera. Therefore, instead of a traditional 2D camera setup from either the top or side or from the bottom, we propose using a multi-camera view to allow the

recording of whole-body movement. While there are depth cameras that can give an extra dimensionality to the recorded data (Hong et al., 2015; Wiltschko et al., 2015), they are limited in tracking the full pose and struggle in naturalistic settings (Alhwarin et al., 2014). The multi-camera setup would include using 3 or 6 cameras positioned to allow the complete 3D reconstruction of the skeletons of the animals (Dunn et al., 2021; Marshall et al., 2021). In addition to this three- or six-camera setup, one can add extra cameras to record from the bottom and top of the behavioral chamber to obtain a comprehensive of the animals' movement. Next to the cameras, one should include microphones to record the vocalizations of the animals as they interact with each other (Sangiamo et al., 2020). A multi-microphone setup similar to the cameras' can help an experimenter triangulate the vocalizations of the animals.

5.3.4 Recording electrophysiological activity during social interaction

Measuring social behavior is a lens to understanding the physiology of the brain, so in addition to quantifying social interactions of prairie voles during pair bond formation, the neural activity needs to be recorded. To increase our knowledge about pair bond formation in prairie voles, we need to record the electrophysiology activity from brain areas, such as the nucleus accumbens and the prefrontal cortex, to understand how they modulate the behavioral actions of the animals. Work from our lab has shown that functional connectivity between the medial prefrontal cortex and nucleus accumbens is predictive of how quickly animals express affiliative behavior towards a partner. This work was based on recording local field potential from these brain areas. Yet to be explored is the recording of single and multi-unit activity from the brain regions to understand how the spiking pattern could influence the social behaviors of the voles. One hypothesis will have held is that there is spike-field coherence (SFC) – a measure of

synchronization between the local field potential (LFP) and spike times – that occurs during affiliative behaviors (e.g., mating). In addition, we hypothesize that during social interactions, striatal neurons will "switch" from gamma oscillation at 50Hz to 80Hz, reflecting reward.

The first hypothesis is premised on the studies that oxytocin is released into the network of social brain centers that drive SFC in the nucleus accumbens (Goto and O'Donnell, 2001, 2002). Therefore, the release of oxytocin during affiliative behaviors is likely to cause SFC. For the second hypothesis, studies have shown that the striatal neural population oscillates in different frequency ranges and can switch from one band to another in a task-dependent manner (Berke, 2009; Gruber et al., 2009). For example, when animals move around, there is a 50Hz oscillation in the striatal neurons. However, if these animals are deprived of water and are cued to obtain a sweetened water reward, striatal neurons "switch" to oscillate at a high 80Hz gamma frequency during the reward period and then back to 50 Hz gamma after the reward ends (Berke, 2009). Consequently, in a rewarding context like during mating, the striatal neural activity would switch 80 Hz oscillations.

5.3.5 How about the arginine vasopressin system?

In chapter 4, we observed that oxytocin receptor knockout female prairie voles could form pair bonds and that although there were subtle behavioral differences between them and the wildtypes, the oxytocin receptors were not necessary for bond formation. These results rise several questions, and one of them is, what if we knocked down the receptors at adult age? Boender from the Young lab performed such an experiment and saw that voles still showed a significant preference for their partner, even after 6 hours of cohabitation and up to 2 weeks (unpublished). How about the neurochemical itself, oxytocin? Before we discuss possible

experiments with it, we would like to consider arginine vasopressin receptors. It is known that there is a crosstalk between the oxytocin and vasopressin systems. AVP can bind to OTRs and its three receptors, while OT has an affinity for its receptor, OTR, V1aR, and V1bR (Kimura et al., 1994; Chini et al., 1995; Hawtin et al., 2000; Song et al., 2014). Therefore, it is possible that oxytocin might be binding to the vasopressin receptors to facilitate pair bonding.

Hence, to rule out this possibility, an experiment to perform is to knock out the vasopressin receptors. This can be done in two ways – first, knock out only the vasopressin receptors without touching the oxytocin receptors in one cohort of animals. Then in a second animal cohort, knock out both oxytocin and receptors. I hypothesize that the second cohort of prairie voles with the oxytocin and vasopressin receptors knocked out will not form pair bonds. Unlike in the first cohort, where the chance of crosstalk remains, the animals in the second cohort would show similar results to those of receptor antagonists experiments. Since using pharmacology antagonists likely blocks both receptors because of their lack of specificity. However, if the first cohort does not show a preference for their partner, then the vasopressin receptors are the primary factor (necessary) for pair bond formation in prairie voles.

What if, even after knocking out both receptors, the voles still show a preference for their partners? Since oxytocin may bind to other receptors that we do not know about or induces the activity of other systems like dopamine to facilitate pair bond formation, the next step should target the neurochemical. One should knock out oxytocin. Although there are several implications of knocking out oxytocin since it mediates reproductive functions and physiological processes (Gimpl and Fahrenholz, 2001), this experiment will hone in on the necessity of oxytocin for pair bond formation.

5.3.6 How much deeper can we go?

In the thesis, we leveraged deep-learning approaches to track the animals' postures and robustly fix swapping issues associated with them. Despite these approaches, maintaining animals' identities remained a challenge leading us to correct switched points manually. We proposed adding a convolutional neural network to the pipeline so that the autoencoder was not solely reliant on the output of the tracking tools (i.e., maDLC and SLEAP). However, one can take it a step further by including transformers.

Transformers are deep-learning networks capable of self-supervised training (i.e., they do not need a training set generated by the user but instead train themselves by finding samples) to learn context and track relationships between sequences in the data (Vaswani et al., 2017). Although we don't fully comprehend how they work, studies show they have been effective in natural language processing for predicting the next word in a sentence (Devlin et al., 2019; Radford Alec et al., 2019). For example, if one uses the most recent version of Microsoft word, one will notice that it suggests the subsequent word or phrase to type as one writes. Given their ability to predict the next sequence based on a context, the transformer could predict an animal's future pose by knowing its current position and posture. maDLC have started experimenting with transformers in their pipeline (Lauer et al., 2022), but it does not yield the desired results of maintaining identities. One possible reason is that their transformer uses the direct tracked output of maDLC, which we have shown in chapter 3 is not good enough. Therefore, applying the transformer to the results from the autoencoder might be the solution.

Chapter 6. APPENDIX A. CHAPTER 4 SUPPLEMENTARY MATERIAL

A.1 Meta Data of prairie voles used in experiments

Note: The Vole #s is not continuous because, in addition to the CRISPR KO and WT animals analyzed in this thesis, I also recorded the behavior of high and low-expressing oxytocin receptors.

Female KO -/- = CRISPR KO female animals

Female KO +/+ = Wild-type female animals (Siblings of CRISPR KO female animals)

Experimental Animal	**Animal Information**	**Details**
Vole 05	DOB	7/11/21
	ID	3346613
	Animal Type	Female - KO +/+
	Generation	48
Partner	DOB	6/12/21
	ID	3340127
	Animal Type	Male - WT reg
	Generation	260
Novel 1	DOB	6/12/21
	ID	3340128
	Animal Type	Male - WT reg
	Generation	260
Novel 2	DOB	6/7/21
	ID	3343003
	Animal Type	Male - WT reg
	Generation	265
Vole 06	DOB	7/11/21
	ID	3346612
	Animal Type	Female - KO +/+

	Generation	48
Partner	DOB	6/12/21
	ID	3340128
	Animal Type	Male - WT reg
	Generation	260
Novel 1	DOB	6/12/21
	ID	3340127
	Animal Type	Male - WT reg
	Generation	260
Novel 2	DOB	6/7/21
	ID	3343002
	Animal Type	Male - WT reg
	Generation	265
Vole 11	DOB	8/11/21
	ID	3352395
	Animal Type	Female - KO -/-
	Generation	38
Partner	DOB	6/7/21
	ID	3343003
	Animal Type	Male - WT reg
	Generation	264
Novel 1	DOB	6/7/21
	ID	3343002
	Animal Type	Male - WT reg
	Generation	265
Novel 2	DOB	9/12/21
	ID	3358403
	Animal Type	Male - WT reg
	Generation	265
Vole 12	DOB	8/11/21
	ID	3352397
	Animal Type	Female - KO +/+
	Generation	53A
Partner	DOB	6/7/21
	ID	3343002
	Animal Type	Male - WT reg
	Generation	265

Novel 1	DOB	6/7/21
	ID	3343003
	Animal Type	Male - WT reg
	Generation	264
Novel 2	DOB	9/12/21
	ID	3358402
	Animal Type	Male - WT reg
	Generation	248
Vole 13	DOB	8/27/21
	ID	3354777
	Animal Type	Female - KO -/-
	Generation	50A
Partner	DOB	6/12/21
	ID	3340126
	Animal Type	Male - WT reg
	Generation	260
Novel 1	DOB	6/7/21
	ID	3343001
	Animal Type	Male - WT reg
	Generation	265
Novel 2	DOB	5/20/21
	ID	3340107
	Animal Type	Male - WT reg
	Generation	270
Vole 14	DOB	8/27/21
	ID	3354776
	Animal Type	Female - KO -/-
	Generation	50A
Partner	DOB	6/7/21
	ID	3343001
	Animal Type	Male - WT reg
	Generation	265
Novel 1	DOB	6/12/21
	ID	3340126
	Animal Type	Male - WT reg
	Generation	260
Novel 2	DOB	5/20/21

	ID	3340106
	Animal Type	Male - WT reg
	Generation	270
Vole 15	DOB	8/27/21
	ID	3354775
	Animal Type	Female - KO -/-
	Generation	50A
Partner	DOB	6/27/21
	ID	3344039
	Animal Type	Male - WT reg
	Generation	263
Novel 1	DOB	6/27/21
	ID	3344038
	Animal Type	Male - WT reg
	Generation	263
Novel 2	DOB	7/15/21
	ID	3349768
	Animal Type	Male - WT reg
	Generation	270
Vole 16	DOB	8/22/21
	ID	3354767
	Animal Type	Female - KO -/-
	Generation	40
Partner	DOB	6/27/21
	ID	3344038
	Animal Type	Male - WT reg
	Generation	263
Novel 1	DOB	6/27/21
	ID	3344039
	Animal Type	Male - WT reg
	Generation	263
Novel 2	DOB	7/15/21
	ID	3349767
	Animal Type	Male - WT reg
	Generation	270
Vole 17	DOB	8/7/21

	ID	3352381
	Animal Type	Female - KO +/+
	Generation	51
Partner	DOB	6/29/21
	ID	3344034
	Animal Type	Male - WT reg
	Generation	264
Novel 1	DOB	6/27/21
	ID	3344037
	Animal Type	Male - WT reg
	Generation	263
Novel 2	DOB	6/20/21
	ID	3340112
	Animal Type	Male - WT reg
	Generation	279
Vole 18	DOB	7/14/21
	ID	3346618
	Animal Type	Female KO +/+
	Generation	46
Partner	DOB	6/27/21
	ID	3344037
	Animal Type	Male - WT reg
	Generation	263
Novel 1	DOB	6/29/21
	ID	3344034
	Animal Type	Male - WT reg
	Generation	264
Novel 2	DOB	6/20/21
	ID	3340104
	Animal Type	Male - WT reg
	Generation	279
Vole 27	DOB	8/31/21
	ID	3356144
	Animal Type	Female - KO -/-
	Generation	49
Partner	DOB	6/20/21
	ID	3340112

	Animal Type	Male - WT reg
	Generation	279
Novel 1	DOB	6/20/21
	ID	3340104
	Animal Type	Male - WT reg
	Generation	279
Novel 2	DOB	9/22/21
	ID	3361176
	Animal Type	Male - WT reg
	Generation	261
Vole 28	DOB	8/31/21
	ID	3356143
	Animal Type	Female - KO -/-
	Generation	49
Partner	DOB	6/20/21
	ID	3340104
	Animal Type	Male - WT reg
	Generation	279
Novel 1	DOB	6/20/21
	ID	3340112
	Animal Type	Male - WT reg
	Generation	279
Novel 2	DOB	9/22/21
	ID	3361175
	Animal Type	Male - WT reg
	Generation	261
Vole 37	DOB	8/7/21
	ID	3352380
	Animal Type	Female - KO +/+
	Generation	51
Partner	DOB	9/21/21
	ID	3361178
	Animal Type	Male - WT reg
	Generation	257
Novel 1	DOB	9/21/21
	ID	3361177
	Animal Type	Male - WT reg

	Generation	257
Novel 2	DOB	10/3/21
	ID	3362206
	Animal Type	Male - WT reg
	Generation	275
Vole 38	DOB	8/28/21
	ID	3354779
	Animal Type	Female - KO +/+
	Generation	46
Partner	DOB	9/21/21
	ID	3361177
	Animal Type	Male - WT reg
	Generation	257
Novel 1	DOB	9/21/21
	ID	3361178
	Animal Type	Male - WT reg
	Generation	257
Novel 2	DOB	10/3/21
	ID	3362205
	Animal Type	Male - WT reg
	Generation	275
Vole 39	DOB	8/16/21
	ID	3353394
	Animal Type	Female - KO -/-
	Generation	47
Partner	DOB	9/22/21
	ID	3361176
	Animal Type	Male - WT reg
	Generation	261
Novel 1	DOB	9/22/21
	ID	3361175
	Animal Type	Male - WT reg
	Generation	261
Novel 2	DOB	10/6/21
	ID	3362208
	Animal Type	Male - WT reg
	Generation	260

Vole 40	DOB	9/21/21
	ID	3360215
	Animal Type	Female - KO +/+
	Generation	55
Partner	DOB	9/22/21
	ID	3361175
	Animal Type	Male - WT reg
	Generation	261
Novel 1	DOB	9/22/21
	ID	3361176
	Animal Type	Male - WT reg
	Generation	261
Novel 2	DOB	10/6/21
	ID	3362208
	Animal Type	Male - WT reg
	Generation	260
Vole 47	DOB	11/20/21
	ID	3369342
	Animal Type	Female - KO -/-
	Generation	53B
Partner	DOB	10/3/21
	ID	3362205
	Animal Type	Male - WT reg
	Generation	275
Novel 1	DOB	10/3/21
	ID	3362204
	Animal Type	Male - WT reg
	Generation	275
Novel 2	DOB	10/6/21
	ID	3362208
	Animal Type	Male - WT reg
	Generation	260
Vole 48	DOB	11/20/21
	ID	3369341
	Animal Type	Female - KO -/-
	Generation	53B

Partner	DOB	10/3/21
	ID	3362204
	Animal Type	Male - WT reg
	Generation	275
Novel 1	DOB	10/3/21
	ID	3362205
	Animal Type	Male - WT reg
	Generation	275
Novel 2	DOB	10/6/21
	ID	3362207
	Animal Type	Male - WT reg
	Generation	260
Vole 49	DOB	11/20/21
	ID	3369344
	Animal Type	Female - KO -/-
	Generation	53B
Partner	DOB	10/6/21
	ID	3362208
	Animal Type	Male - WT reg
	Generation	260
Novel 1	DOB	10/6/21
	ID	3362207
	Animal Type	Male - WT reg
	Generation	260
Novel 2	DOB	10/6/21
	ID	3364356
	Animal Type	Male - WT reg
	Generation	265
Vole 50	DOB	11/20/21
	ID	3369343
	Animal Type	Female - KO -/-
	Generation	53B
Partner	DOB	10/6/21
	ID	3362207
	Animal Type	Male - WT reg
	Generation	260
Novel 1	DOB	10/6/21

	ID	3362208
	Animal Type	Male - WT reg
	Generation	260
Novel 2	DOB	10/6/21
	ID	3364355
	Animal Type	Male - WT reg
	Generation	265
Vole 51	DOB	11/9/21
	ID	3368133
	Animal Type	Female - KO -/-
	Generation	57
Partner	DOB	10/6/21
	ID	3365356
	Animal Type	Male - WT reg
	Generation	265
Novel 1	DOB	10/6/21
	ID	3365355
	Animal Type	Male - WT reg
	Generation	265
Novel 2	DOB	10/10/21
	ID	3363661
	Animal Type	Male - WT reg
	Generation	248
Vole 52	DOB	11/9/21
	ID	3368132
	Animal Type	Female - KO -/-
	Generation	58
Partner	DOB	10/6/21
	ID	3365355
	Animal Type	Male - WT reg
	Generation	265
Novel 1	DOB	10/6/21
	ID	3365356
	Animal Type	Male - WT reg
	Generation	265
Novel 2	DOB	10/10/21
	ID	3363660

	Animal Type	Male - WT reg
	Generation	248
Vole 53	DOB	12/5/21
	ID	3371326
	Animal Type	Female - KO +/+
	Generation	54
Partner	DOB	10/13/21
	ID	3363658
	Animal Type	Male - WT reg
	Generation	257
Novel 1	DOB	10/13/21
	ID	3363657
	Animal Type	Male - WT reg
	Generation	257
Novel 2	DOB	10/11/21
	ID	3364342
	Animal Type	Male - WT reg
	Generation	274
Vole 54	DOB	12/5/21
	ID	3371327
	Animal Type	Female - KO +/+
	Generation	54
Partner	DOB	10/13/21
	ID	3363657
	Animal Type	Male - WT reg
	Generation	257
Novel 1	DOB	10/13/21
	ID	3363658
	Animal Type	Male - WT reg
	Generation	257
Novel 2	DOB	10/11/21
	ID	3364343
	Animal Type	Male - WT reg
	Generation	274
Vole 55	DOB	11/7/21
	ID	3368141

	Animal Type	Female - KO +/+
	Generation	54
Partner	DOB	10/10/21
	ID	3363661
	Animal Type	Male - WT reg
	Generation	248
Novel 1	DOB	10/10/21
	ID	3363660
	Animal Type	Male - WT reg
	Generation	248
Novel 2	DOB	10/11/21
	ID	3364343
	Animal Type	Male - WT reg
	Generation	274
Vole 56	DOB	11/7/21
	ID	3368140
	Animal Type	Female - KO +/+
	Generation	56
Partner	DOB	10/10/21
	ID	3363660
	Animal Type	Male - WT reg
	Generation	248
Novel 1	DOB	10/10/21
	ID	3363661
	Animal Type	Male - WT reg
	Generation	248
Novel 2	DOB	10/11/21
	ID	3364342
	Animal Type	Male - WT reg
	Generation	274
Vole 57	DOB	10/19/21
	ID	3364382
	Animal Type	Female - KO -/-
	Generation	58
Partner	DOB	10/13/21
	ID	3363656
	Animal Type	Male - WT Reg

	Generation	257
Novel 1	DOB	10/10/21
	ID	3363659
	Animal Type	Male - WT Reg
	Generation	248
Novel 2	DOB	10/11/21
	ID	3364342
	Animal Type	Male - WT reg
	Generation	274
Vole 58	DOB	11/7/21
	ID	3368137
	Animal Type	Female - KO -/-
	Generation	51
Partner	DOB	10/10/21
	ID	3363659
	Animal Type	Male - WT Reg
	Generation	248
Novel 1	DOB	10/13/21
	ID	3363656
	Animal Type	Male - WT Reg
	Generation	257
Novel 2	DOB	10/11/21
	ID	3364341
	Animal Type	Male - WT reg
	Generation	274

A.2 Supplemental Figures

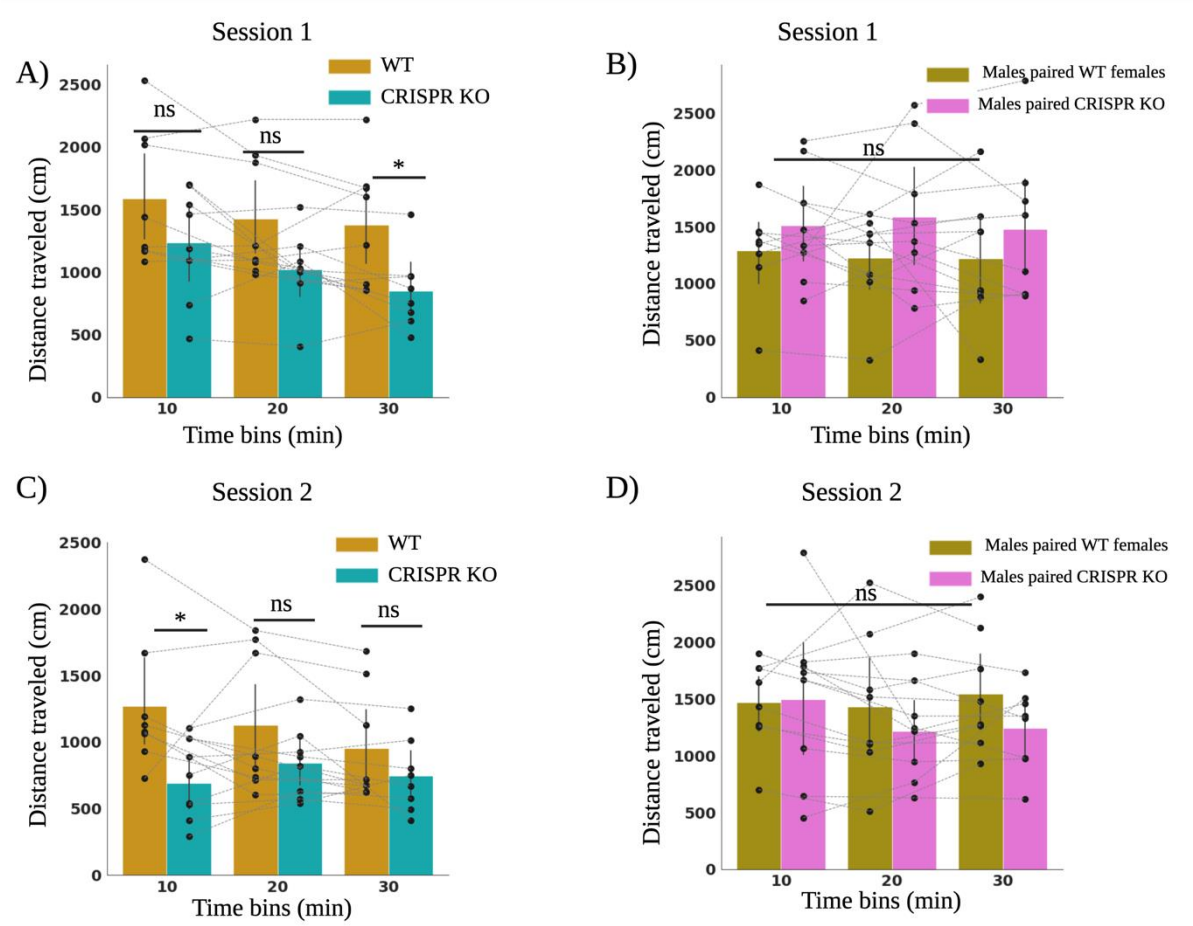

Appendix A.2.1 Locomotor activity of voles during the modified open field test. The total distance traveled by female animals in the first session (A) and second session(C). The total distance traveled by male animals in the first (B) and second sessions (D). *p<0.05, **p<0.01, ***p<0.0001; N.S., not significant

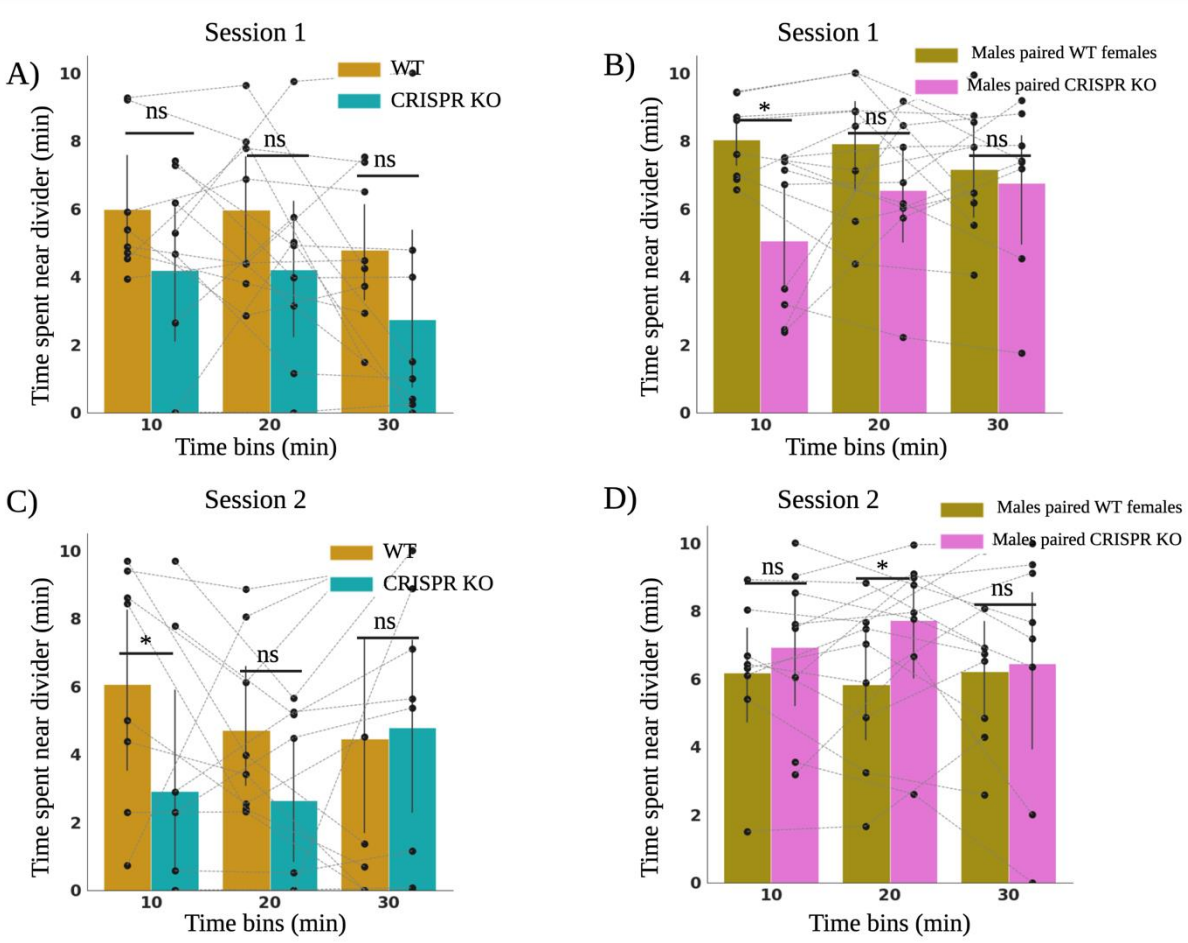

Appendix A.2.2 Time spent near divider by voles during the modified open field test. The time spent near divider by female animals in the first session (A) and second session(C). The time spent by male animals in the first (B) and second sessions (D). *p<0.05, **p<0.01, ***p<0.0001; N.S., not significant

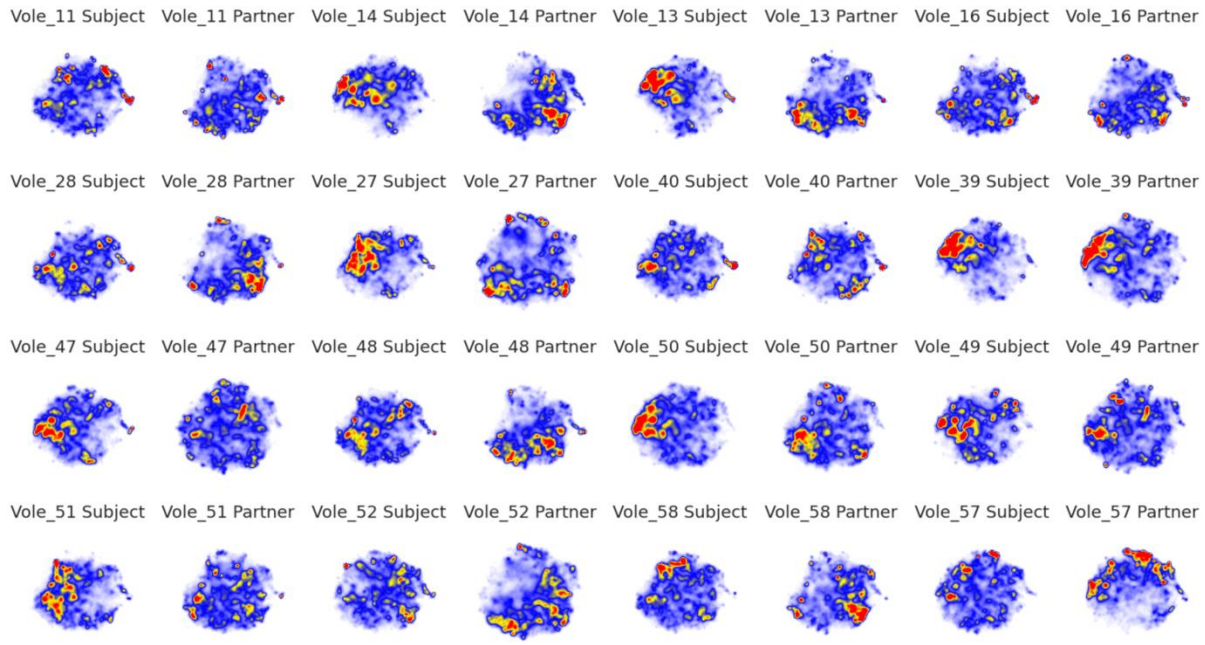

Appendix A.2.3 Individual behavioral maps of CRISPR KO animals

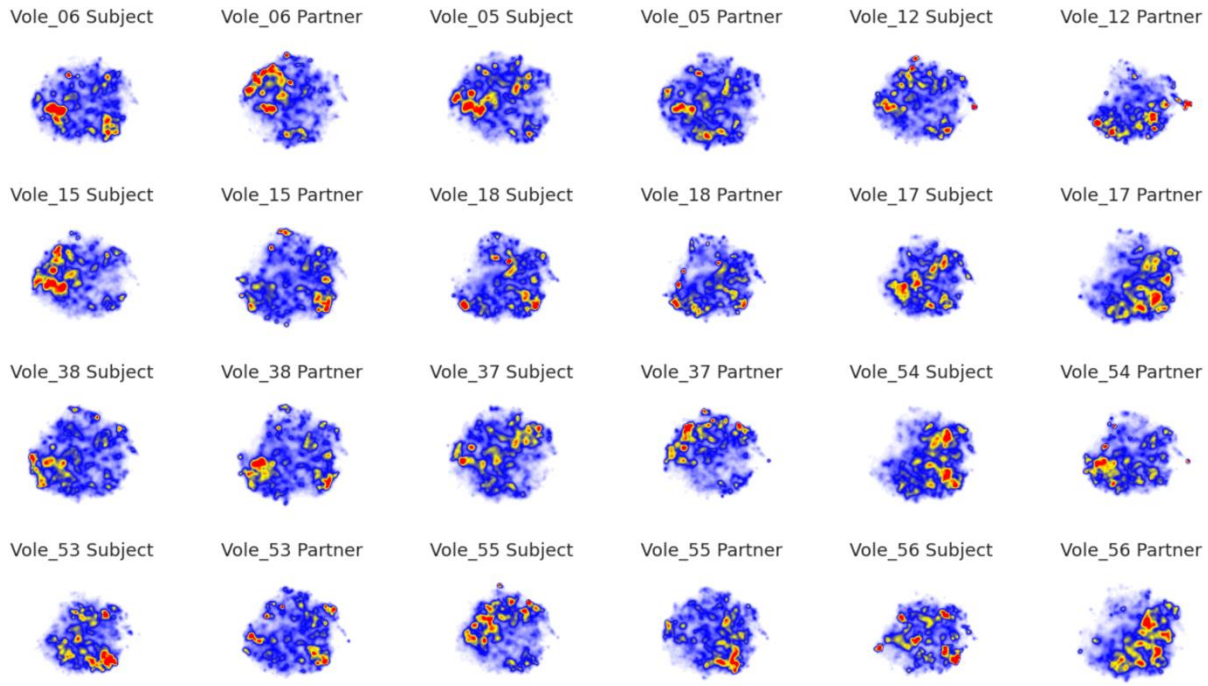

Appendix A.2.4 Individual behavioral maps of WT animals

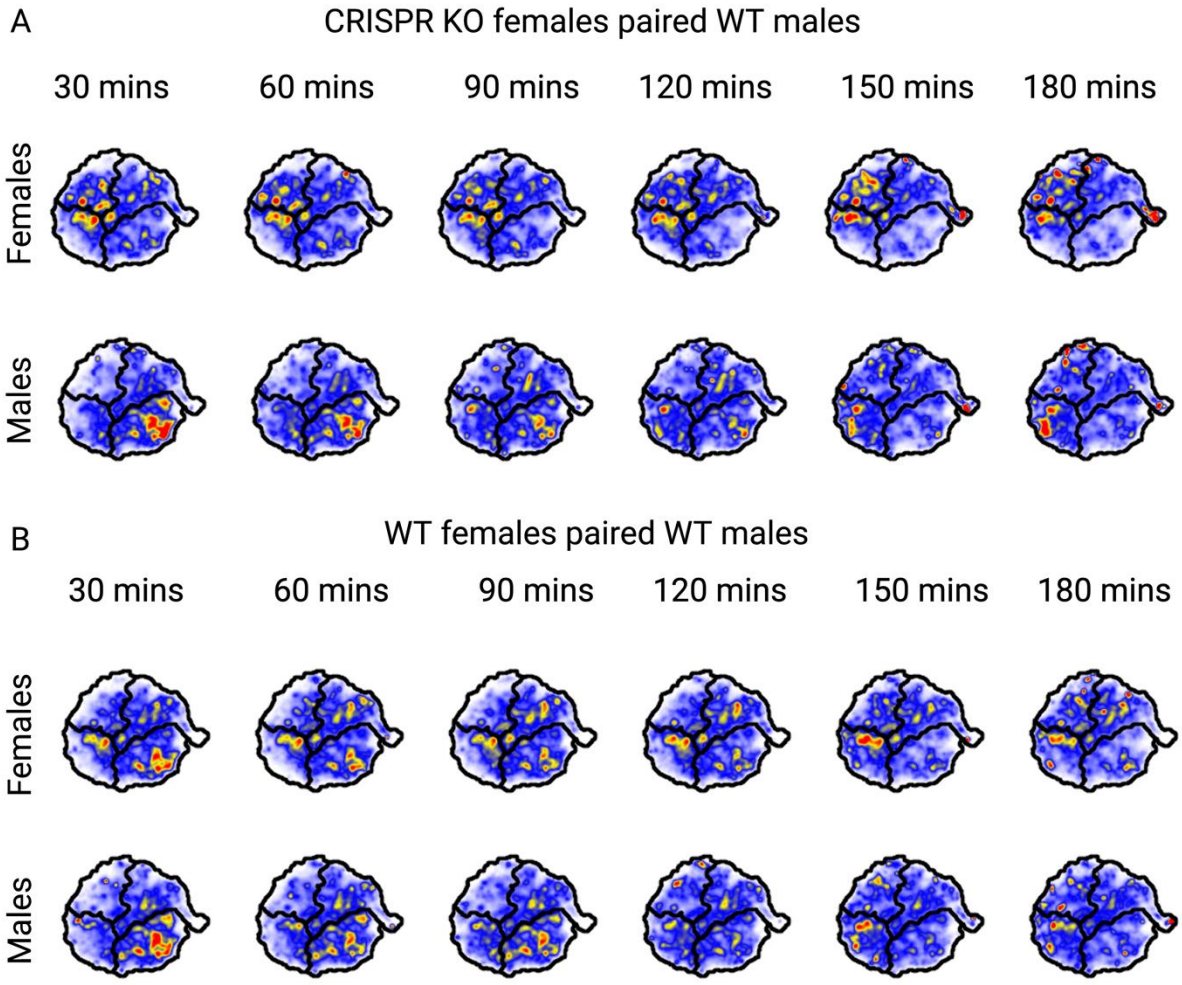

Appendix A.2.5 Behavioral densities as a function of time. Behavioral densities for CRISPR KO female and WT male voles (A) and WT female and male voles (B) are broken down into 30-minute intervals. WT females and males perform very active-like behavior during the early part of cohabitation and gradually transition to idle-like behavior later. In contrast, CRISPR KO females are more idle-like during the entire period

Reference

Acher R, Chauvet J, Chauvet MT (1996) Man and the Chimaera: Selective versus Neutral Oxytocin Evolution. Adv Exp Med Biol 395.

Alhwarin F, Ferrein A, Scholl I (2014) IR stereo kinect: Improving depth images by combining structured light with IR stereo. Lect Notes Comput Sci (including Subser Lect Notes Artif Intell Lect Notes Bioinformatics) 8862.

Andari E, Duhamel J-R, Zalla T, Herbrecht E, Leboyer M, Sirigu A (2010) Promoting social behavior with oxytocin in high-functioning autism spectrum disorders. Proc Natl Acad Sci 107:4389–4394 Available at: https://pnas.org/doi/full/10.1073/pnas.0910249107.

Anderson DJ, Perona P (2014) Toward a Science of Computational Ethology. Neuron 84:18–31 Available at: https://linkinghub.elsevier.com/retrieve/pii/S0896627314007934.

Anderson JR (1998) Social stimuli and social rewards in primate learning and cognition. Behav Processes.

Andriluka M, Pishchulin L, Gehler P, Schiele B (2014) 2D human pose estimation: New benchmark and state of the art analysis. In: Proceedings of the IEEE Computer Society Conference on Computer Vision and Pattern Recognition.

Anpilov S, Shemesh Y, Eren N, Harony-Nicolas H, Benjamin A, Dine J, Oliveira VEM, Forkosh O, Karamihalev S, Hüttl RE, Feldman N, Berger R, Dagan A, Chen G, Neumann ID, Wagner S, Yizhar O, Chen A (2020) Wireless Optogenetic Stimulation of Oxytocin Neurons in a Semi-natural Setup Dynamically Elevates Both Pro-social and Agonistic Behaviors. Neuron 107.

Aoki (1980) An analysis of the schooling behavior of fish: Internal organization and communication process. Bull Ocean Res Inst - Univ Tokyo (Japan) no 12 Available at: https://agris.fao.org/agris-search/search.do?recordID=JP19810659327 [Accessed December 11, 2022].

Aragona BJ, Liu Y, Curtis JT, Stephan FK, Wang Z (2003) A critical role for nucleus accumbens dopamine in partner-preference formation in male prairie voles. J Neurosci.

Aragona BJ, Liu Y, Yu YJ, Curtis JT, Detwiler JM, Insel TR, Wang Z (2006) Nucleus accumbens dopamine differentially mediates the formation and maintenance of monogamous pair bonds. Nat Neurosci.

Auyeung B, Lombardo M V., Heinrichs M, Chakrabarti B, Sule A, Deakin JB, Bethlehem RAI, Dickens L, Mooney N, Sipple JAN, Thiemann P, Baron-Cohen S (2015) Oxytocin increases eye contact during a real-time, naturalistic social interaction in males with and without

autism. Transl Psychiatry.

Avery L, Horvitz HR (1990) Effects of starvation and neuroactive drugs on feeding in Caenorhabditis elegans. J Exp Zool 253:263–270 Available at: https://pubmed.ncbi.nlm.nih.gov/2181052/ [Accessed January 10, 2023].

Bar-Shalom Y, Fortmann TE, Cable PG (1990) Tracking and Data Association . J Acoust Soc Am 87.

Barberis C, Tribollet E (1996) Vasopressin and oxytocin receptors in the central nervous system. Crit Rev Neurobiol 10.

Bargmann W, Scharrer E (1951) The site of origin of the hormones of the posterior pituitary. Am Sci.

Barrett CE, Keebaugh AC, Ahern TH, Bass CE, Terwilliger EF, Young LJ (2013) Variation in vasopressin receptor (Avpr1a) expression creates diversity in behaviors related to monogamy in prairie voles. Horm Behav 63.

Bayne BL, Scullard C (1978) Rates of feeding by Thais (Nucella) Lapillus (L.). J Exp Mar Bio Ecol 32.

Becker JB, Rudick CN, Jenkins WJ (2001) The role of dopamine in the nucleus accumbens and striatum during sexual behavior in the female rat. J Neurosci 21.

Berendzen KM, Sharma R, Mandujano MA, Wei Y, Rogers FD, Simmons TC, Seelke AHM, Bond JM, Larios RD, Sherman M, Parthasarathy S, Espineda I, Knoedler JR, Beery A, Bales KL, Shah NM, Manoli DS (2022) Oxytocin receptor is not required for social attachment in prairie voles. bioRxiv:2022.07.22.501192 Available at: https://www.biorxiv.org/content/10.1101/2022.07.22.501192v1 [Accessed January 2, 2023].

Berke JD (2009) Fast oscillations in cortical-striatal networks switch frequency following rewarding events and stimulant drugs. Eur J Neurosci.

Berman GJ (2018) Measuring behavior across scales. BMC Biol 16:23 Available at: https://bmcbiol.biomedcentral.com/articles/10.1186/s12915-018-0494-7.

Berman GJ, Bialek W, Shaevitz JW (2016) Predictability and hierarchy in Drosophila behavior. Proc Natl Acad Sci U S A 113.

Berman GJ, Choi DM, Bialek W, Shaevitz JW (2014) Mapping the stereotyped behaviour of freely moving fruit flies. J R Soc Interface 11:20140672 Available at: https://royalsocietypublishing.org/doi/10.1098/rsif.2014.0672.

Bialek W, Cavagna A, Giardina I, Mora T, Pohl O, Silvestri E, Viale M, Walczak AM (2014) Social interactions dominate speed control in poising natural flocks near criticality. Proc Natl Acad Sci U S A 111:7212–7217 Available at: https://www.pnas.org/doi/abs/10.1073/pnas.1324045111 [Accessed December 14, 2022].

Borie AM, Agezo S, Lunsford P, Boender AJ, Guo J-D, Zhu H, Berman GJ, Young LJ, Liu RC (2021) Social Experience Alters Oxytocinergic Modulation in the Nucleus Accumbens of Female Prairie Voles. SSRN Electron J.

Branson K, Robie AA, Bender J, Perona P, Dickinson MH (2009) High-throughput ethomics in large groups of Drosophila. Nat Methods 6:451–457 Available at: http://www.nature.com/articles/nmeth.1328.

Brown AEX, De Bivort B (2018) Ethology as a physical science. Nat Phys 14.

Buelthoff H, Poggio T, Wehrhahn C (1980) 3-D Analysis of the flight trajectories of flies (drosophila melanogaster). Zeitschrift fur Naturforsch - Sect C J Biosci 35.

Burbach PJ, Young LJ, Russell JA (2006) OxytocinSynthesis, Secretion, and Reproductive Functions. In: Knobil and Neill's Physiology of Reproduction, pp 3055–3128. Elsevier. Available at: https://linkinghub.elsevier.com/retrieve/pii/B9780125154000500634.

Burkett JP, Spiegel LL, Inoue K, Murphy AZ, Young LJ (2011) Activation of-opioid receptors in the dorsal striatum is necessary for adult social attachment in monogamous prairie voles. Neuropsychopharmacology.

Caldwell HK, Young WS (2006) Oxytocin and Vasopressin: Genetics and Behavioral Implications. In: Handbook of Neurochemistry and Molecular Neurobiology.

Carter CS, Witt DM, Thompson EG, Carlstead K (1988) Effects of hormonal, sexual, and social history on mating and pair bonding in prairie voles. Physiol Behav 44:691–697 Available at: https://linkinghub.elsevier.com/retrieve/pii/0031938488900492.

Castillo PE, Younts TJ, Chávez AE, Hashimotodani Y (2012) Endocannabinoid Signaling and Synaptic Function. Neuron 76.

Chapais B (2021) The Evolutionary History of Pair-Bonding. In: Primeval Kinship.

Chen S, Lee AY, Bowens NM, Huber R, Kravitz EA (2002) Fighting fruit flies: A model system for the study of aggression. Proc Natl Acad Sci U S A 99.

Cheriyamkunnel SJ, Rose S, Jacob PF, Blackburn LA, Glasgow S, Moorse J, Winstanley M, Moynihan PJ, Waddell S, Rezaval C (2021) A neuronal mechanism controlling the choice

between feeding and sexual behaviors in Drosophila. Curr Biol 31:4231-4245.e4 Available at: https://pubmed.ncbi.nlm.nih.gov/34358444/ [Accessed January 10, 2023].

Chiel HJ, Beer RD (1997) The brain has a body: adaptive behavior emerges from interactions of nervous system, body and environment. Trends Neurosci 20:553–557 Available at: https://linkinghub.elsevier.com/retrieve/pii/S0166223697011491.

Chini B, Mouillac B, Ala Y, Balestre MN, Trumpp-Kallmeyer S, Hoflack J, Elands J, Hibert M, Manning M, Jard S, Barberis C (1995) Tyr115 is the key residue for determining agonist selectivity in the V1a vasopressin receptor. EMBO J 14.

Cho MM, DeVries AC, Williams JR, Carter CS (1999a) The effects of oxytocin and vasopressin on partner preferences in male and female prairie voles (Microtus ochrogaster). Behav Neurosci.

Cho MM, DeVries AC, Williams JR, Carter CS (1999b) The effects of oxytocin and vasopressin on partner preferences in male and female prairie voles (Microtus ochrogaster). Behav Neurosci 113:1071–1079 Available at: http://doi.apa.org/getdoi.cfm?doi=10.1037/0735-7044.113.5.1071.

Chong KK, Anandakumar DB, Dunlap AG, Kacsoh DB, Liu RC (2020) Experience-dependent coding of time-dependent frequency trajectories by off responses in secondary auditory cortex. J Neurosci 40.

Clutton-Brock TH, Gaynor D, McIlrath GM, Maccoll ADC, Kansky R, Chadwick P, Manser M, Skinner JD, Brotherton PNM (1999) Predation, group size and mortality in a cooperative mongoose, Suricata suricatta. J Anim Ecol 68:672–683 Available at: http://doi.wiley.com/10.1046/j.1365-2656.1999.00317.x.

Cockburn A (2006) Prevalence of different modes of parental care in birds. Proc R Soc B Biol Sci 273:1375–1383 Available at: https://royalsocietypublishing.org/doi/10.1098/rspb.2005.3458.

Cohen D, Shamay-Tsoory SG (2018) Oxytocin regulates social approach. Soc Neurosci 13.

Couzin ID, Krause J (2003) Self-Organization and Collective Behavior in Vertebrates. In: Advances in the Study of Behavior, pp 1–75 Available at: https://linkinghub.elsevier.com/retrieve/pii/S0065345403010015.

D'Amato FR, Moles A (2001) Ultrasonic vocalizations as an index of social memory in female mice. Behav Neurosci 115.

Dale HH (1906) On some physiological actions of ergot. J Physiol 34:163–206 Available at: https://onlinelibrary.wiley.com/doi/10.1113/jphysiol.1906.sp001148.

Dankert H, Wang L, Hoopfer ED, Anderson DJ, Perona P (2009) Automated monitoring and analysis of social behavior in Drosophila. Nat Methods 6.

Datta SR, Anderson DJ, Branson K, Perona P, Leifer A (2019) Computational Neuroethology: A Call to Action. Neuron 104:11–24 Available at: https://linkinghub.elsevier.com/retrieve/pii/S0896627319308414.

Dawkins R (1976) Hierarchical organisation: A candidate principle for ethology. In: Growing points in ethology.

De Bono M, Tobin DM, Davis MW, Avery L, Bargmann CI (2002) Social feeding in Caenorhabditis elegans is induced by neurons that detect aversive stimuli. Nature 419.

de Chaumont F, Coura RD-S, Serreau P, Cressant A, Chabout J, Granon S, Olivo-Marin J-C (2012) Computerized video analysis of social interactions in mice. Nat Methods 9:410–417 Available at: http://www.nature.com/articles/nmeth.1924.

de Kock CPJ, Wierda KDB, Bosman LWJ, Min R, Koksma J-J, Mansvelder HD, Verhage M, Brussaard AB (2003) Somatodendritic Secretion in Oxytocin Neurons Is Upregulated during the Female Reproductive Cycle. J Neurosci 23:2726–2734 Available at: https://www.jneurosci.org/lookup/doi/10.1523/JNEUROSCI.23-07-02726.2003.

Deban SM, Richardson JC (2011) Cold-blooded snipers: Thermal independence of ballistic tongue projection in the salamander Hydromantes platycephalus. J Exp Zool Part A Ecol Genet Physiol 315 A.

Dell AI, Bender JA, Branson K, Couzin ID, de Polavieja GG, Noldus LPJJ, Pérez-Escudero A, Perona P, Straw AD, Wikelski M, Brose U (2014) Automated image-based tracking and its application in ecology. Trends Ecol Evol 29:417–428 Available at: https://linkinghub.elsevier.com/retrieve/pii/S0169534714001074.

Devlin J, Chang MW, Lee K, Toutanova K (2019) BERT: Pre-training of deep bidirectional transformers for language understanding. In: NAACL HLT 2019 - 2019 Conference of the North American Chapter of the Association for Computational Linguistics: Human Language Technologies - Proceedings of the Conference.

Dikker S, Wan L, Davidesco I, Kaggen L, Oostrik M, McClintock J, Rowland J, Michalareas G, Van Bavel JJ, Ding M, Poeppel D (2017) Brain-to-Brain Synchrony Tracks Real-World Dynamic Group Interactions in the Classroom. Curr Biol 27.

Dölen G, Darvishzadeh A, Huang KW, Malenka RC (2013) Social reward requires coordinated activity of nucleus accumbens oxytocin and serotonin. Nature.

Dunlap AG, Besosa C, Pascual LM, Chong KK, Walum H, Kacsoh DB, Tankeu BB, Lu K, Liu RC (2020) Becoming a better parent: Mice learn sounds that improve a stereotyped maternal behavior. Horm Behav 124:104779 Available at: https://linkinghub.elsevier.com/retrieve/pii/S0018506X20301057.

Dunn TW, Marshall JD, Severson KS, Aldarondo DE, Hildebrand DGC, Chettih SN, Wang WL, Gellis AJ, Carlson DE, Aronov D, Freiwald WA, Wang F, Ölveczky BP (2021) Geometric deep learning enables 3D kinematic profiling across species and environments. Nat Methods 18.

Durisko Z, Kemp R, Mubasher R, Dukas R (2014) Dynamics of social behavior in fruit fly larvae. PLoS One 9.

Duvernoy HM (1988) The Human Hippocampus.

Ekanadham C, Tranchina D, Simoncelli EP (2014) A unified framework and method for automatic neural spike identification. J Neurosci Methods 222.

Ferguson JN, Aldag JM, Insel TR, Young LJ (2001) Oxytocin in the Medial Amygdala is Essential for Social Recognition in the Mouse. J Neurosci 21:8278–8285 Available at: https://www.jneurosci.org/lookup/doi/10.1523/JNEUROSCI.21-20-08278.2001.

Ferguson JN, Young LJ, Hearn EF, Matzuk MM, Insel TR, Winslow JT (2000) Social amnesia in mice lacking the oxytocin gene. Nat Genet 25:284–288 Available at: http://www.nature.com/articles/ng0700_284.

Ferris CF, Melloni RH, Koppel G, Perry KW, Fuller RW, Delville Y (1997) Vasopressin/serotonin interactions in the anterior hypothalamus control aggressive behavior in golden hamsters. J Neurosci 17.

Floresco SB (2015) The nucleus accumbens: An interface between cognition, emotion, and action. Annu Rev Psychol 66.

Floresco SB, Braaksma DN, Phillips AG (1999) Thalamic-cortical-striatal circuitry subserves working memory during delayed responding on a radial arm maze. J Neurosci 19.

Floresco SB, McLaughlin RJ, Haluk DM (2008) Opposing roles for the nucleus accumbens core and shell in cue-induced reinstatement of food-seeking behavior. Neuroscience 154.

Floresco SB, Seamans JK, Phillips AG (1997) Selective roles for hippocampal, prefrontal cortical, and ventral striatal circuits in radial-arm maze tasks with or without a delay. J Neurosci 17.

Francis DD, Young LJ, Meaney MJ, Insel TR (2002) Naturally occurring differences in maternal care are associated with the expression of oxytocin and vasopressin (V1a) receptors: Gender differences. J Neuroendocrinol 14.

François Chollet (2017) Deep Learning with Python & Keras. Manning Publ 80.

Freeman SM, Samineni S, Allen PC, Stockinger D, Bales KL, Hwa GGC, Roberts JA (2016) Plasma and CSF oxytocin levels after intranasal and intravenous oxytocin in awake macaques. Psychoneuroendocrinology.

Freund-mercier M-J, Moos F, Poulain DA, Richard P, Rodriguez F, Theodosis DT, Vincent J (1988) Role of central oxytocin in the control of the milk ejection reflex. Brain Res Bull 20:737–741 Available at: https://linkinghub.elsevier.com/retrieve/pii/0361923088900858.

Freund-Mercier MJ, Stoeckel ME, Palacios JM, Pazos A, Reichhart JM, Porte A, Richard P (1987) Pharmacological characteristics and anatomical distribution of [3H]oxytocin-binding sites in the wistar rat brain studied by autoradiography. Neuroscience 20.

Froemke RC, Young LJ (2021) Oxytocin, Neural Plasticity, and Social Behavior. Annu Rev Neurosci 44:359–381 Available at: https://www.annualreviews.org/doi/10.1146/annurev-neuro-102320-102847.

Gavish L, Sue Carter C, Getz LL (1983) Male-female interactions in prairie voles. Anim Behav 31:511–517 Available at: https://linkinghub.elsevier.com/retrieve/pii/S0003347283800736.

Gavrilets S (2012) Human origins and the transition from promiscuity to pair-bonding. Proc Natl Acad Sci 109:9923–9928 Available at: https://pnas.org/doi/full/10.1073/pnas.1200717109.

Géron A (2019) Hands-on machine learning with Scikit-Learn and TensorFlow : concepts, tools, and techniques to build intelligent systems.

Getz LL., Carter CS (1980) Social Organization in Microtus ochrogaster Populations. Biol 62.

Getz LL, Carter CS, Gavish L (1981) The mating system of the prairie vole, Microtus ochrogaster: Field and laboratory evidence for pair-bonding. Behav Ecol Sociobiol 8:189–194 Available at: http://link.springer.com/10.1007/BF00299829.

Getz LL, McGuire B, Pizzuto T, Hofmann JE, Frase B (1993) Social organization of the prairie vole (Microtus ochrogaster). J Mammal 74.

Gimpl G, Fahrenholz F (2001) The Oxytocin Receptor System: Structure, Function, and Regulation. Physiol Rev.

Gomez-Marin A, Stephens GJ, Brown AEX (2016) Hierarchical compression of Caenorhabditis elegans locomotion reveals phenotypic differences in the organization of behaviour. J R Soc Interface 13.

Goodfellow Ian, Bengio Yoshua CA (2016) Deep Learning - Ian Goodfellow, Yoshua Bengio, Aaron Courville - Google Books. MIT Press.

Goto Y, O'Donnell P (2001) Network Synchrony in the Nucleus Accumbens In Vivo. J Neurosci 21:4498–4504 Available at: http://www.jneurosci.org/lookup/doi/10.1523/JNEUROSCI.21-12-04498.2001.

Goto Y, O'Donnell P (2002) Timing-dependent limbic-motor synaptic integration in the nucleus accumbens. Proc Natl Acad Sci U S A.

Graving JM, Chae D, Naik H, Li L, Koger B, Costelloe BR, Couzin ID (2019) Deepposekit, a software toolkit for fast and robust animal pose estimation using deep learning. Elife 8.

Gruber AJ, Hussain RJ, O'Donnell P (2009) The nucleus accumbens: A switchboard for goal-directed behaviors. PLoS One.

Guastella AJ, Mitchell PB, Dadds MR (2008) Oxytocin Increases Gaze to the Eye Region of Human Faces. Biol Psychiatry 63.

Günel S, Rhodin H, Morales D, Campagnolo J, Ramdya P, Fua P (2019) Deepfly3D, a deep learning-based approach for 3D limb and appendage tracking in tethered, adult Drosophila. Elife 8.

Hammerschmidt K, Radyushkin K, Ehrenreich H, Fischer J (2009) Female mice respond to male ultrasonic "songs" with approach behaviour. Biol Lett 5.

Hanson JL, Hurley LM (2012) Female presence and estrous state influence mouse ultrasonic courtship vocalizations. PLoS One 7.

Hawtin SR, Wesley VJ, Parslow RA, Patel S, Wheatley M (2000) Critical role of a subdomain of the N-terminus of the V(1a) vasopressin receptor for binding agonists but not antagonists; functional rescue by the oxytocin receptor N-terminus. Biochemistry 39.

Hess EH, Hodges AW, Lorenz KZ, Lorenz K, Kickert RW (1982) The Foundations of Ethology. Am J Psychol 95:521.

Hong W, Kennedy A, Burgos-Artizzu XP, Zelikowsky M, Navonne SG, Perona P, Anderson DJ (2015) Automated measurement of mouse social behaviors using depth sensing, video tracking, and machine learning. Proc Natl Acad Sci 112 Available at: https://pnas.org/doi/full/10.1073/pnas.1515982112.

Horie K, Inoue K, Suzuki S, Adachi S, Yada S, Hirayama T, Hidema S, Young LJ, Nishimori K (2019) Oxytocin receptor knockout prairie voles generated by CRISPR/Cas9 editing show reduced

preference for social novelty and exaggerated repetitive behaviors. Horm Behav 111.

Horie K, Nishimori K (2022) CRISPR/Cas9-Mediated Genetic Engineering to Generate a Disease Model Prairie Vole, Based on Species-Optimized Assisted Reproductive Technology. In: Methods in Molecular Biology.

House J, Landis K, Umberson D (1988) Social relationships and health. Science (80-) 241:540–545 Available at: https://www.sciencemag.org/lookup/doi/10.1126/science.3399889.

Inoue T, Kimura T, Azuma C, Inazawa J, Takemura M, Kikuchi T, Kubota Y, Ogita K, Saji F (1994) Structural organization of the human oxytocin receptor gene. J Biol Chem 269.

Insafutdinov E, Pishchulin L, Andres B, Andriluka M, Schiele B (2016) DeeperCut: A Deeper, Stronger, and Faster Multi-person Pose Estimation Model. In: Lecture Notes in Computer Science (including subseries Lecture Notes in Artificial Intelligence and Lecture Notes in Bioinformatics), pp 34–50 Available at: http://link.springer.com/10.1007/978-3-319-46466-4_3.

Insel TR, Hulihan TJ (1995) A Gender-Specific Mechanism for Pair Bonding: Oxytocin and Partner Preference Formation in Monogamous Voles. Behav Neurosci.

Insel TR, Young LJ (2001) The neurobiology of attachment. Nat Rev Neurosci 2:129–136 Available at: http://www.nature.com/articles/35053579.

Ioffe S, Szegedy C (2015) Batch normalization: Accelerating deep network training by reducing internal covariate shift. In: 32nd International Conference on Machine Learning, ICML 2015.

Jones FN, Skinner BF (1939) The Behavior of Organisms: An Experimental Analysis. Am J Psychol 52.

Kappeler PM (1997) Determinants of primate social organization: Comparative evidence and new insights from malagasy lemurs. Biol Rev 72.

Kappeler PM, Van Schaik CP (2002) Evolution of primate social systems. Int J Primatol 23.

Kawasaki M, Yamada Y, Ushiku Y, Miyauchi E, Yamaguchi Y (2013) Inter-brain synchronization during coordination of speech rhythm in human-to-human social interaction. Sci Rep 3.

Keebaugh AC, Barrett CE, Laprairie JL, Jenkins JJ, Young LJ (2015) RNAi knockdown of oxytocin receptor in the nucleus accumbens inhibits social attachment and parental care in monogamous female prairie voles. Soc Neurosci.

Keebaugh AC, Young LJ (2011) Increasing oxytocin receptor expression in the nucleus

accumbens of pre-pubertal female prairie voles enhances alloparental responsiveness and partner preference formation as adults. Horm Behav 60:498–504 Available at: https://linkinghub.elsevier.com/retrieve/pii/S0018506X11001796.

Keller BL, Krebs CJ (1970) Microtus Population Biology; III. Reproductive Changes in Fluctuating Populations of M. ochrogaster and M. pennsylvanicus in Southern Indiana, 1965-67. Ecol Monogr 40:263–294 Available at: https://onlinelibrary.wiley.com/doi/10.2307/1942284.

Kiecolt-Glaser JK, Loving TJ, Stowell JR, Malarkey WB, Lemeshow S, Dickinson SL, Glaser R (2005) Hostile Marital Interactions, Proinflammatory Cytokine Production, and Wound Healing. Arch Gen Psychiatry 62:1377 Available at: http://archpsyc.jamanetwork.com/article.aspx?doi=10.1001/archpsyc.62.12.1377.

Kiecolt-Glaser JK, Newton TL (2001) Marriage and health: His and hers. Psychol Bull 127:472–503 Available at: http://doi.apa.org/getdoi.cfm?doi=10.1037/0033-2909.127.4.472.

Kimura T, Makino Y, Saji F, Takemura M, Inoue T, Kikuchi T, Kubota Y, Azuma C, Nobunaga T, Tokugawa Y, Tanizawa O (1994) Molecular characterization of a cloned human oxytocin receptor. Eur J Endocrinol 131.

King LB, Walum H, Inoue K, Eyrich NW, Young LJ (2016) Variation in the Oxytocin Receptor Gene Predicts Brain Region–Specific Expression and Social Attachment. Biol Psychiatry.

Kingma DP, Ba JL (2015) Adam: A method for stochastic optimization. In: 3rd International Conference on Learning Representations, ICLR 2015 - Conference Track Proceedings.

Kirsch P, Esslinger C, Chen Q, Mier D, Lis S, Siddhanti S, Gruppe H, Mattay VS, Gallhofer B, Meyer-Lindenberg A (2005) Oxytocin modulates neural circuitry for social cognition and fear in humans. J Neurosci 25.

Klambauer G, Unterthiner T, Mayr A, Hochreiter S (2017) Self-Normalizing Neural Networks. Adv Neural Inf Process Syst 2017-December:972–981 Available at: https://arxiv.org/abs/1706.02515v5 [Accessed January 20, 2023].

Klibaite U, Shaevitz JW (2020) Paired fruit flies synchronize behavior: Uncovering social interactions in Drosophila melanogaster Flack JC, ed. PLOS Comput Biol 16:e1008230 Available at: https://dx.plos.org/10.1371/journal.pcbi.1008230.

Knobloch HS, Charlet A, Hoffmann LC, Eliava M, Khrulev S, Cetin AH, Osten P, Schwarz MK, Seeburg PH, Stoop R, Grinevich V (2012) Evoked Axonal Oxytocin Release in the Central Amygdala Attenuates Fear Response. Neuron 73:553–566 Available at: https://linkinghub.elsevier.com/retrieve/pii/S0896627312000347.

Kosfeld M, Heinrichs M, Zak PJ, Fischbacher U, Fehr E (2005) Oxytocin increases trust in

humans. Nature 435.

Kravitz EA, Huber R (2003) Aggression in invertebrates. Curr Opin Neurobiol 13:736–743 Available at: https://linkinghub.elsevier.com/retrieve/pii/S0959438803001582.

Lauer J, Zhou M, Ye S, Menegas W, Nath T, Rahman MM, Santo V Di, Soberanes D, Feng G, Murthy VN, Lauder G, Dulac C, Mathis MW, Mathis A (2021) Multi-animal pose estimation and tracking with DeepLabCut. bioRxiv.

Lauer J, Zhou M, Ye S, Menegas W, Schneider S, Nath T, Rahman MM, Di Santo V, Soberanes D, Feng G, Murthy VN, Lauder G, Dulac C, Mathis MW, Mathis A (2022) Multi-animal pose estimation, identification and tracking with DeepLabCut. Nat Methods 19:496–504 Available at: https://www.nature.com/articles/s41592-022-01443-0 [Accessed January 3, 2023].

Lim MM, Young LJ (2004) Vasopressin-dependent neural circuits underlying pair bond formation in the monogamous prairie vole. Neuroscience 125.

Liu X Le, Yu SY, Flierman NA, Loyola S, Kamermans M, Hoogland TM, De Zeeuw CI (2021) OptiFlex: Multi-Frame Animal Pose Estimation Combining Deep Learning With Optical Flow. Front Cell Neurosci 15.

Liu Y, Curtis JT, Wang Z (2001) Vasopressin in the lateral septum regulates pair bond formation in male prairie voles (Microtus ochrogaster). Behav Neurosci 115.

Liu Y, Wang ZX (2003) Nucleus accumbens oxytocin and dopamine interact to regulate pair bond formation in female prairie voles. Neuroscience.

Lorenz K (1966) Evolution and Modification of Behavior.

Lukas D, Clutton-Brock TH (2013) The Evolution of Social Monogamy in Mammals. Science (80-) 341:526–530 Available at: https://www.science.org/doi/10.1126/science.1238677.

MacBeth AH, Lee HJ, Edds J, Young WS (2009) Oxytocin and the oxytocin receptor underlie intrastrain, but not interstrain, social recognition. Genes, Brain Behav 8.

Mann K, Gordon MD, Scott K (2013) A pair of interneurons influences the choice between feeding and locomotion in Drosophila. Neuron 79:754 Available at: /pmc/articles/PMC3750742/ [Accessed January 10, 2023].

Marshall JD, Klibaite U, Gellis A, Aldarondo DE, Ölveczky BP, Dunn TW (2021) The PAIR-R24M Dataset for Multi-animal 3D Pose Estimation. bioRxiv:2021.11.23.469743 Available at: http://biorxiv.org/content/early/2021/11/25/2021.11.23.469743.abstract.

Masters WM, Jacobs SC (1989) Target detection and range resolution by the big brown bat (Eptesicus fuscus) using normal and time-reversed model echoes. J Comp Physiol A 166.

Mathis A, Mamidanna P, Cury KM, Abe T, Murthy VN, Mathis MW, Bethge M (2018) DeepLabCut: markerless pose estimation of user-defined body parts with deep learning. Nat Neurosci 21:1281–1289 Available at: http://www.nature.com/articles/s41593-018-0209-y.

Mehta P, Bukov M, Wang CH, Day AGR, Richardson C, Fisher CK, Schwab DJ (2019) A high-bias, low-variance introduction to Machine Learning for physicists. Phys Rep 810.

Mermelstein PG, Becker JB (1995) Increased Extracellular Dopamine in the Nucleus Accumbens and Striatum of the Female Rat During Paced Copulatory Behavior. Behav Neurosci.

Modi ME, Connor-Stroud F, Landgraf R, Young LJ, Parr LA (2014) Aerosolized oxytocin increases cerebrospinal fluid oxytocin in rhesus macaques. Psychoneuroendocrinology 45.

Moran G, Fentress JC, Golani I (1981) A description of relational patterns of movement during “ritualized fighting” in wolves. Anim Behav 29.

Morgan BJT, Okubo A (1981) Diffusion and Ecological Problems: Mathematical Models. Biometrics 37.

Musstafa (2021) Optimizers in Deep Learning. What is an optimizer? | by Musstafa | MLearning.ai | Medium. Available at: https://medium.com/mlearning-ai/optimizers-in-deep-learning-7bf81fed78a0 [Accessed December 5, 2022].

Nath T, Mathis A, Chen AC, Patel A, Bethge M, Mathis MW (2019) Using DeepLabCut for 3D markerless pose estimation across species and behaviors. Nat Protoc 14.

Neumann ID, Maloumby R, Beiderbeck DI, Lukas M, Landgraf R (2013) Increased brain and plasma oxytocin after nasal and peripheral administration in rats and mice. Psychoneuroendocrinology 38.

Noldus LPJJ, Spink AJ, Tegelenbosch RAJ (2001) EthoVision: A versatile video tracking system for automation of behavioral experiments. Behav Res Methods, Instruments, Comput 33.

Numan M, Young LJ (2016) Neural mechanisms of mother–infant bonding and pair bonding: Similarities, differences, and broader implications. Horm Behav 77:98–112 Available at: https://linkinghub.elsevier.com/retrieve/pii/S0018506X15001038.

Oettl L-L, Ravi N, Schneider M, Scheller MF, Schneider P, Mitre M, da Silva Gouveia M, Froemke RC, Chao MV, Young WS, Meyer-Lindenberg A, Grinevich V, Shusterman R, Kelsch W (2016)

Oxytocin Enhances Social Recognition by Modulating Cortical Control of Early Olfactory Processing. Neuron 90:609–621 Available at: https://linkinghub.elsevier.com/retrieve/pii/S0896627316300241.

Okuyama T, Kitamura T, Roy DS, Itohara S, Tonegawa S (2016) Ventral CA1 neurons store social memory. Science (80-) 353:1536–1541 Available at: https://www.science.org/doi/10.1126/science.aaf7003.

Olazábal DE, Young LJ (2006) Species and individual differences in juvenile female alloparental care are associated with oxytocin receptor density in the striatum and the lateral septum. Horm Behav 49.

Ophir AG, Phelps SM, Sorin AB, Wolff JO (2007) Morphological, Genetic, and Behavioral Comparisons of Two Prairie Vole Populations in the Field and Laboratory. J Mammal 88:989–999 Available at: https://academic.oup.com/jmammal/article-lookup/doi/10.1644/06-MAMM-A-250R.1.

Overman KE, Choi DM, Leung K, Shaevitz JW, Berman GJ (2022) Measuring the repertoire of age-related behavioral changes in Drosophila melanogaster. PLoS Comput Biol 18.

Owen SF, Tuncdemir SN, Bader PL, Tirko NN, Fishell G, Tsien RW (2013) Oxytocin enhances hippocampal spike transmission by modulating fast-spiking interneurons. Nature.

Pachitariu M, Steinmetz N, Kadir S, Carandini M, Harris K (2016) Fast and accurate spike sorting of high-channel count probes with KiloSort. In: Advances in Neural Information Processing Systems.

Peciña S, Berridge KC (2005) Hedonic hot spot in nucleus accumbens shell: Where do μ-Opioids cause increased hedonic impact of sweetness? J Neurosci 25.

Pedersen CA, Ascher JA, Monroe YL, Prange AJ (1982) Oxytocin Induces Maternal Behavior in Virgin Female Rats. Science (80-) 216:648–650 Available at: https://www.science.org/doi/10.1126/science.7071605.

Pereira TD et al. (2022) SLEAP: A deep learning system for multi-animal pose tracking. Nat Methods 19:486–495 Available at: https://www.nature.com/articles/s41592-022-01426-1.

Pereira TD, Aldarondo DE, Willmore L, Kislin M, Wang SSH, Murthy M, Shaevitz JW (2019) Fast animal pose estimation using deep neural networks. Nat Methods 16.

Pereira TD, Shaevitz JW, Murthy M (2020) Quantifying behavior to understand the brain. Nat Neurosci 23.

Pérez-Escudero A, Vicente-Page J, Hinz RC, Arganda S, de Polavieja GG (2014) idTracker:

tracking individuals in a group by automatic identification of unmarked animals. Nat Methods 11:743–748 Available at: http://www.nature.com/articles/nmeth.2994.

Pisansky MT, Hanson LR, Gottesman II, Gewirtz JC (2017) Oxytocin enhances observational fear in mice. Nat Commun 2017 81 8:1–11 Available at: https://www.nature.com/articles/s41467-017-02279-5 [Accessed January 8, 2023].

Popik P, van Ree JM (1991) Oxytocin but not vasopressin facilities social recognition following injection into the medial preoptic area of the rat brain. Eur Neuropsychopharmacol 1.

Post AM, Weyers P, Holzer P, Painsipp E, Pauli P, Wultsch T, Reif A, Lesch KP (2011) Gene-environment interaction influences anxiety-like behavior in ethologically based mouse models. Behav Brain Res 218.

Raam T, McAvoy KM, Besnard A, Veenema A, Sahay A (2017) Hippocampal oxytocin receptors are necessary for discrimination of social stimuli. Nat Commun 8.

Radford Alec, Wu Jeffrey, Child Rewon, Luan David, Amodei Dario, Sutskever Ilya (2019) Language Models are Unsupervised Multitask Learners | Enhanced Reader. OpenAI Blog 1.

Resendez SL, Dome M, Gormley G, Franco D, Nevarez N, Hamid AA, Aragona BJ (2013) -Opioid Receptors within Subregions of the Striatum Mediate Pair Bond Formation through Parallel Yet Distinct Reward Mechanisms. J Neurosci 33:9140–9149 Available at: https://www.jneurosci.org/lookup/doi/10.1523/JNEUROSCI.4123-12.2013.

Resendez SL, Keyes PC, Day JJ, Hambro C, Austin CJ, Maina FK, Eidson LN, Porter-Stransky KA, Nevárez N, McLean JW, Kuhnmuench MA, Murphy AZ, Mathews TA, Aragona BJ (2016) Dopamine and opioid systems interact within the nucleus accumbens to maintain monogamous pair bonds. Elife.

Resendez SL, Kuhnmuench M, Krzywosinski T, Aragona BJ (2012) κ-opioid receptors within the nucleus accumbens shell mediate pair bond maintenance. J Neurosci 32.

Reynolds CW (1987) FLOCKS, HERDS, AND SCHOOLS: A DISTRIBUTED BEHAVIORAL MODEL. Comput Graph 21.

Richard, Dawkins M (1973) Decisions and The Uncertainty Of Behaviour. Behaviour.

Richard, Dawkins M (1976) Hierachical organization and postural facilitation: Rules for grooming in flies. Anim Behav 24.

Ridley AR, Nelson-Flower MJ, Thompson AM (2013) Is sentinel behaviour safe? An experimental investigation. Anim Behav 85:137–142 Available at: https://linkinghub.elsevier.com/retrieve/pii/S0003347212004770.

Robie AA, Seagraves KM, Egnor SER, Branson K (2017) Machine vision methods for analyzing social interactions Levine JD, Kronauer DJC, Dickinson MH, eds. J Exp Biol 220:25–34 Available at: https://journals.biologists.com/jeb/article/220/1/25/33433/Machine-vision-methods-for-analyzing-social.

Romero-Ferrero F, Bergomi MG, Hinz RC, Heras FJH, de Polavieja GG (2019) idtracker.ai: tracking all individuals in small or large collectives of unmarked animals. Nat Methods 16.

Ross HE, Cole CD, Smith Y, Neumann ID, Landgraf R, Murphy AZ, Young LJ (2009) Characterization of the oxytocin system regulating affiliative behavior in female prairie voles. Neuroscience 162:892–903 Available at: http://www.ncbi.nlm.nih.gov/pubmed/19482070 [Accessed June 5, 2019].

Sangiamo DT, Warren MR, Neunuebel JP (2020) Ultrasonic signals associated with different types of social behavior of mice. Nat Neurosci 23.

Schwarz RF, Branicky R, Grundy LJ, Schafer WR, Brown AEX (2015) Changes in Postural Syntax Characterize Sensory Modulation and Natural Variation of C. elegans Locomotion. PLoS Comput Biol 11.

Seeds AM, Ravbar P, Chung P, Hampel S, Midgley FM, Mensh BD, Simpson JH (2014) A suppression hierarchy among competing motor programs drives sequential grooming in Drosophila. Elife 3.

Shamay-Tsoory SG, Abu-Akel A (2016) The Social Salience Hypothesis of Oxytocin. Biol Psychiatry.

Shapiro LE, Insel TR (1992) Oxytocin Receptor Distribution Reflects Social Organization in Monogamous and Polygamous Voles. Ann N Y Acad Sci.

Shukla S, Arac A (2020) A step-by-step implementation of deepbehavior, deep learning toolbox for automated behavior analysis. J Vis Exp 2020.

Song Z, McCann KE, McNeill JK, Larkin TE, Huhman KL, Albers HE (2014) Oxytocin induces social communication by activating arginine-vasopressin V1a receptors and not oxytocin receptors. Psychoneuroendocrinology 50.

Spink AJ, Tegelenbosch RAJ, Buma MOS, Noldus LPJJ (2001) The EthoVision video tracking system - A tool for behavioral phenotyping of transgenic mice. Physiol Behav 73.

Srivastava N, Hinton G, Krizhevsky A, Sutskever I, Salakhutdinov R (2014) Dropout: A simple way to prevent neural networks from overfitting. J Mach Learn Res 15.

Stafflinger E, Hansen KK, Hauser F, Schneider M, Cazzamali G, Williamson M, Grimmelikhuijzen CJP (2008) Cloning and identification of an oxytocin/vasopressin-like receptor and its ligand from insects. Proc Natl Acad Sci 105:3262–3267 Available at: https://pnas.org/doi/full/10.1073/pnas.0710897105.

Stephens GJ, Johnson-Kerner B, Bialek W, Ryu WS (2008) Dimensionality and Dynamics in the Behavior of C. elegans Sporns O, ed. PLoS Comput Biol 4:e1000028 Available at: https://dx.plos.org/10.1371/journal.pcbi.1000028.

Stevens Negus S (2011) Effects of peripherally restricted kappa opioid receptor agonists on pain-stimulated and pain-depressed behavior in rats. Neuropsychopharmacology 36.

Sue Carter C, Courtney Devries A, Getz LL (1995) Physiological substrates of mammalian monogamy: The prairie vole model. Neurosci Biobehav Rev 19:303–314 Available at: https://linkinghub.elsevier.com/retrieve/pii/014976349400070H.

Summerlee AJS, Lincoln DW (1981) ELECTROPHYSIOLOGICAL RECORDINGS FROM OXYTOCINERGIC NEURONES DURING SUCKLING IN THE UNANAESTHETIZED LACTATING RAT. J Endocrinol 90:255–265 Available at: https://joe.bioscientifica.com/view/journals/joe/90/2/joe_90_2_013.xml.

Swaney WT, Dubose BN, Curley JP, Champagne FA (2012) Sexual experience affects reproductive behavior and preoptic androgen receptors in male mice. Horm Behav.

Tan Y, Singhal SM, Harden SW, Cahill KM, Nguyen D-TM, Colon-Perez LM, Sahagian TJ, Thinschmidt JS, de Kloet AD, Febo M, Frazier CJ, Krause EG (2019) Oxytocin Receptors Are Expressed by Glutamatergic Prefrontal Cortical Neurons That Selectively Modulate Social Recognition. J Neurosci 39:3249–3263 Available at: https://www.jneurosci.org/lookup/doi/10.1523/JNEUROSCI.2944-18.2019.

Terburg D, Scheggia D, Triana del Rio R, Klumpers F, Ciobanu AC, Morgan B, Montoya ER, Bos PA, Giobellina G, van den Burg EH, de Gelder B, Stein DJ, Stoop R, van Honk J (2018) The Basolateral Amygdala Is Essential for Rapid Escape: A Human and Rodent Study. Cell 175:723 Available at: /pmc/articles/PMC6198024/ [Accessed January 8, 2023].

Thalmann U (2001) Food resource characteristics in two nocturnal lemurs with different social behavior: Avahi occidentalis and Lepilemur edwardsi. Int J Primatol 22.

Tinbergen N (1952) The Study of Instinct. N. Tinbergen. New York: Oxford Univ. Press, 1951. 228 pp. $7.00. Science (80-).

Tinbergen N (1963) On aims and methods of Ethology. Z Tierpsychol 20.

Tishby N, Pereira FC, Bialek W (2000) The information bottleneck method. Neural Comput.

Todd JG, Kain JS, De Bivort BL (2017) Systematic exploration of unsupervised methods for mapping behavior. Phys Biol 14.

Vaccari C, Lolait SJ, Ostrowski NL (1998) Comparative distribution of vasopressin V1B and oxytocin receptor messenger ribonucleic acids in brain. Endocrinology 139.

van den Pol AN (2012) Neuropeptide Transmission in Brain Circuits. Neuron 76:98–115 Available at: https://linkinghub.elsevier.com/retrieve/pii/S0896627312008471.

Van Der Maaten L, Hinton G (2008) Visualizing data using t-SNE. J Mach Learn Res 9.

Varley M, Symmes D (1966) The Hierarchy of Dominance in a Group of Macaques. Behaviour 27:54–74 Available at: https://brill.com/view/journals/beh/27/1-2/article-p54_3.xml.

Vaswani A, Shazeer N, Parmar N, Uszkoreit J, Jones L, Gomez AN, Kaiser Ł, Polosukhin I (2017) Attention is all you need. In: Advances in Neural Information Processing Systems.

Veenema AH, Bredewold R, Neumann ID (2007) Opposite effects of maternal separation on intermale and maternal aggression in C57BL/6 mice: Link to hypothalamic vasopressin and oxytocin immunoreactivity. Psychoneuroendocrinology 32.

Veenema AH, Neumann ID (2008) Central vasopressin and oxytocin release: regulation of complex social behaviours. Prog Brain Res 170.

Walum H, Young LJ (2018) The neural mechanisms and circuitry of the pair bond. Nat Rev Neurosci 19:643–654 Available at: http://www.nature.com/articles/s41583-018-0072-6.

Wang Z, Yu G, Cascio C, Liu Y, Gingrich B, Insel TR (1999) Dopamine D2 receptor-mediated regulation of partner preferences in female prairie voles (Microtus ochrogaster): A mechanism for pair bonding? Behav Neurosci 113.

Warren TL, Tumer EC, Charlesworth JD, Brainard MS (2011) Mechanisms and time course of vocal learning and consolidation in the adult songbird. J Neurophysiol 106:1806–1821 Available at: https://www.physiology.org/doi/10.1152/jn.00311.2011.

White NR, Prasad M, Barfield RJ, Nyby JG (1998) 40- and 70-kHz Vocalizations of Mice (Mus musculus) during Copulation. Physiol Behav 63:467–473 Available at: https://linkinghub.elsevier.com/retrieve/pii/S0031938497004848.

Williams JR, Catania KC, Carter SC (1992) Development of partner preferences in female prairie voles (Microtus ochrogaster): The role of social and sexual experience. Horm Behav 26:339–349 Available at: https://linkinghub.elsevier.com/retrieve/pii/0018506X9290004F.

Williams JR, Insel TR, Harbaugh CR, Carter CS (1994) Oxytocin Administered Centrally Facilitates Formation of a Partner Preference in Female Prairie Voles (Microtus ochrogaster). J Neuroendocrinol 6:247–250 Available at: http://doi.wiley.com/10.1111/j.1365-2826.1994.tb00579.x.

Wiltschko AB, Johnson MJ, Iurilli G, Peterson RE, Katon JM, Pashkovski SL, Abraira VE, Adams RP, Datta SR (2015) Mapping Sub-Second Structure in Mouse Behavior. Neuron 88:1121–1135 Available at: https://linkinghub.elsevier.com/retrieve/pii/S0896627315010375.

Winslow JT, Hastings N, Carter CS, Harbaugh CR, Insel TR (1993) A role for central vasopressin in pair bonding in monogamous prairie voles. Nature 365:545–548 Available at: http://www.nature.com/articles/365545a0.

Young LJ, Lim MM, Gingrich B, Insel TR (2001) Cellular mechanisms of social attachment. In: Hormones and Behavior.

Young LJ, Wang Z (2004) The neurobiology of pair bonding. Nat Neurosci 7:1048–1054 Available at: http://www.nature.com/articles/nn1327.

Zhang W, Yartsev MM (2019) Correlated Neural Activity across the Brains of Socially Interacting Bats. Cell 178.